

DEVELOPMENT OF FLAT GAIN AND WIDE-BAND  
ERBIUM DOPED FIBER AMPLIFIER USING HYBRID  
ACTIVE MEDIUM

AYA ALI HASAN ALMUKHTAR

FACULTY OF ENGINEERING  
UNIVERSITY OF MALAYA  
KUALA LUMPUR

2019

**DEVELOPMENT OF FLAT GAIN AND WIDE-BAND  
ERBIUM DOPED FIBER AMPLIFIER USING HYBRID  
ACTIVE MEDIUM**

**AYA ALI HASAN ALMUKHTAR**

**THESIS SUBMITTED IN FULFILMENT OF THE  
REQUIREMENTS FOR THE DEGREE OF DOCTOR OF  
PHILOSOPHY**

**DEPARTMENT OF ELECTRICAL ENGINEERING  
FACULTY OF ENGINEERING  
UNIVERSITY OF MALAYA  
KUALA LUMPUR**

**2019**

**UNIVERSITY OF MALAYA**  
**ORIGINAL LITERARY WORK DECLARATION**

Name of Candidate: Aya Ali Hasan Almkhtar

Matric No: KVA170019

Name of Degree: Doctor of Philosophy

Title of Project Paper/Research Report/Dissertation/Thesis (“this Work”):

DEVELOPMENT OF FLAT GAIN AND WIDE-BAND ERBIUM DOPED FIBER  
AMPLIFIER USING HYBRID ACTIVE MEDIUM

Field of Study: Photonics

I do solemnly and sincerely declare that:

- (1) I am the sole author/writer of this Work;
- (2) This Work is original;
- (3) Any use of any work in which copyright exists was done by way of fair dealing and for permitted purposes and any excerpt or extract from, or reference to or reproduction of any copyright work has been disclosed expressly and sufficiently and the title of the Work and its authorship have been acknowledged in this Work;
- (4) I do not have any actual knowledge nor do I ought reasonably to know that the making of this work constitutes an infringement of any copyright work;
- (5) I hereby assign all and every rights in the copyright to this Work to the University of Malaya (“UM”), who henceforth shall be owner of the copyright in this Work and that any reproduction or use in any form or by any means whatsoever is prohibited without the written consent of UM having been first had and obtained;
- (6) I am fully aware that if in the course of making this Work I have infringed any copyright whether intentionally or otherwise, I may be subject to legal action or any other action as may be determined by UM.

Candidate’s Signature

Date:

Subscribed and solemnly declared before,

Witness’s Signature

Date:

Name:

Designation:

## ABSTRACT

Efficient L-band amplifiers were successfully achieved using two types of new Erbium-doped fiber; Zr-EDF and HB-EDF as a gain medium. Both fibers have a significantly high Erbium ions concentration. For instance, the enhanced Zr-EDF has an erbium ion concentration of 4000 ppm while the HB-EDF has ion concentration of 12500 ppm. For enhance Zr-EDF, a significant flat gain of about 17.1 dB was achieved with gain variance of less than 1 dB within band over 40 nm wavelength region for double-pass setup at input power of -10 dBm. The noise figure for double-pass was provided higher spectrum as compared with single-pass. For new HB-EDF, an efficient flat gain of about 15 dB was achieved at gain variance of around 1 dB over wavelength area from 1560 to 1605 nm in double-pass configuration. The performance of HB-EDFA was compared with enhance Zr-EDFA performance in double-pass configuration. The Zr-EDFA has relatively higher gain as compared to that of HB-EDFA over wavelength region from 1565 to 1610 nm at input signal power of -10 dBm. However, a shorter length of 1.5 m was used for the HB-EDF amplifier which is half of the Zr-EDF length as well as the new HB-EDFA provided wider bandwidth amplification started from 1545 nm. The corresponding noise figure of the proposed HB-EDFA was lower as compared to that of Zr-EDFA. An efficient hybrid amplifier with wideband and flat gain characteristics was demonstrated using a combination of Bi-EDF and HB-EDF with total optimal length of 1.99 m in double-pass parallel configuration. This amplifier provided flat gain of 14 dB with gain fluctuation less than 1.5 dB over 75 nm wavelengths at high input power of -10 dBm. An efficient wideband EDFA operating in wideband wavelength region was also obtained using two pieces of Zr-EDFs as gain media for both stages, with total length of 3.5 m in double-pass parallel configuration. The proposed amplifier also provided a wideband and high flat gain of 17.1 dB with gain fluctuation less than 1.5 dB within wavelength region from 1525 to 1600 nm at input signal power of -10 dBm. A wideband

flat gain amplification was investigated using partial double-pass which is using both HB-EDF and Zr-EDF as the gain mediums. At input signal of -10 dBm, a flat gain of around 17.2 dB is obtained with a gain fluctuation of less than 2.3 dB within the 55 nm wavelength region from 1540 to 1595 nm. A novel dual-stage with triple-pass hybrid amplifier is investigated by comprise 2 stages of EDFA using both HB-EDF and Bi-EDF, as the gain medium. At high input power of -10 dBm, a flat gain of about 18.5 dB with gain variation less than 2 dB is observed across 45 nm bandwidth. The noise figure varied from 4.8 to 9.3 dB within the flat gain region. The triple-pass EDFA has been enhanced by utilizing distribution pumping scheme to minimize the cost of the amplifier yet having the comparable performance with the dual-pump configuration.

Keywords: Wideband optical amplifier, Erbium doped fiber amplifier, Flat gain, Hybrid active medium,

## ABSTRAK

Kecekapan L-band amplifier berjaya diperolehi dengan menggunakan dua jenis Erbium-doped fiber yang baru iaitu Zr-EDF dan HB-EDF sebagai gain medium. Kedua-dua gentian mempunyai kepekatan ion Erbium yang tinggi. Sebagai contoh, Zr-EDF yang dipertingkatkan mempunyai kepekatan ion erbium sebanyak 4000 ppm manakala HB-EDF mempunyai kepekatan ion sebanyak 12500 ppm. Bagi Zr-EDF yang telah dipertingkatkan, kira-kira 17.1 dB gandaan mendatar telah diperolehi dengan gandaan varians kurang daripada 1 dB dalam jalur melebihi 40 nm jarak kawasan gelombang bagi persiapan double-pass untuk kuasa input -10 dBm. Noise figure untuk double pass diberikan spektrum yang lebih tinggi dibandingkan dengan single pass. Untuk HB-EDF yang baru, gandaan rata yang lebih cekap kira-kira 15 dB telah dicapai pada gandaan varians 1 dB lebih dari jarak kawasan gelombang diantara 1560 hingga 1605 nm dalam konfigurasi double pass. Prestasi HB-EDFA telah dibandingkan dengan prestasi Zr-EDFA yang telah dipertingkatkan dalam konfigurasi double pass. Zr-EDFA mempunyai gandaan yang lebih tinggi berbanding dengan HB-EDFA lebih dari jarak kawasan gelombang diantara 1565 hingga 1610 nm pada kekuatan isyarat input -10 dBm. Walau bagaimanapun, ukuran yang lebih pendek sebanyak 1.5 m digunakan untuk HB-EDF amplifier iaitu separuh daripada panjang Zr-EDF serta HB-EDFA yang baru telah memberikan penguat jalur lebar yang lebih luas bermula dari 1545 nm. Noise figure HB-EDFA yang telah dicadangkan adalah lebih rendah dibandingkan dengan Zr-EDFA. Amplifier hibrid yang lebih cekap dengan ciri-ciri wideband dan gandaan rata telah ditunjukkan menggunakan kombinasi diantara Bi-EDF dan HB-EDF dengan jumlah panjang optimum 1.99 m dalam konfigurasi selari double pass. Amplifier ini menyediakan gandaan rata 14 dB dengan gandaan turun naik kurang daripada 1.5 dB bagi 75 nm jarak gelombang pada kuasa input tinggi -10 dBm. Jalur lebar EDFA yang lebih cekap beroperasi dalam jarak gelombang jalur lebar telah diperolehi dengan

menggunakan dua keping Zr-EDFs sebagai gain medium untuk kedua-dua peringkat, dengan jumlah panjang 3.5 m dalam konfigurasi selari double pass. Amplifier yang dicadangkan juga telah menyediakan jalur lebar dan gandaan rata yang tinggi iaitu 17.1 dB dengan turun naik gandaan kurang daripada 1.5 dB dalam rantau jarak gelombang dari 1525 hingga 1600 nm pada kekuatan isyarat input -10 dBm. Penguat jalur lebar gandaan rata diselidiki menggunakan separa double pass yang menggunakan kedua-dua HB-EDF dan Zr-EDF sebagai gain medium. Pada isyarat input -10 dBm, gandaan rata sekitar 17.2 dB diperoleh dengan turun naik gandaan kurang daripada 2.3 dB diantara 55 nm jarak kawasan gelombang dari 1540 hingga 1595 nm. Satu penemuan baru dual-stage dengan hybrid triple-pass amplifier diselidiki dengan merangkumi 2 peringkat EDFA menggunakan kedua HB-EDF dan Bi-EDF, sebagai gain medium. Pada kuasa input lebih tinggi pada -10 dBm, gandaan rata kira-kira 18.5 dB dengan gandaan varians kurang daripada 2 dB diperhatikan diantara 45 nm jalur lebar. Noise figure bervariasi dari 4.8 hingga 9.3 dB di dalam kawasan gandaan rata. EDFA triple-pass telah dipertingkatkan dengan menggunakan skim mengepam agihan untuk meminimumkan kos amplifier, namun mempunyai prestasi setanding dengan konfigurasi dual-pump.

## ACKNOWLEDGEMENTS

Firstly, I would like to express my sincere gratitude to my advisor Prof. Sulaiman Wadi Harun for the continuous support of my Ph.D study and related research, for his patience, motivation, and immense knowledge. His guidance helped me in all the time of research and writing of this thesis. I could not have imagined having a better advisor and mentor for my Ph.D study. I would like to thank and appreciate my Co-supervisor Prof. Dr. Harith Bin Ahmed who gave his kind permission to access to the laboratory (Photonics Research Center). Without his precious support it would not be possible to conduct this research.

I would like to thank and dedicate this thesis to my loving parents, Dr. Ali Almkhtar and Mrs. Rafah Alsalem, for their moral, financial and emotional support in my life. Furthermore, a beautiful and kind thank to my lovely sisters Dr. Jana Ali and Dr. Nabaa Ali, who supporting me spiritually throughout doing my research.

A special thanks to my research's friend Dr. Alabbas A. Alazzawi for his co-operation and helpness throughout this journey. My sincere thanks also goes to Dr. Bilal, Dr. X.S. Cheng, and Dr. Jassim K. Hamood, who shared their knowledge and scientific experience with me. I would love to thank my fellow labmates, Aminah Ahmed, Muhammad Farid, and Ahmed Haziq, for the stimulating discussions, cooperating, and for all the fun talking we have had in last two years.

## TABLE OF CONTENTS

Abstract .....	iii
Abstrak .....	v
Acknowledgements .....	vii
Table of Contents .....	viii
List of Figures .....	xii
List of Tables.....	xvi
List of Symbols and Abbreviations.....	xvii
<b>CHAPTER 1: INTRODUCTION.....</b>	<b>1</b>
1.1 An overview on optical communication.....	1
1.2 Optical Amplifier.....	4
1.3 Problem statement .....	9
1.4 The objective of the research.....	10
1.5 Research contributions.....	11
1.6 Thesis organization.....	12
<b>CHAPTER 2: LITRATURE REVIEW .....</b>	<b>15</b>
2.1 Introduction.....	15
2.2 Working principle of erbium doped fiber amplifier (EDFA).....	16
2.3 Theoretical model .....	21
2.3.1 Emission and absorption cross sections .....	22
2.3.2 Rate equations .....	22
2.3.3 Propagating equations .....	24

2.4	EDFA characteristics .....	25
2.4.1	Gain .....	25
2.4.2	Noise figure .....	27
2.4.3	Amplified spontaneous emission.....	28
2.5	EDFA configurations.....	29
2.5.1	Single-pass EDFA .....	29
2.5.2	Dual-stage EDFA .....	31
2.6	Wide-band and hybrid optical amplifier.....	32
2.7	Related previous works.....	34

**CHAPTER 3: DEVELOPMENT OF EFFICIENT AND FLAT GAIN L-BAND EDFA WITH HIGHLY DOPED ERBIUM-DOPED FIBERS.....41**

3.1	Introduction.....	41
3.2	Zirconia-Yttria-Alumium erbium co-doped fiber (Zr-EDF) .....	42
3.2.1	Fabrication and optical characterization of the Zr-EDF .....	42
3.2.2	Amplified Spontaneous Emission (ASE) and amplification characteristics at L-band region .....	46
3.2.3	Double-pass L-band Zr-EDFA .....	50
3.2.4	Effect pumping wavelength on the performance of the double-pass Zr-EDFA.....	55
3.2.5	Effect of Erbium dopant concentration on the performance of the Zr-EDFA	
58		
3.3	Hafnium bismuth erbium co-doped fiber (HB-EDF) .....	61
3.3.1	Fabrication and Characterization.....	61
3.3.2	ASE characteristics.....	64
3.3.3	Amplification performances in single-pass and double-pass set-up .....	65
3.3.4	Effect of pumping wavelength .....	71

3.3.5	Performance comparison with Zr-EDFA .....	74
3.4	Summary .....	80
<b>CHAPTER 4: WIDE-BAND AND FLAT GAIN ERBIUM DOPED FIBER AMPLIFIER USING PARALLEL CONFIGURATION .....</b>		<b>82</b>
4.1	Introduction.....	82
4.2	Development of efficient Bi-EDFA.....	83
4.3	Wide-band and flat gain optical amplifier using a hybrid gain medium .....	88
4.4	Wide-band and flat gain using enhanced Zr-EDF as gain medium.....	97
4.5	Summary .....	100
<b>CHAPTER 5: FLAT GAIN AND WIDE-BAND PARTIAL DOUBLE-PASS ERBIUM CO-DOPED FIBER AMPLIFIER WITH HYBRID GAIN MEDIUM</b>		<b>103</b>
5.1	Introduction.....	103
5.2	Partial double-pass amplifier .....	104
5.2.1	The effect of changing pump power.....	106
5.2.2	The effect of changing EDF lengths.....	109
5.2.3	Amplification characteristics of each stages and the combined stages ..	111
5.3	Triple-pass hybrid EDFA using a novel dual-stage configuration .....	116
5.3.1	The effect of changing pump power.....	117
5.3.2	The effect of changing the HB-EDF length .....	119
5.3.3	Amplification performance comparison.....	121
5.3.4	New pump power distribution scheme .....	125
5.4	Summary .....	127
<b>CHAPTER 6: CONCLUSIONS AND FUTURE WORKS .....</b>		<b>129</b>
6.1	Conclusions .....	129

6.2 Future works .....	132
References .....	134
List of Publications and Papers Presented .....	142
List of conference paper .....	143

University of Malaya

## LIST OF FIGURES

Figure 1.1: The basic fiber optic communication system. ....	1
Figure 1.2: The attenuation spectrum at three operating windows in optical fiber communication. ....	4
Figure 1.3: Optical amplifier diagram. ....	5
Figure 2.1: Basic configuration of Erbium doped fiber amplifier (EDFA). ....	16
Figure 2.2: Energy levels of Er <sup>3+</sup> with the possible pump bands (Norouzi & Briley, 2013). ....	18
Figure 2.3: Schematic representation of absorption and emission between energy level 1 and 2: (a) absorption (b) spontaneous emission (c) stimulated emission. ....	20
Figure 2.4: Atom density curve at two system (a) Thermal Equilibrium and (b) population inversion (Naji et al., 2011). ....	21
Figure 2.5: The EDFA input and output power spectral parameters. ....	28
Figure 2.6: single-stage EDFA configuration with (a) single-pass and (b) double-pass scheme. ....	30
Figure 2.7: Dual-stage EDFA configurations with (a) two-pass, and (b) Triple-pass. ....	32
Figure 3.1: Setup of the MCVD system used in the doped fiber fabrication. ....	42
Figure 3.2: (a) Cross-sectional view and (b) Dopant distribution profile of the fabricated Zr-EDF. ....	44
Figure 3.3: (a) Refractive index profile and (b) Absorption loss curve of the Zr-EDF. ....	45
Figure 3.4: Experimental setup for investigating ASE generation and single-pass amplification. ....	46
Figure 3.5: ASE spectrum for different lengths of Zr-EDF. ....	47
Figure 3.6: Gain and noise figure spectra with two different Zr-EDF length in single-pass setup at input signal powers of (a) -10 dBm and (b) -30 dBm. ....	49
Figure 3.7: Double-pass configuration. ....	50
Figure 3.8: Gain and noise figure spectra for the double-pass Zr-EDFA at two input signal powers of (a)-10 dBm and (b)-30 dBm. ....	52

Figure 3.9: Gain and noise figure spectrum of the single and double-pass Zr-EDFA configured with 3 m long Zr-EDF at input signal powers of (a) -10 dBm and (b) -30 dBm. ....	54
Figure 3.10: Comparison of ASE characteristics for the Zr-EDF at two pumping wavelengths.....	55
Figure 3.11: The gain and noise figure of the double-pass Zr-EDFA at two different pump wavelengths when the input signal is fixed at (a) -10 dBm and (b) -30 dBm.....	57
Figure 3.12: Comparison of the gain and noise figure spectra between enhanced Zr-EDFA (ER-3) and the conventional Zr-EDFA (NER-6) at input signal power of (a) -10 dBm and (b) -30 dBm. ....	60
Figure 3.13: HB-EDF characteristics: (a) Microscopic view (b) Refractive index profile, and (c) Absorption loss curve. ....	63
Figure 3.14: ASE spectrum for various lengths of HB-EDF as they were pumped at 170 mW using 1480 nm LD in single pass configuration.....	64
Figure 3.15: Gain and noise figure performances with different length of HB-EDF in single-pass setup at input signal power of (a) -10 dBm and (b) -30 dBm. ....	66
Figure 3.16: Gain and noise figure performances with different length of HB-EDF in double-pass setup at input signal power of (a) -10 dBm and (b) -30 dBm.....	68
Figure 3.17: Gain and noise figure spectrum of single and double-pass of the 1.5 m long HB-EDFA at input signal power of (a) -10 dBm and (b) -30 dBm.....	70
Figure 3.18: Comparison the characteristics of amplified spontaneous emission for HB-EDFA at two pumping wavelengths. ....	71
Figure 3.19: The HB-EDF amplifier characteristics in term of gain and noise figure for different pump wavelengths at two input signal powers.....	73
Figure 3.20: Comparison of the gain and noise figure spectra between HB-EDFA and the conventional Zr-EDFA at input signal power of (a) -10 dBm and (b) -30 dBm. ....	76
Figure 3.21: Comparison of the gain and noise figure spectra between HB-EDFA and the enhanced Zr-EDFA at input signal power of (a) -10 dBm and (b) -30 dBm.....	79
Figure 4.1: ASE spectrum for the Bi-EDFA at 170 mW pump power.....	84
Figure 4.2: Double-pass configuration for Bi-EDFA. ....	85
Figure 4.3: Single and double-pass comparison for Bi-EDFA at two input signals power of (a) -10 dBm and (b) -30 dBm. ....	87

Figure 4.4: Gain and noise figure performances of Bi-EDFA against pump power at two input signals power of -30 dBm and -10 dBm. ....	88
Figure 4.5: Dual-stage configuration for the proposed hybrid amplifier. ....	89
Figure 4.6: Gain (solid symbol) and noise figure (hollow symbol) performances of the parallel amplifier at different length of HB-EDF for L-band region at input signal power of -10 dBm. ....	91
Figure 4.7: Gain and noise figure spectrum characteristics for the proposed wide-band amplifier with parallel configuration at two different input signal powers of -30 and -10 dBm. ....	92
Figure 4.8: Gain (solid symbol) and noise figure (hollow symbol) performances of different parallel hybrid amplifier at input signal power of (a) -10 dBm and (b) -30 dBm. ....	94
Figure 4.9: Gain (solid symbol) and noise figure (hollow symbol) spectrum of single and double-pass of the 3 m long Zr-EDFA at input signal power of (a) -10 dBm and (b) -30 dBm. ....	98
Figure 4.10: Gain (solid symbol) and noise figure (hollow symbol) performances of the parallel amplifier at different length of Zr-EDF for C-band region at input signal power of -10 dBm. ....	99
Figure 5.1: The experimental setup for partial double-pass amplifier. ....	105
Figure 5.2: Gain (solid symbol) and noise figure (hollow symbol) performances at various LD pump powers for input signal power of (a) -10 dBm and (b) -30dBm. ....	108
Figure 5.3: Comparison of gain (solid symbol) and noise figure (hollow symbol) among three hybrid lengths of gain medium at input signal power of -10 dBm. ....	110
Figure 5.4: Gain and noise figure performances of the hybrid amplifier at input signal power of (a)-10 dBm (b) -30 dBm. ....	113
Figure 5.5: The gain improvement percentage of the hybrid gain amplifier as compared to that of the single-pass HB-EDFA and the double-pass Zr-EDFA. ....	115
Figure 5.6: The proposed triple-pass hybrid EDFA. ....	117
Figure 5.7: Gain and noise figure performance of the proposed triple-pass amplifier with different combinations of LD pump power at input signal power of (a) -10 dBm and (b) -30 dBm. ....	119

Figure 5.8: The comparison of the gain and noise figure of the triple-pass EDFA at different lengths of HB-EDF at two input signal powers of (a) -10 dBm and (b) -30 dBm. ....	121
Figure 5.9: The ASE spectra from HB-EDF and Bi-EDF under pump power of 170 mW. ....	123
Figure 5.10: Comparison of the gain and noise figure performances of the proposed triple-pass amplifier with single-pass Bi-EDFA and double-pass HB-EDFA at input signal powers of (a) -10 dBm and (b) -30 dBm. ....	124
Figure 5.11: The enhanced triple-pass hybrid EDFA with distribution pumping scheme. ....	125
Figure 5.12: Gain and noise figure characteristics for two different configurations at high input signal power of -10 dBm. ....	126

University of Malaya

## LIST OF TABLES

Table 2.1: Summary of the previous recent works on EDFAs .....	34
Table 3.1: Specification comparison between the newly developed and the previous (conventional) Zr-EDF .....	58
Table 3.2: Specification comparison between the previous Zr-EDF and HB-EDF .....	74
Table 3.3: Specification comparison between Enhance Zr-EDF and HB-EDF .....	77
Table 4.1: The specification of the Bi-EDF and HB-EDF .....	90
Table 4.2: Summary of the amplification performance of the hybrid amplifiers. ....	96
Table 4.3: Summary of the performance comparison for two types of parallel EDFAs. ....	101
Table 5.1: The optical characteristics of the Zr-EDF and HB-EDF .....	106
Table 5.2: Performance summary of partial double-pass and triple-pass amplifiers....	128

## LIST OF SYMBOLS AND ABBREVIATIONS

GaAs	:	Gallium Arsenide
InGaAsP	:	Indium Gallium Arsenide Phosphate
WDM	:	Wavelength Division Multiplexing
SOA	:	Semiconductor Optical Amplifier
RA	:	Raman Amplifier
EDFA	:	Erbium Doped Fiber Amplifier
EDF	:	Erbium Doped Fiber
SRS	:	Stimulated Raman Scattering
DFA	:	Doped Fiber Amplifier
La	:	Lanthanum
Yb	:	Ytterbium
ESA	:	Excited State Absorption
RI	:	Reflective Index
F-P	:	Resonant Fabry-Perot
FBG	:	Chirped Fiber Bragg Grating
L-band	:	Long-Band
C-band	:	Conventional-Band
DWDM	:	Dense Wavelength Division Multiplexing
WSC	:	Wavelength Selective Coupler
Zr-EDF	:	Zirconia-Erbium Doped Fiber
HB-EDF	:	Hafnium-Bismuth Erbium Doped Fiber
ASE	:	Amplified Spontaneous Emission
G	:	Gain
NF	:	Noise Figure

SNR	:	Signal to Noise Ratio
HOA	:	Hybrid Optical Amplifier
Si-EDF	:	Silica-Erbium Doped Fiber
EDPF	:	Erbium-Doped Phosphate glass Fiber
OFA	:	Optical Fiber Amplifier
MCVD	:	Modified Chemical Vapor Deposition
SD	:	Solution Doping
EPMA	:	Electron Probe Micro Analysis
NA	:	Numerical Aperture
NIR	:	Near Infra-red region
LD	:	Laser Diode
TLS	:	Tunable Laser Source
OSA	:	Optical Spectrum Analyzer
POA	:	Programmable Optical Attenuator
PI	:	Population Inversion
OC	:	Optical Circulator
Bi-EDF	:	Bismuth-Erbium Doped Fiber
SMF	:	Single Mode Fiber
PCE	:	Pump Conversion Efficiency
SP	:	Single-pass
DP	:	Double-pass

University of Malaya

## CHAPTER 1: INTRODUCTION

### 1.1 An overview on optical communication

Optical communication is one of the most effective means of communication for transferring information and data through transmission medium such as optical fiber. An optical fiber is a cylindrical dielectric waveguide produced from low loss glasses, generally silicon dioxide. The reflective index of the waveguide core is somewhat higher than that cladding (the outer medium), so that light pulses are guided along the fiber axis through total internal reflection (Idachaba, Ike, & Orovwode, 2014). It provides many features such as low loss of transmission, broad bandwidth, light weight, non-conductivity, signal safety compared to standard copper wire-based system. The optical communication system comprises a transmitter, that converts the electrical signal into optical signal, an optical fiber which is act as transmission medium, and the receiver. The optical signal is converted back into electrical signal at the receiver. Figure 1.1 illustrates a simplified illustration of the basic fiber optic communication system.

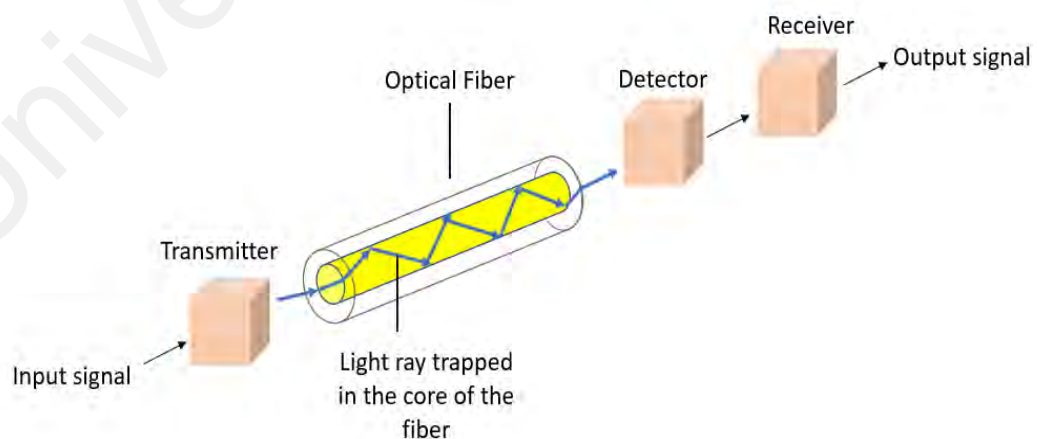


**Figure 1.1:** The basic fiber optic communication system.

The construction of optical fiber contains core, which is made of a very thin silica fiber or plastic of high reflective index with diameter varies from 10 to 100. The core is covered by a cladding made of glass or plastic. As the light propagates through the optical fiber, its parameter degrades due to attenuation, noise, dispersion, and nonlinearities. The main causes of impairments in optical fiber communication is optical attenuation, which is caused by scattering, absorption and bending losses. The optical fiber was firstly developed in 1970's by the company called Corning Glass work and it has attenuation of about 20 dB/km. Immediately after that, they have managed to reduce the optical fiber attenuation to about 0.2 dB/km, which meets the requirement for optical communication.

Fiber-optic communication system have been developed after that, which the first generation of optical communication system was introduced in 1975. The system was based on 0.8  $\mu\text{m}$  wavelength and used a light source of Gallium Arsenide (GaAs) semiconductor. The operation bit rate of the first generation was 45 Mbit/s with repeater spacing up to 10 km. During 1980s, the second generation of fiber-optic communication system was developed for commercial use, operated at 1.3  $\mu\text{m}$  and used semiconductor lasers from Indium gallium arsenide phosphate (InGaAsP) (Htein, Fan, Watekar, & Han, 2012). Within those years, the systems were restricted by dispersion since they employed multi-mode fiber as transmission medium until 1981 where the single-mode fiber was detected to enhance the performance of the systems. However, it was hard to develop practical connectors capable that operating with single mode fiber. The operation bit rate of this generation was around 1.7 Gbit/s with repeater spacing up to 50 Km. The system operation was developed at 1.55 with losses up to 0.2 dB/km. Engineers used traditional InGaAsP semiconductor lasers to overcome previous difficulties with pulse-spreading at that wavelength. These advances ultimately enabled the third-generation system to function commercially at 2.5 Gbit/s with a repeater distance of more than 100 km (Jia et al., 2014; Urquhart, 1988). Optical amplification and wavelength division multiplexing

were successfully used within the fourth-generation system to minimize the use of repeaters and improve the data capacity. The use of optical amplifiers has successfully increased the bit rate to 14 Tbit/s with single line of 160 km. The Dense Wave Division Multiplexing (DWDM) system is used by the fifth-generation fiber optic communication systems to further improve information rates. In addition, the notion of optical solitons is also being studied, which are pulses that can maintain their form by counteracting the negative influences of dispersion (Mynbaev & Systems, 2016).

In the early 1980s, the attenuation spectrum of a standard silica-based single mode fiber and the telecommunication transmission windows are shown in Figure 1.2. As illustrated from the figure, the shadow curve represented the previous optical fiber while the clear curve represents the modern optical fiber. Rayleigh scattering is the basic contribution of the absorption loss. The band around 800-900 nm was used since start of the optical fiber systems, with fiber attenuation of about 3 dB/km. this window was suitable only for short distance transmission. As technology advance, the band around 1310 nm was produced with low loss and property of zero dispersion of light wave. This window had fiber attenuation of about 0.35-0.4 dB/km. In latest years, the 3<sup>rd</sup> window with band from around 1510-1625 nm was generated. this window had the lowest attenuation about 0.2 dB/km available on current optical fiber. Furthermore, this band could operate the optical amplifiers.

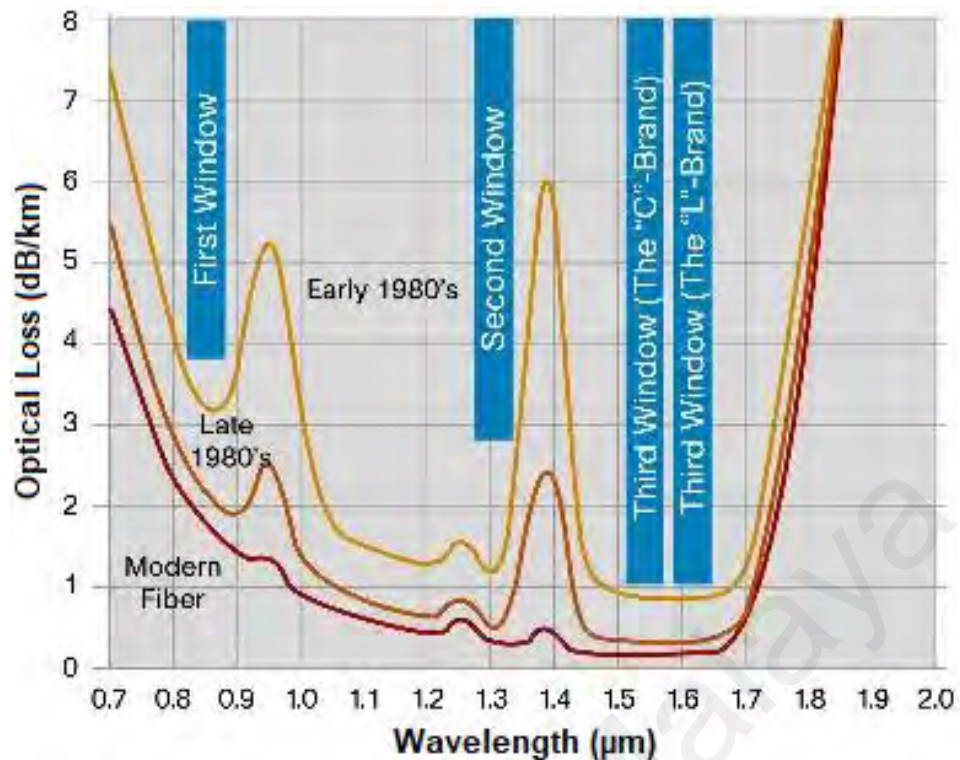


**Figure 1.2:** The attenuation spectrum at three operating windows in optical fiber communication.

## 1.2 Optical Amplifier

It is important to compensate for attenuation losses within the fiber to transmit data over long distances ( $> 100$  km). This compensation is done by using optical amplifier, which is a device that immediately amplifies an optical signal without converting it to an electrical signal as shown in Figure 1.3. Initially, electrical regenerators were used to amplify the degraded signal before optical amplifiers were reachable. The first transatlantic cable, 6700 km wide, used 95 electronic regenerators to restore signals (Mariyam et al., 2018). The electric regenerator puts a modulated optical signal through three stages, optical-to-electronic conversion, electronic signal amplification, reshaping and retiming, and finally electronic to optical conversion. However, there are many limitations in using electrical regenerators, such as high cost, limited capacity,

complexity, etc. With the introduction of optical amplifier, it overcomes the limitations of electrical regenerator. An optical amplifier amplifies the incoming light signal directly, without the need for the conversion and regeneration of the information carried.

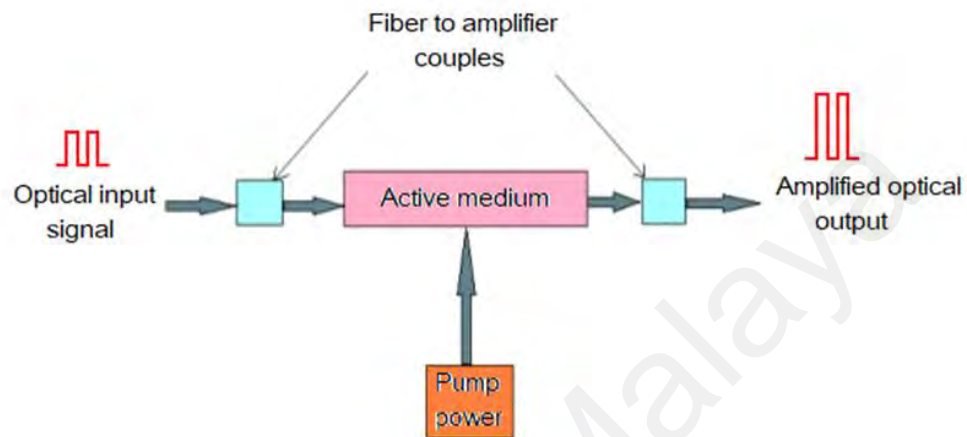


**Figure 1.3:** Optical amplifier diagram.

The reasons of using optical amplifier are due to their reliability, flexibility, wavelength division multiplexing (WDM) and low cost. Besides being used on optical links, optical amplifiers also can be used to boost signal power after multiplexing or before demultiplexing, both of which can introduce loss into the system. All optical amplifiers increase the power level of incident light through a stimulated emission process. The main optical amplifier types can be classified as follows: semiconductor optical amplifier (SOA), Raman amplifier (RA) and Erbium doped fiber amplifier (EDFA).

SOA structures are similar to laser diodes but with fiber attached to both ends. The advantages of SOA are related to small size, work with low power laser, operate for 1310 nm or 1550 nm systems and lastly, providing light through electrical means (Ghosh et al.,

2011). On the other hand, the disadvantages of the SOAs include high-coupling loss, polarization dependence, and a higher noise figure (Volet et al., 2017).

RAs differ in principle from EDFAs or conventional lasers in that they utilize stimulated Raman scattering (SRS) to create optical gain. These amplifiers have a wide gain bandwidth (up to 10 nm). RAs have several advantages such as amplification in any type of conventional fiber, broad band spectrum, non-linearity insensitive system and provide low noise figure. However, the disadvantages of these amplifiers include required high pump power, polarization of pump and crosstalk between pump and signal Rayleigh scattering (Mahran & Aly, 2016).

The benefit of rare-earth doped fiber amplifiers (DFAs) is in their achievement of low noise figure and higher gain as compared to that of SOAs. However, these amplifiers provide same advantages compared to RAs in case of their lower cost and usage of higher pump power. Furthermore, the DFAs could cover wide range of wavelengths. The range could be from visible to infrared depending on the rare-earth material used as a dopant (Bebawi et al., 2018). Lanthanum (La) (Liu et al., 2018) and Ytterbium (Yb) (Jauregui et al., 2016; Jayarajan et al., 2018) are other materials dopant in rare-earth fiber. These materials have been used in several applications such as: improve the mechanical properties of some aluminum alloys and usage of amplification within wavelength range from 975 to 1200 nm. To date, work on rare-earth-doped fiber amplifiers has concentrated on the erbium dopant (Becker & Simpson, 1999). This is attributed to its ability on operating in the wide-band range of the third transmission window at 1550 nm, which is characterized by its minimum attenuation. In this case, the amplifier is called Erbium doped fiber amplifier (EDFA). The pumping laser wavelength of EDFA should be 980 nm and 1480 nm. the 1480 nm has advantages over 980 nm where it is lowly affected by excited state absorption (ESA). the ESA is outcome from diffident transitions in case of high pumping schemes (C. Berkdemir & S. J. O. C. Özsoy, 2005; Geguo & Guofu, 1999)

as well as the pump absorption along the fiber. Several host materials such as Tellurite (Dong et al., 2011), phosphate (Goel et al., 2014), Bismuth (Firstov et al., 2016) and Zirconia (Duarte et al., 2019) have been proposed to enhance the erbium ion concentration. However, the noise figure of those materials based EDFA are still relatively high due to many reasons such as it cannot be effectively pumped by 980 nm laser diode. Among these amplifiers, silica based EDFAs seem to be the most practical amplifier. These materials also change the characteristic of the Erbium lifetime that can influence the EDFA performance. Some of these elements attain greater erbium ion concentrations that avoid damaging and clustering effects and thus decrease the length of the effective fiber to produce a more compact amplifier. Others attain a wider emission wavelength which is compatible with DWDM technology (Harun et al., 2011). Recently, Hafnia-Bismuth co-doped erbium fiber (HB-EDF) was shown to be useful for near infrared applications (Pal et al., 2010) (Kir'yanov et al., 2017). The choice of SiO<sub>2</sub>-HfO<sub>2</sub> network of core-glass stems from the fact that HfO<sub>2</sub> is a material with a high refractive index (RI) and transparent over a wide wavelength range of 0.4-6.0 μm (Wood, Nassau, Kometani, & Nash, 1990).

The tremendous growth of communication traffic in recent years has created an enormous demand for transmission bandwidth in optical communication systems based on DWDM technology. The transmission bandwidth of the DWDM system can be increased by using a wide-band amplifier to cover the full range of operating window of silica fibers. EDFA can be used to amplify the signal with high gain and low noise figure and thus it plays an important role in the DWDM system. Furthermore, it has the advantages in terms of insertion loss, low crosstalk and polarization insensitivity compared to other types of optical amplifier. Gain equalization is one of the critical factors for achieving flat gain spectrum in EDFAs. In this regard, the complexity of gain equalizer design is directly influenced by the erbium gain profile.

A wide-band optical amplifier can be realized by combining the C- and L-band amplifiers. L-band EDFA requires a significantly longer gain medium or larger amount of Erbium ions to transfer the gain from C-band to L-band through a reabsorption process in the gain medium. Therefore, many researches have been focused on this amplifier especially on controlling and flattening the gain spectrum (Durak et al., 2018; Durak & Altuncu, 2017). Owing to its simplicity, the all-optical based lasing-control technique is more common in gain clamping than electrical and hybrid methods (Qureshi et al., 2012; Yi et al., 2005). However, the penalty is to produce a clear loss at the lasing wavelength that can lead to unexpected gain-compression and flatness-aggravation (Bakar et al., 2009; Yang et al., 2014). A resonant Fabry-Perot (F-P) laser structure is realized using a pair of C-band fiber Bragg gratings (FBGs) to effectively control L-EDFA gain (Anthony et al., 2014; Yang et al., 2016). According to (Gangwar et al., 2010; Xia et al., 2003), the two stages structures are proven to efficiently ensure the high output gain, and their flatness also can be obviously improved by optimizing parameters, filters and gratings. The two stages optical amplifier usually employs a hybrid system that combines several amplifiers with different gain media. It can easily be achieved by connecting two amplifiers operating in different region in parallel (Liaw & Hsiao et al., 2008). The hybrid amplifier is advantageous due to its extensibility, where each amplifier can work independently while another amplifier can be added later into the system according to the demand for expansion (Harun et al., 2011).

### 1.3 Problem statement

The one of major drawback for long-haul transmission is high signal attenuation. Therefore, optical amplifiers are required and become one of important devices in DWDM to compensate for the transmission loss (Firstov et al., 2017). The wide-band operation in the DWDM system requires the operating band of erbium doped fiber amplifiers (EDFAs) to be extended from C-band (1530-1565 nm) to L-band (1565-1610 nm). Comparatively, L-band EDFAs received more attention since many issues such as gain flatness, gain-enhancement and gain-clamping need to be resolved so that the DWDMs system can be upgraded (Nilsson et al., 1998; Yeniay et al., 2001).

One of the critical factors in achieving flat gain spectrum in EDFAs is gain equalization. The erbium gain profile directly influences the complexity of gain equalizer design. Gain variability is the determining factor in the industry of gain equalizer, where if there is a large gain variation, the production of the gain equalizer becomes more complicated (Yusoff et al., 2012). In constructing an L-EDFA, a longer erbium-doped fiber (EDF) is required to achieve sufficient gain in the L band since it lies at the tail of the erbium amplification window where pump conversion efficiency (PCE) is low (Firat Ertaç Durak & Altuncu, 2017). All optical lasing-control technique is more common in gain clamping than in electrical and hybrid methods because of its simplicity (Qureshi, 2014; Yi et al., 2005). However, this method results in a clear loss of lasing wavelength that can lead to unexpected gain-compression and flatness-aggravation (Bhadra & Ghatak, 2016). Another effectively method to control the gain-clamped operation for a large dynamic range and wide gain spectrum is obtained by using a resonant F-P lasing cavity (Qiao, 2019; Wang & Zhang, 2018). According to the previous reports (Gangwar et al., 2010; Yucel et al., 2012), the dual-stage hybrid configurations are proven to efficiently ensure the high and flat output gain, low noise figures and wide bandwidth

amplification. The hybrid EDFAs is obtained by connecting several amplifiers with different gain bandwidths (Ellison et al., 1999; Hamida et al., 2016; Xunsi et al., 2008).

On the other hand, extensive researches have been carried out on developing new EDFAs using different glass host and co-dopant materials such as phosphate (Jianga et al., 2000), telluride (Mori, 2008) and bismuth (Cheng et al., 2011) to extend the operation bandwidth, flattening the gain spectrum, and to reduce the length of the active fiber. In this work, wide-band and flat gain amplifiers are developed based on new configuration arrangement and new active fibers based on Zr-EDF and HB-EDF. These active fibers are expected to perform better than the conventional silica based EDF, which provides all the benefits of a highly doped fiber without the drawbacks typically associated with such fibers, such as incompatibilities with conventional Single-Mode Fibers.

#### **1.4 The objective of the research**

This research work aims to develop an advanced EDFA with wide-band and flat gain spectrum characteristics, which are essential to increase the capacity of DWDM system. To guide our work, the following objectives are outlined:

- a) To propose and develop a flat gain and compact EDFA operating in Long-wavelength band (L-band) region using a highly doped Erbium-doped fiber as an active medium.
- b) To demonstrate and develop wideband EDFA with flat gain characteristics operating at broadband (C+L) wavelength regions, using short length of the erbium fibers in parallel double-pass setup.

- c) To propose and demonstrate a dual-stage amplifier based on partial double-pass using hybrid active gain medium.
- d) To implement a new scheme of triple-pass with shorter length of hybrid gain medium.
- e) To demonstrate an EDFA realizing not only the functional requirements as well as the economically viable, using pump distribution technique.

### **1.5 Research contributions**

This thesis focuses on the development of enhanced L-band as well as wide-band amplifications using a short length of highly concentrated EDF. The research methodology and achievement are summarized as follows:

- a) A compact flat gain L-band EDFA has been investigated and achieved using a short length of EDF significantly high erbium ion concentration.
- b) Single and double-pass EDFAs have been designed using an enhanced Zirconia-Yttria-Aluminium based EDF (Zr-EDF) as a gain medium to achieve a reasonably high flat gain characteristic but using only 3 m long active fiber. Single and double-pass of HB-EDF amplifiers (HB-EDFAs) have also been demonstrated to achieve a flat gain operation operating at L-band region using only 1.5 m long active fiber. Finally, the performance of HB-EDFA was compared with the Zr-EDFA in double-pass configuration.
- c) An efficient wide-band and flat gain EDFA, which operating within a wavelength region from 1535 to 1590 nm was also successfully demonstrated using hybrid amplifier with a combination of Bi-EDF and HB-EDF with total

optimal length of 1.99 m in double-pass parallel configuration. In addition, an efficient wide-band EDFA operating in C- and L- band wavelength regions from 1525 to 1600 nm was investigated and demonstrated using two sections of Zr-EDF as gain media, with total length of 3.5 m in double-pass parallel configuration.

- d) A compact flat gain hybrid EDFA was also achieved over wide-band span from 1540 to 1590 nm. This amplifier employs a 1 m long of HB-EDF and 2 m long of Zr-EDF as the gain media to enhance the amplification performance across C- and L-band wavelength region.
- e) A novel dual-stage EDFA design was also successfully developed based on triple-pass amplification by incorporating 1.5 m long HB-EDF and 0.49 m long Bi-EDF in first and second stage, respectively to improve the gain with a minimum noise figure penalty over wide-band wavelength region.
- f) The new triple-pass hybrid amplifier was also proposed and demonstrated using a single laser diode for pumping the EDF in both stages. In this amplifier, a 1480 nm optical coupler with splitting ratio of 40/60 was integrated to efficiently distribute the 1480 nm pump power to both stages. The improvised amplifier was successfully proved not only the functional requirements but also the economically viable, by reduction the complication of the design and equipment used.

## **1.6 Thesis organization**

This thesis contains six main chapters to demonstrate the development of wide-band and flat gain EDFA using hybrid active medium. Chapter 1 briefly described an

overview of optical communication systems. Moreover, the problem statement, the research objectives and brief research methodology are also presented in this chapter. Chapter 2 presents the theory of optical amplifier and literature reviews on optical transmission system relevant to the study.

Chapter 3 presents experimentally an efficient L- band amplifier EDFA with shorter length of fiber as the gain medium. The fabrication and characterization of the Zr-EDF and HB-EDF are also discussed in this chapter. The amplification performances of both EDFs are investigated at single and double-pass configurations. The effect of pumping wavelength on the amplifier performance is also investigated. Finally, the performance of the EDFAs configured with the newly developed highly concentrated active fiber is compared the conventional EDFA.

Chapter 4 proposes new wide-band and flat gain amplifier based on a double-pass approach in parallel configuration, using shorter length of active fibers. At first, a combination of 0.49 m long of Bi-EDF and 1.5 m long of HB-EDF is examined as hybrid active medium. The double-pass parallel EDFA operating in C- and L- band wavelength region is also examined in this chapter to provide higher gain and lower noise figure, using two pieces of Zr-EDFs as gain media with a total length of 3.5 m.

A novel optical amplifier is then proposed in Chapter 5 based on partial double-pass configuration with a hybrid gain medium. In order to achieve a wide-band and flat gain EDFA, a dual-stage hybrid optical amplifier was proposed with total EDF's length of only 3 meters. This amplifier combines 1 m long of HB-EDF and 2 m long of Zr-EDF as the gain mediums. The second section of this chapter is clarified the amplification performance of new triple-pass configuration to realize wide-band and flat gain with very short length fibers of 1.99 m. Eventually, the triple-pass configuration is improved by

using a new pumping distribution technique. Chapter 6 concludes all findings of the research work with suggestions and recommendations for future work.

University of Malaya

## CHAPTER 2: LITRATURE REVIEW

### 2.1 Introduction

Optical fiber communication is vital for both medium and long-distance data transmissions. In optical communication systems, the information could be rapidly transferred over long distance by using a semiconductor laser as a light source and a silica optical fiber as a transmission medium. In order to carry transmit multiple information signals at different wavelength simultaneously using the same fiber, dense wavelength division multiplexing (DWDM) transmission technique is used, in which increases the information-carrying capacity (M. J. J. o. O. C. Singh, 2018). In the DWDM transmission system, each information signal is assigned to a special wavelength from the low loss wavelength region. The channel spacing between the two channels of the DWDM scheme can be as small as 1 nm. Optical amplifier is the basic component of a DWDM transmission system.

Erbium doped fiber amplifiers (EDFAs) are typically used in a DWDM system to amplify a multiple signal simultaneously. In this regard, EDFAs should have a high gain and flat gain characteristics to improve the transmission distance over broad bandwidth (Durak & Altuncu, 2018; Kumar & Kumar, 2019). The purpose of the thesis is to develop and demonstrate new configurations for an EDFA to provide flat gain, low noise and wide-band optical amplification using a highly doped erbium fiber as a gain medium. This chapter provides a thorough review on EDFA and its recent development especially on achieving flat gain and wide-band operation.

## 2.2 Working principle of erbium doped fiber amplifier (EDFA)

Erbium doped fiber amplifier (EDFA) was firstly introduced in the 1980s and is one of the most significant milestones in the growth of fiber optic communication. The basic configuration of the EDFA consists of a section of an erbium doped fiber (EDF), a pump laser with pumping wavelength of 980 nm or 1480 nm and a wavelength selective coupler (WSC) for merging the input signal and the pump wavelength as shown in Figure 2.1.

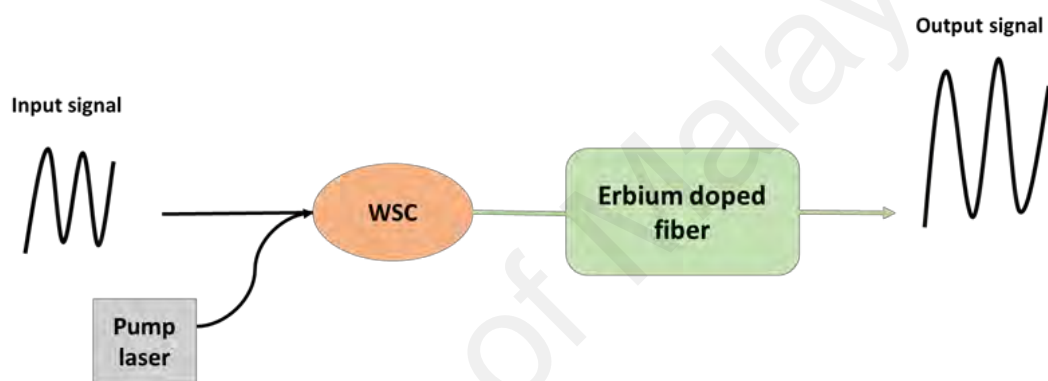


**Figure 2.1:** Basic configuration of Erbium doped fiber amplifier (EDFA).

EDF is a silica fiber which is doped with few hundred parts per million (by weight) of erbium ions. It is normally pumped by 980 nm or 1480 nm photons to emit light at 1550 nm region based on spontaneous and stimulated emission processes. With the pumping, the erbium ions are excited from the ground state to higher energy level to achieve the population inversion. The energy level refers to an amount of particular energy contained by the ion corresponding either to absorb or emitted energy. As the pump photons are launched into the EDF, amplified spontaneous emission (ASE) in 1550 nm region can be generated. When an input signal at a certain wavelength is injected into the EDF, it stimulates the excited ions to produce energy as photons with the same wavelength as the input signal. This stimulated emission process amplifies the input

signal along the EDF (Pradhan & Mishra, 2015). There are two basic parameters of EDF: absorption and emission cross sections, which are material characteristics that quantifies the absorption or stimulated emission transition. Several techniques have been used to measure absorption and emission cross sections, McCumber relation (Ladaci et al., 2018) is the most used owing to its simplicity. The relation between the emission and absorption cross-section is given as follows:

$$\sigma_e(\lambda) = \sigma_a(\lambda) \cdot e^{\frac{\varepsilon - h\nu}{KT}} \quad (2.1)$$

where  $\varepsilon$ ,  $h$ ,  $\nu$ ,  $K$ , and  $T$  are the energy required to excite one erbium ion, Plank's constant, operating frequency, Boltzmann's constant, and the absolute temperature, respectively. However, the absorption and emission cross sections are represented by  $\sigma_a$  and  $\sigma_e$ , respectively (J. Bebawi et al., 2018).

Figure 2.2 shows the possible energy levels for Erbium ions as well as possible pumping wavelength. The levels are  $^4I_{11/2}$ ,  $^4I_{13/2}$  and  $^4I_{15/2}$ , which represents excited, metastable and ground level, respectively. The wavelength scale corresponds to the wavelength of the transition from a given energy level to the ground state. The tendency to radiate a photon when jumping to lower energy levels increases with the energy gap. From the energy level diagram, it is observed that the upper level of the amplifying transition,  $^4I_{13/2}$ , is separated by a large energy gap from the next lowest level,  $^4I_{15/2}$ . The lifetime of this upper level is very long and hence mostly radiative. The value of the lifetime is around 10 ms and varies depending on the host and erbium concentration. With sufficient pump power, this long lifetime creates the population inversion between the levels  $^4I_{13/2}$  and  $^4I_{15/2}$  for stimulated emission to occur.

To excite  $Er^{3+}$  ions from the ground state to higher states  $^4I_{11/2}$  and  $^4I_{13/2}$ , two common pump wavelength bands are used, specifically 980 nm and 1480 nm for their

higher pumping efficiency (Pedersen et al., 1992). The erbium ions in the ground state will absorb the pump wavelength that enters the EDF. The 980 nm pump excites the ions from ground state  $^4I_{15/2}$  to the higher level  $^4I_{11/2}$  excited state, the ions stay at the excited state for about 1  $\mu$ s and then decay to the metastable state through a nonradiative transition. The lifetime of the metastable state is approximately 10 ms.

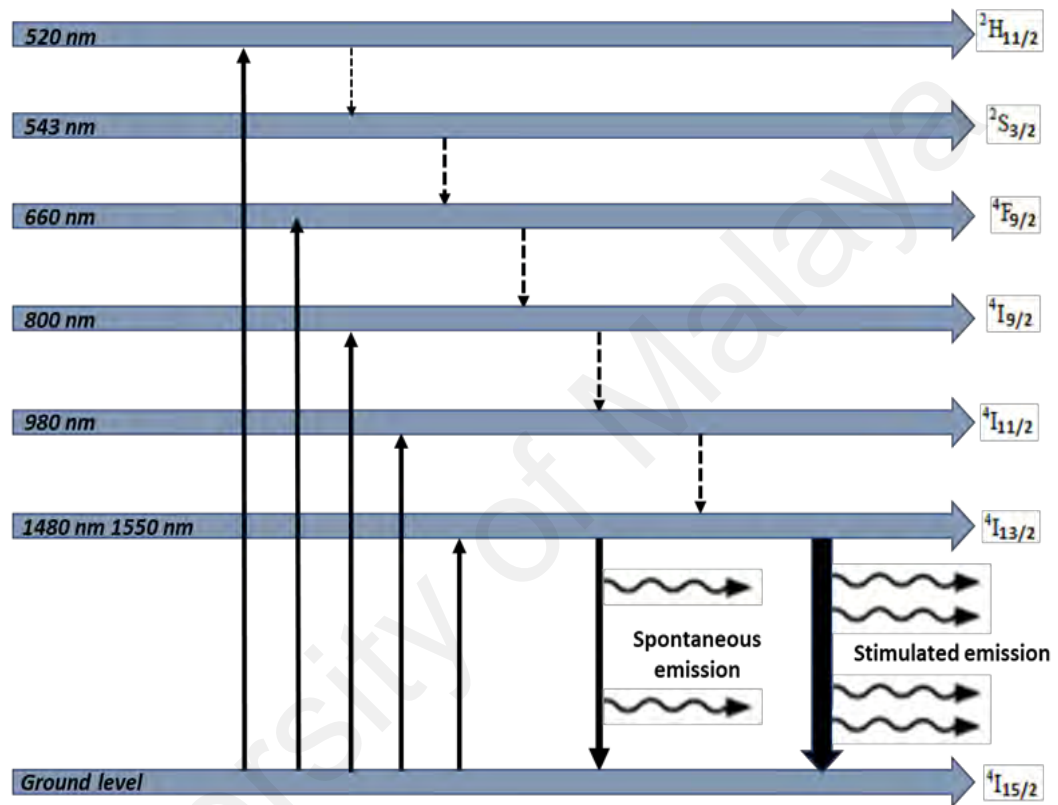


**Figure 2.2:** Energy levels of Er<sup>3+</sup> with the possible pump bands (Norouzi & Briley, 2013).

Non-equilibrium distribution of atoms can be created in EDF by providing a constant pump power. This causes the population of the higher energy level is greater than the lower energy level. This condition is known as population inversion, and it could be achieved between metastable state  $^4I_{13/2}$  and ground state  $^4I_{15/2}$ . From the metastable

state  ${}^4I_{13/2}$ , the ions will decay to the ground state by emitting photons with frequency corresponds to the energy difference between  ${}^4I_{13/2}$  and  ${}^4I_{15/2}$ , the relationship is given by:

$$E_2 - E_1 = hf \quad (2.2)$$

where  $E_1$  and  $E_2$  are the energy levels in  ${}^4I_{15/2}$  and  ${}^4I_{13/2}$ , respectively,  $h = 6.626 \times 10^{-34}$  J.s is the Planck's constant and  $f$  is photon frequency. The emitted photons have wavelength characteristics around the 1550 nm region.

Figure 2.3 shows the absorption and emission processes in an active fiber. The process of pumping is also referred to light absorption as illustrated in Figure 2.3(a). The ions absorb the pump light to excite to higher energy level  $E_2$ . When the ions from high energy level goes down to the lower energy level, they emit light in two ways; spontaneous and stimulated emission as illustrated in Figures 2.3(b) and (c), respectively. Spontaneous light emission occurs when ions return to lower energy level randomly. This emission would become the noise as it is further amplified in the gain medium. This noise is referred to as amplified spontaneous emission (ASE). Stimulated emission occurs when photons having energy equal to the energy difference between high level energy ( $E_2$ ) and lower level energy ( $E_1$ ) are launched into the gain medium. This process multiplies the number of photons to amplify the incoming signal.

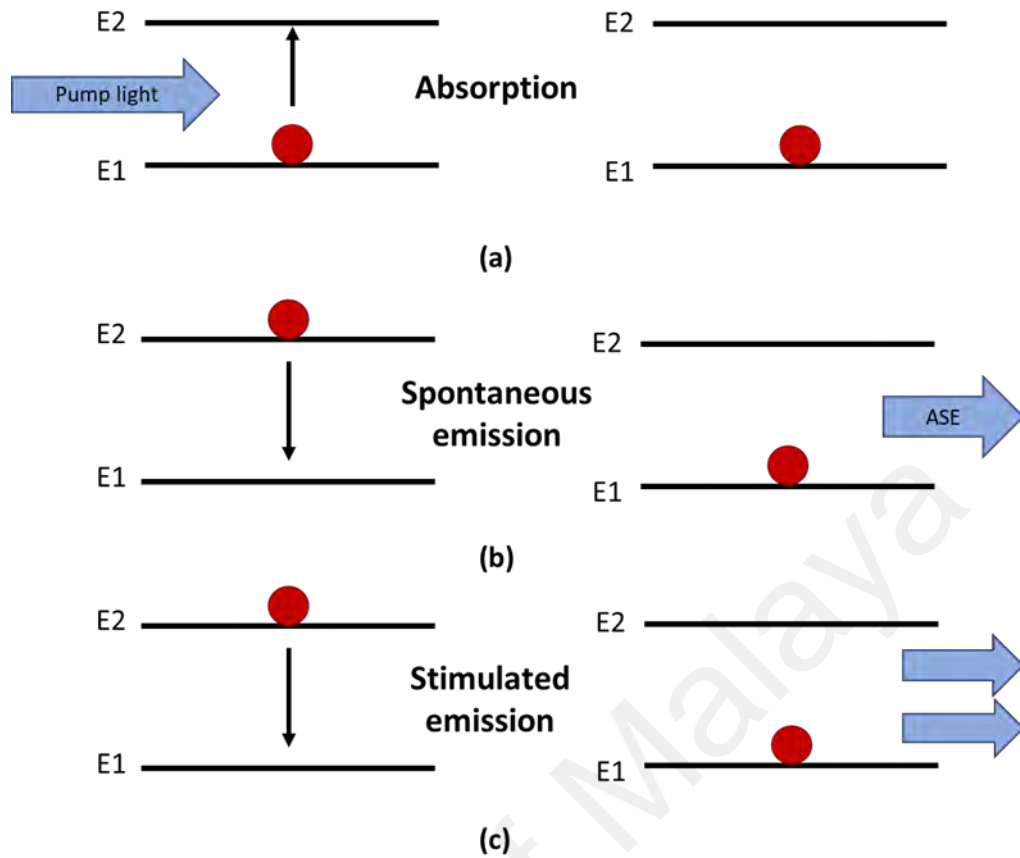


**Figure 2.3:** Schematic representation of absorption and emission between energy level 1 and 2: (a) absorption (b) spontaneous emission (c) stimulated emission.

In a normal atom system, the stimulated absorption become greater than stimulated emission. This case caused when the atom density ( $N_1$ ) at E1 is much higher than the atom density ( $N_2$ ) at E2. This situation is recognized as thermal equilibrium, where the atoms enforce with the Boltzmann distribution as shown in the following equation:

$$\frac{N_2}{N_1} = e^{-\left[\frac{(E_2-E_1)}{KT}\right]} \quad (2.3)$$

Here, E1 and E2 represents the lower and higher energy level, respectively. Boltzmann constant and absolute temperature are represented by K and T, respectively.

Optical amplification can be achieved by increasing the number of atoms in N2 so that its population is much higher than that in N1. In this case, the stimulated emission will be much higher than the stimulated absorption and cause the population inversion (Naji et al., 2011). The population inversion could be produced by pumping the EDF so excite the ions to higher energy level. The density curve of the atom in case of thermal equilibrium and population inversion are illustrated in Figure 2.4.

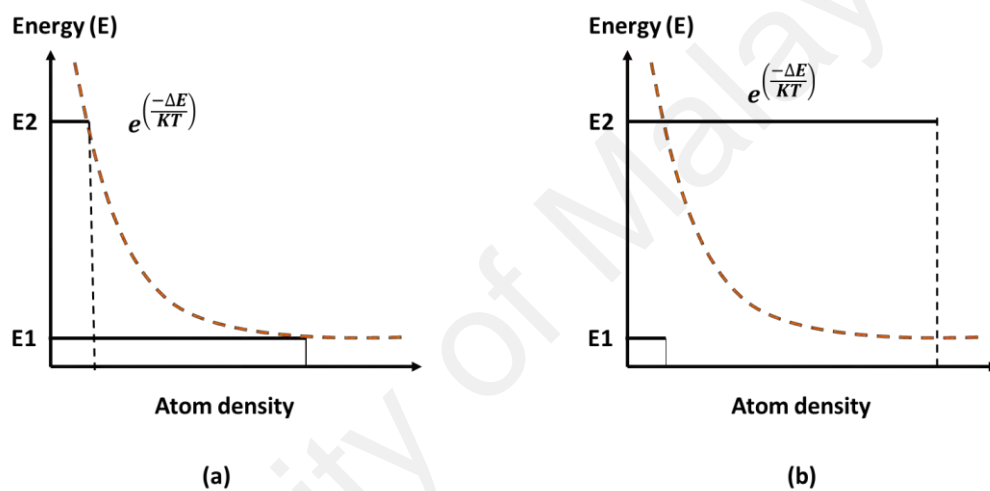


**Figure 2.4:** Atom density curve at two system (a) Thermal Equilibrium and (b) population inversion (Naji et al., 2011).

### 2.3 Theoretical model

The input signal is multiplexed together with the pump signal into the erbium doped fiber via wavelength selective coupler (WSC) to achieve the amplified signal. The amplification occurs due to stimulated emission, on the other hand, the spontaneous emission is reduced the efficiency of the amplified signal through amplified spontaneous emission. the erbium doped silica fiber provides a three-energy level which is used for pumping wavelength of 980 nm and a two energy level for 1480 nm pumping (Berkdemir

et al., 2005; Desurvire et al., 1992) as shown in Figure 2.2. In this section, two basic sets of equations are discussed to study erbium doped fiber amplifier, which are rely on absorption and emission cross sections of the erbium dopant. these sets are the propagating equation and the rate equations.

### 2.3.1 Emission and absorption cross sections

The optical transitions have two basic parameters which are absorption and emission cross sections. these parameters are essential to get exact solution for both propagating and rate equations. In order to calculate the absorption and emission cross sections, the McCumber relation is used due to its simplicity (Martin Becker et al., 1999; et al., 2006) as shown in equation below:

$$\sigma_e(\lambda) = \sigma_a(\lambda) e^{\frac{\epsilon - h\nu}{k_B T}} \quad (2.4)$$

Where  $\sigma_e$  and  $\sigma_a$  represented emission and absorption cross sections.  $h, k_B, T, \nu$ , and  $\epsilon$  are represent Plank constant, Boltzmann' constant, absolute temperature, operating frequency and energy required to excite the erbium to upper level, respectively.

### 2.3.2 Rate equations

In this subsection, the three level model is consider as shown in figure 2.2. the ions population density in the ground state level (N1), metastable state level (N2) and pumping state level (N3). The system of differential rate equations is driven as follows (Novak et al., 2002):

$$\frac{dN1}{dt} = -R_{13}N1 + R_{13}N3 - W_{12}N1 + W_{21}N2 + A_{21}N2 \quad (2.5)$$

$$\frac{dN2}{dt} = W_{12}N1 - W_{12}N2 - A_{21}N2 + A_{32}N3 \quad (2.6)$$

$$\frac{dN3}{dt} = R_{13}N1 - R_{31}N3 - A_{32}N3 \quad (2.7)$$

By assuming the condition  $(\frac{dN1}{dt}, \frac{dN2}{dt}, \frac{dN3}{dt})$  equal zero then:

$$N2 = \frac{R_{13} + W_{12}}{\frac{1}{\tau} + R_{13} + R_{13} + W_{12} + W_{21}} N \quad (2.8)$$

N represent the total  $N1 = N - N2$  and  $N3$  is neglected due to lifetime rate which is about 1  $\mu$ s. The emission and absorption cross sections rate represented by  $R_{13}, R_{13}, W_{12}, W_{21}$ . (Lin & Chi, 1992)

$$W_{12} = \frac{\sigma_s^e \Gamma_s (P_s + P_{ASE}^+ + P_{ASE}^-)}{h\nu_s A_{eff}} \quad (2.9)$$

$$W_{21} = \frac{\sigma_s^a \Gamma_s (P_s + P_{ASE}^+ + P_{ASE}^-)}{h\nu_s A_{eff}} \quad (2.10)$$

$$R_{13} = \frac{\sigma_p^a \Gamma_s P_p}{h\nu_p A_{eff}} \quad (2.11)$$

$$R_{31} = \frac{\sigma_p^e \Gamma_s P_p}{h\nu_p A_{eff}} \quad (2.12)$$

The following illustrate the acronyms of the equations above:

$\sigma_s^a, \sigma_p^a$ : Absorption cross section at signal and pump

$\sigma_s^e, \sigma_p^e$ : Emission cross section at signal and pump

$A_{eff}$ : Fiber effective area

$P_p$  and  $P_s$  : signal power transmitted through the fiber and the pump power driven into the fiber.

$\Gamma_s$  : Signal wavelength

$P_{ASE}^+$  and  $P_{ASE}^-$  : Forward and backward ASE

In multichannel case when several signal with different wavelengths are multiplexed together with pump signal into the gain medium, the equation will be as follow:

$$N_2 = \frac{\frac{\sigma_p^a \Gamma_p}{h\nu_p A_{eff}} P_p + \sum_{i=1}^{s_i} \frac{\sigma_{si}^a \Gamma_{si}}{h\nu_{si} A_{eff}} (P_{si} + P_{ASE}^+ + P_{ASE}^-)}{\frac{1}{\tau} + \frac{(\sigma_p^a + \sigma_p^e) \Gamma_p}{h\nu_p A_{eff}} P_p + \sum_{i=1}^{s_i} \frac{(\sigma_{si}^a + \sigma_{si}^e) \Gamma_{si}}{h\nu_{si} A_{eff}} (P_{si} + P_{ASE}^+ + P_{ASE}^-)} \quad (2.13)$$

### 2.3.3 Propagating equations

In order to perform propagation of each signal through the fiber, the propagating equations are discussed in the sub-section. the equations are clarified as follow based on (Giles & Desurvire, 1991) model:

$$\frac{dP_p}{dz} = P_p \Gamma_p (\beta \sigma_p^e N_2 - \sigma_p^a N_1) - \alpha_p P_p \quad (2.14)$$

$$\frac{dP_s}{dz} = P_s \Gamma_s (\sigma_s^e N_2 - \sigma_s^a N_1) - \alpha_s P_s \quad (2.15)$$

$$\frac{dP_{ASE}^\pm}{dz} = \pm P_{ASE}^\pm \Gamma_s (\sigma_s^e N_2 - \sigma_s^a N_1) \pm 2\sigma_s^e N_2 \Gamma_s P_{ASE}^\pm \Delta\nu \mp \alpha_s P_{ASE}^\pm \quad (2.16)$$

Here  $z$ ,  $\Delta\nu$ ,  $\alpha_s$ , and  $\alpha_p$  are represent the direction of propagating, the bandwidth, the loss for signal and the loss for pump. The Boltzmann factor here is singed by  $\beta$

(Bedawi et al., 2018) that can be achieved by following equation and E2 defined the difference in energy:

$$\beta = e^{\left(-\frac{\Delta E_2}{K_B T}\right)} \quad (2.17)$$

## 2.4 EDFA characteristics

In this section, the common characteristics of EDFA are described. The amplification is achieved due to the stimulated emission process in Erbium-doped fiber (EDF). This process is realized by pumping the EDF with 980 nm or 1480 nm laser diode to create a population inversion condition in the gain medium.

### 2.4.1 Gain

The function of an EDFA is to provide gain by multiplying the number of photons through a process of stimulated emission. Signal gain is an essential parameter that measures the performance of EDFA. The ratio of the output signal power,  $P_{out}$  to the input signal power,  $P_{in}$ , is known as Gain (G). It is normally expressed in dB as shown in the following equation:

$$G = 10 \log \left( \frac{P_{out}}{P_{in}} \right) \quad (2.4)$$

Essentially, the gain of the EDFA is limited by secondary physical effects which include self-saturation by amplified spontaneous emission (ASE), pump excited state absorption (ESA), concentration quenching and inhomogeneous broadening (Suzuki et al., 2016). The input and output power levels measured are usually the sum of the signal power and a small amount of spontaneous emission power. It becomes an important factor

when high spontaneous emission levels are present. The gain is defined as Equation (2.5) when  $P_{ASE}$  represent the ASE noise power.

$$G = 10 \log \left( \frac{P_{out} - P_{ASE}}{P_{in}} \right) \quad (2.5)$$

The principle of energy conservation is one of physical limitation that effect on the signal gain. It explains that the maximum output signal energy could not exceed the summation of input and pump signals energies (Abu-Aisheh & Moslehpour, 2010). Equation (2.6) shows the  $P_{out}$  and the gain can be derived and expressed in term of gain as illustrated in the Equation (2.7);

$$P_{out} \leq P_{in} + \frac{\lambda_p}{\lambda_{in}} P_p \quad (2.6)$$

$$G \leq 1 + \frac{\lambda_p}{\lambda_{in}} \frac{P_p}{P_{in}} \quad (2.7)$$

Here,  $P_p$  is pump power,  $\lambda_p$  is pump wavelength and  $\lambda_{in}$  is input signal wavelength. The gain is determined by saturation effect while the pump photon absorption is determined by the erbium ion concentration and the fiber length (Emmanuel & Zervas, 1994). The pump power is proportional with the amplifier's gain. However, the gain reduces and saturate at certain level of pump power due to saturation effect (Kaler & Kaler, 2011). This situation happened owing to the limited number of erbium ions in the gain medium and thus limits the population inversion. The gain also reduces at higher input signal power. This is attributed to the stimulated emission rate, which reduces at high input signal power (Cokrak & Altuncu, 2004).

### 2.4.2 Noise figure

The second parameter of EDFA is noise figure (NF) where it serves as a measure of the quality of a signal. Noise figure is a measure of the signal-to-noise power ratio (SNR) degradation encountered by the signal after passing through the amplifier. The definition of noise figure is the ratio of the signal-to-noise ratio at the input ( $SNR_{in}$ ) of the amplifier to that at the output ( $SNR_{out}$ ) of the amplifier.

$$NF = \frac{SNR_{out}}{SNR_{in}} \quad (2.5)$$

For further derivation of the noise figure, the shot noise of an ideal photo detector is used to determine the  $SNR_{in}$  at the input of the amplifier while, the noise figure and signal spontaneous noise are used to calculate the  $SNR_{out}$  at output of amplifier. The equations below illustrate the derivation of noise figure:

$$NF = 2n_{sp} \frac{(G - 1)}{G} + \frac{1}{G} \quad (2.6)$$

While  $G \gg 1$ , the noise figure can be simplified as:

$$NF = 2n_{sp} \quad (2.7)$$

Here  $2n_{sp}$  represent the spontaneous emission factor which has value of one or greater. Figure 2.5 illustrates the EDFA input and output power spectral showing the signal, spontaneous emission and amplifier gain. The standard level of noise figure should

be more than 3 dB for EDFA. The noise figure can also be expressed based on ASE power where  $h$  is Planck constant,  $f$  is the frequency of signal and  $\Delta\nu$  is bandwidth.

$$NF = \frac{P_{ASE}}{hf \Delta\nu G} + \frac{1}{G} \quad (2.8)$$

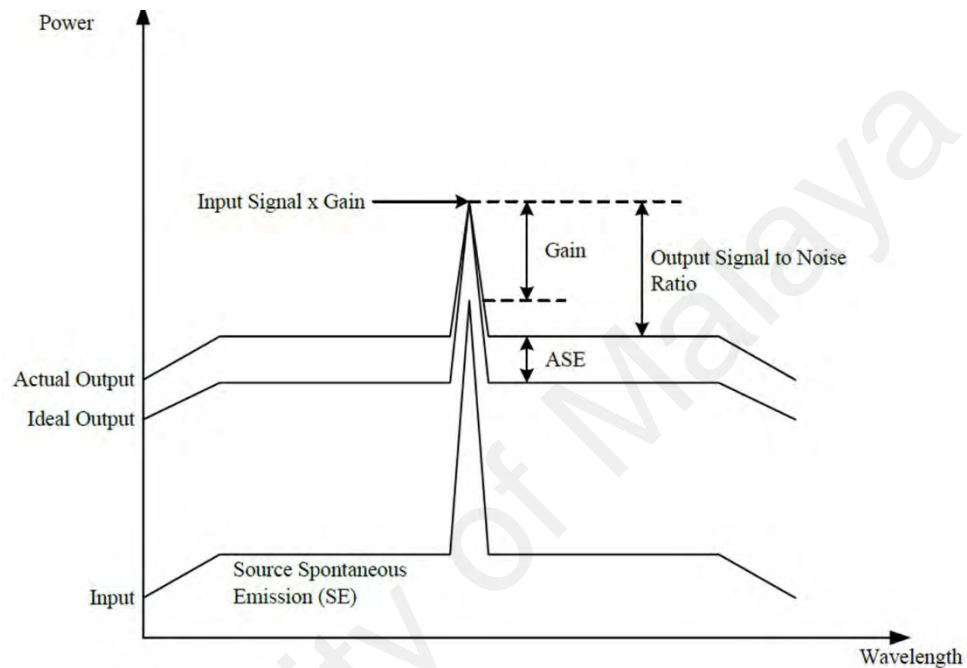


**Figure 2.5:** The EDFA input and output power spectral parameters.

### 2.4.3 Amplified spontaneous emission

Amplified spontaneous emission (ASE) is an important factor in determining the EDFA performance. When the EDF is pumped by either 980 nm or 1480 nm laser diode, population inversion is achieved, and ASE will be produced. As described previously, the ions at the excited state can spontaneously return to the ground state and generate incoherent radiation. These spontaneously emitted photons can be amplified as they travel down the fiber and stimulate the emission of more photons from the excited ions, photons that belong to the same mode of the electromagnetic field as the original spontaneous

photons (Liu, Xiang, Zhang, & Li, 2015). The number of excited ions for stimulated emission with the signal photons is reduced by the ASE process. As a result, the amplifier gain is also reduced. By taking ASE into consideration, the absolute amplifier gain is given by:

$$G = \frac{P_{out} - P_{ASE}}{P_{in}} \quad (2.8)$$

where  $P_{ASE}$  is the ASE output power.

## 2.5 EDFA configurations

The EDFA has several types of configurations according to its stages and passes, which are dependent on the kind of application. In this section, various schemes for implementing single-stage and dual-stage amplifiers are discussed.

### 2.5.1 Single-pass EDFA

Figure 2.7 shows two types of single-stage amplifier, which deploys a single piece of EDF as an active gain medium. The laser diode pump can be connected either in forward or backward pumping direction. The single-stage EDFA possibly be single or double-pass propagation as illustrated in Figure 2.6 (a) and (b), respectively. The difference between single and double-pass scheme is that the latter scheme uses a kind of mirror to retro-back the amplified signal into the active gain medium. An optical circulator or a chirped Fiber Bragg Grating (FBG) can also be used to replace the mirror. Hamida et al., (2012) has previously compared the performance of single and double-pass EDFA, which was configured based on single-stage configuration. They employed EDF

length of 1.5 m and 9 m for C-band and L-band operation, respectively. The results show that the average flat gain of approximately 25 and 30 dB for experimental and simulation results, respectively, are obtained by double-pass EDFA at input signal power of -30 dBm. The corresponding noise figure is maintained at 5 dB with noise figure variation  $\pm 0.5$  dB.

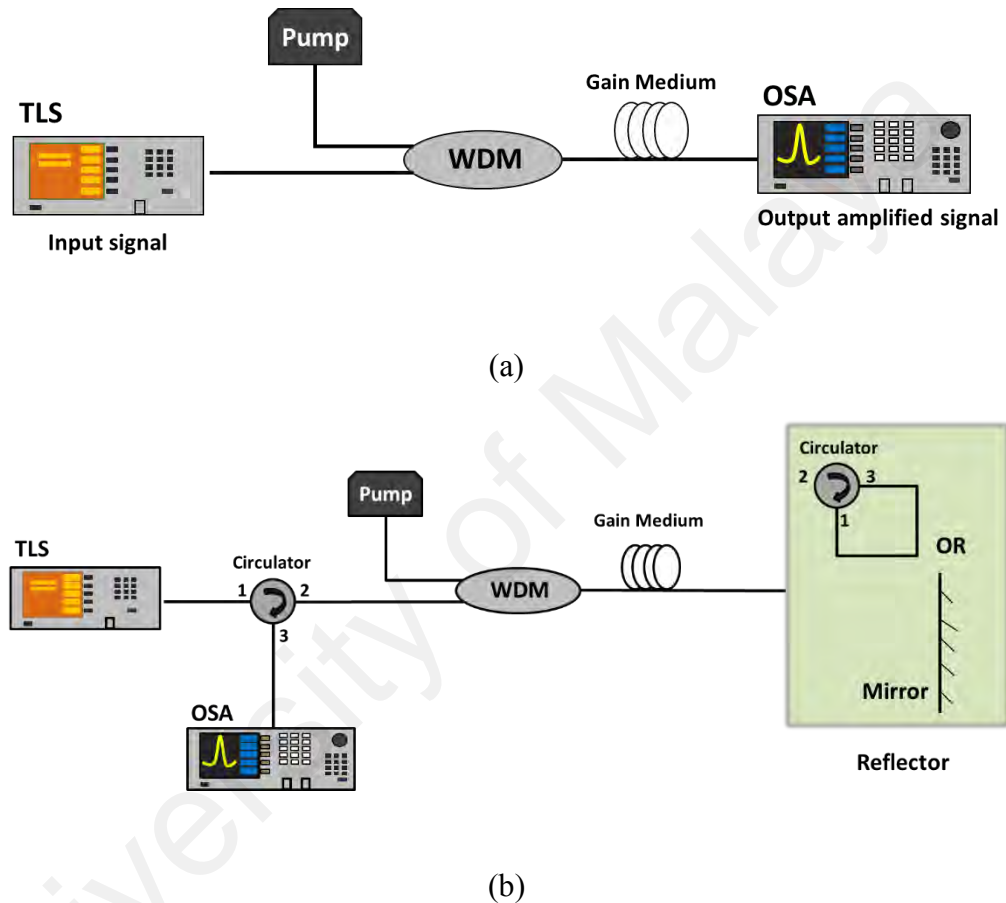


**Figure 2.6:** single-stage EDFA configuration with (a) single-pass and (b) double-pass scheme.

In another work, Saries et. al, (2017) investigated and compared the performance of double-pass EDFA with single and dual-pump configurations using stimulatory demonstrate a comparison of gain improvement OptiSystem simulation software. It was found that the proposed dual-pump amplifier provides a better gain performance

especially at lower input signal power compared to that of single-pump system. Abass et al. (2014) compared and investigated the performance of single-stage EDFA with single and double-pass arrangements, under different input and pump signals powers. The simulation results show that the gain was improved in double-pass EDFA, using a broadband optical mirror. The gain improvement of 37.13% was obtained at input signal power of -40 dBm. In addition, a 25mW pump power in double-pass configuration can provide the same gain level in a single-pass configuration at a pump power of 100 mW and an input signal power of -20 dBm at 1530nm.

### **2.5.2 Dual-stage EDFA**

Dual-stage EDFA can be configured to provide a two-pass or triple-pass amplification as shown in Figure 2.7 (a) and (b), respectively. At low input single power of -30 dBm, dual-stage two-pass EDFA could achieve gain up to 32.64 dB and noise figure of less than 5 dB (Allah et al., 2011). On the other hand, a triple-pass EDFA can achieve gain as high as 37 dB with a noise figure of 6.5 dB at input signal power of around -40 dBm (Khairil et al., 2006). Naji, et al. (2010) proposed and investigated two configurations of EDFA with dual-stage triple-pass. The first configuration consists of single and two-pass amplifiers at the first and second stages, respectively (similar to Figure 2.8 (b)). In another configuration, the second stage is single-pass amplifier and the first stage is two-pass EDFA. In the experiment, a 1480 nm laser diode with pump power of 100 mW was used for each stage of both configurations. The results show the gain of the second configuration is higher than the gain of first configuration. However, the noise figure spectra are almost same for both configurations.

In another work, Cheng et al., (2011) investigated dual-stage EDFA using two pieces of Bi-EDF with a total length of 67 cm as a gain medium in the parallel

configuration. Gain improvement of 10.8 dB was obtained by the proposed EDFA at input signal wavelength of 1560 nm. For input signal of -30 dBm, the average gains of the EDFA are obtained at approximately 18 dB within the wavelength region from 1530 to 1605 nm. However, the noise figures are maintained below 10 dB at wavelength region from 1535 nm to 1620 nm.

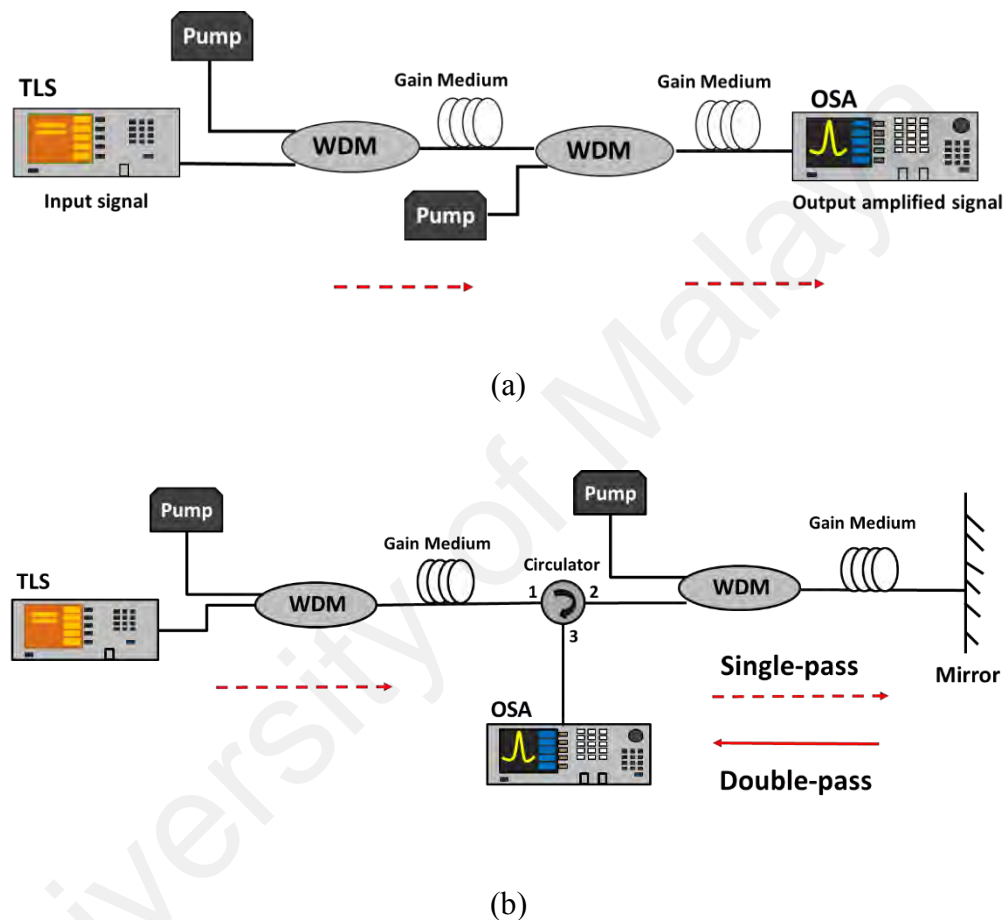


**Figure 2.7:** Dual-stage EDFA configurations with (a) two-pass, and (b) Triple-pass.

## 2.6 Wide-band and hybrid optical amplifier

In hybrid amplifier technology, different optical amplifiers operating at different gain spectra are coupled together in different combinations in order to achieve desirous gain bandwidth as per the requirement of the transmission system. Different optical amplifiers can either be connected in series combination or in parallel combination and

this configuration is known as hybrid amplifiers. In the parallel combination of hybrid optical amplifiers; first, the DWDM information signal is divided into separate wavelength groups using a de-multiplexer. Then each of the wavelength group is amplified by different amplifiers having gain in the respective wavelengths band and then these wavelength groups are again multiplexed with the application of an optical coupler. The implementation of the parallel configuration of hybrid optical amplifiers is very simple and applicable to all optical amplifiers. The main limitation of the parallel configuration of hybrid optical amplifiers is the presence of unutilized wavelength which exists in between gain bands of individual amplifiers due to the presence of guard band in the optical coupler. Also, the noise figure of the system degrades due to the losses introduced in the system by optical couplers used in front of amplifiers. In series configuration of hybrid optical amplifiers, optical couplers are not required, and gain bandwidth is relatively wide.

Huri et al., (2011) proposed an efficient flat gain C-band optical amplifier using hybrid configuration, which is combined Zr-EDFA and semiconductor optical amplifier (SOA). This amplifier utilizes a two-stage structure with a midway isolator to improve flat gain characteristic and reduce noise figure. At input signal power of  $-30$  dBm, a flat gain of 28 dB is obtained from wavelength region of 1530 to 1560 nm with gain variation of less than 4 dB. The noise figure is maintained below 11 dB at the flat gain region. This amplifier has the potential to be used in the high channel count dense wavelength division multiplexing system due to its simplicity and compact design.

Hybrid optical amplifiers (HOA) are the most suitable and widely accepted technology which can meet the requirements of the high capacity of DWDM systems (Singh & Kaler, 2012). The HOA are designed so as to maximize the link distance with acceptable performance levels, to enhance the capacity of the communication link in terms of channel bandwidth and a number of channels, and to minimize the signal

degradation due to nonlinear effects present in the optical fiber (Singh et al., 2013; Singh & Kaler, 2015). The optical amplifiers must have a large gain bandwidth in order to ensure proper transmission of a number of information signals from a large number of users. The gain of the amplifier is dependent on the operating wavelength and on the width of the energy bands. Therefore, HOA can be considered as the best alternative as they have large gain bandwidth with a flat gain response with deploying any gain flattening technique. Amplifier saturation is another reason leading to large gain bandwidths.

## 2.7 Related previous works

In this section, various related previous works on EDFA are discussed. Table 2.1 shows the summary of the work., which focuses on highlighting the findings of the previous researches and their drawbacks. The parameters of interests are gain, noise figure, configurations, amplification wavelength, the flat gain characteristic, and the length of the active fibers.

**Table 2.1:** Summary of the previous recent works on EDFAs

Title	Authors	Findings	Drawbacks
Experimental and theoretical studies on a double-pass C-band bismuth-based erbium-doped fiber amplifier.	Harun et al., (2010)	Experimentally and theoretically proposed the performance of Bi-EDFA utilizing 1480 nm pumping with double-pass scheme. At input signal power of 0 dBm,	The achievement of noise figure is higher as compared to the attainable gain, which is about 12 dB within that region.

**Table 2.1**, continued

<b>Title</b>	<b>Authors</b>	<b>Findings</b>	<b>Drawbacks</b>
		<p>a gain of 14.5 dB is obtained experimentally with gain variation of less than 1 dB within the wavelength region from 1530 to 1565 nm</p>	
<p>67 cm long bismuth-based erbium doped fiber amplifier with wideband operation.</p>	<p>Cheng et al. (2011)</p>	<p>Demonstrate a wide-band Bi-EDFA using two pieces of Bi-EDF with a total length of 67 cm as gain media in a double pass parallel configuration. The proposed Bi-EDFA achieved a Wide-band gain of around 18 dB within the wavelength region from 1530 to 1565 nm.</p>	<p>This amplifier could not achieve flat gain. Furthermore, the noise figure of about 10 dB is achieved which is too high as compared with attainable gain. EDFs have a problem in splicing with standard SMFs by utilizing a standard splicing machine due to the variance in melting temperature.</p>
<p>Optical amplifier with</p>	<p>Hamida et al., (2012)</p>	<p>A flat-gain and wide-band EDFA using Bi-EDF and Si-</p>	<p>A high noise figures of about 12 dB were</p>

**Table 2.1**, continued

Title	Authors	Findings	Drawbacks
Flat-gain and wideband operation utilizing high concentrated erbium-doped fibers.		EDF with two FBG in serial configuration for double-pass operation. It observed that flat gain spectrum is achieved within a wavelength region from 1535 nm to 1605 nm with a gain variation of less than 2 dB at input signal of 0 dBm.	observed as compared to the achieved gain. Long active fiber length of about 9.49 m was used. Furthermore, Bi-EDFs have a problem in splicing with standard SMFs by utilizing a standard splicing machine due to the variance in melting temperatures.
Comparative Study on Single and Double-Pass Configurations for Serial Dual-Stage High Concentration EDFA.	Latiff et al. (2013)	A wide-band optical amplifier using two pieces of silica erbium doped fibers (Si-EDFs) was proposed. Two series stages were used in conjunction with single and double -pass configurations.	The total length of the Si-EDFs used were 10.5 m which are long. Besides, at low input signal power, a high noise figure was observed

**Table 2.1**, continued

Title	Authors	Findings	Drawbacks
		<p>The better performance was observed with series double-pass amplifier. At input signal power of -30 dBm, a flat gain of 22 dB was realized with a gain ripple of less than 3 dB.</p>	<p>as compared to the achieved gain. The average gain was about 11.5 dB while the noise figure fluctuated from 8 dB to 12 dB. The series single-pass EDFA achieved a flat gain only in the L-band region.</p>
<p>An optical amplifier having 5 cm long silica clad erbium doped phosphate glass fiber fabricated by “core-suction” technique.</p>	<p>Goel et al. (2014)</p>	<p>An optical amplifier was introduced using only 5 cm of the new fabricated erbium - doped phosphate glass fiber (EDPF). A double pass configuration was used with backward pumping technique. A wide gain spectrum was observed in this amplifier.</p>	<p>The gain was very low. The maximum gain of 5 dB was observed at 1535 nm wavelength. Further investigations aimed at improving the gain are required.</p>

**Table 2.1**, continued

Title	Authors	Findings	Drawbacks
Enhanced erbium-Zirconia-Yttria-Aluminum co-doped fiber amplifier.	Paul et al. (2015)	An efficient optical amplifier is demonstrated using 1m of enhanced Zr-EDF as the gain medium. Zr-EDFA produces a flat gain of 38 dB within a wavelength region between 1530 and 1565 nm with a gain variation of less than 3 dB when the input signal power and 980 nm pump power is fixed at -30 dBm and 130 mW, respectively.	This amplifier could not achieve a flat gain for L-band region. Besides, at high input signal power of -10 dBm, the gain ripple and noise figure were high, within the C-band wavelength span.
Flat-gain wide-band erbium doped fiber amplifier with hybrid gain medium.	Hamida et al. (2016)	A combination of Zr-EDF with Si-EDF were used as a hybrid active fiber to achieve a wide-band EDFA. At high input signal power, a flat gain of 15 dB was realized with a gain ripple of less than 1 dB. Noise figure fluctuated from 6.2 dB to 10.8 dB.	The total length of the EDFs used were 11 m which is very long. Besides, the series amplifier could not achieve a flat gain over the wide-band operation region.
Performance comparison of enhanced	Markom et al., (2017)	A flat-gain single and double pass optical amplifier was	This amplifier used 1 m long of Zr-EDF

**Table 2.1**, continued

<b>Title</b>	<b>Authors</b>	<b>Findings</b>	<b>Drawbacks</b>
Erbium-Zirconia-Yttria-Aluminum co-doped conventional erbium-doped fiber amplifiers.		proposed using a Zr-EDF as the gain medium. The performance of the proposed amplifier was compared with the conventional Si-EDFA. A better gain and noise figure characteristics were observed with the Zr-EDFA.	to achieve a flat gain only at C-band region. This length is still long for C-band region as compared to that of previous active fiber like Bi-EDF.
Flat-gain and Wideband EDFA by using Dual Stage Amplifier Technique.	Hamza et al., (2018)	A wide-band and flat gain amplification of two stages EDFA was investigated under different EDF lengths and pump powers. Compared to one stage EDFA, the two stages EDFA obtained a better performance for all experiments. At 0 dBm of input signal power and 100 mW of pump power, a flat gain of about 15 dB was realized throughout a wide-band region.	The total length of the EDFs used were 22 m which is very long. On the other hand, this study focused only on the gain characteristic where the noise figure was ignored.

**Table 2.1**, continued

<b>Title</b>	<b>Authors</b>	<b>Findings</b>	<b>Drawbacks</b>
Optical Fiber Amplifiers: Optimization and Performance Evaluation	Abbas et al., (2019)	demonstrated the simulation of two different types of optical fiber amplifiers (OFA) using OptiSystem10 for 7 km Raman fiber and 3 m EDF. The EDFA shows best performance at conventional band (C-band) within the pump power of 30 mW. While the better performance is observed at long band (L-band) within the pump power of 600 mW for the RA.	These amplifiers utilizing very long fibers. The proposed amplifier achieved very low flat gain of about 3 dB.

## **CHAPTER 3: DEVELOPMENT OF EFFICIENT AND FLAT GAIN L-BAND EDFA WITH HIGHLY DOPED ERBIUM-DOPED FIBERS**

### **3.1 Introduction**

Due to the Internet and new data-communications services, the demand for bandwidth in long-haul communication networks drastically increased in recent years. L-band Erbium-doped fiber amplifiers (EDFAs) provide an attractive option for expanding bandwidth. These amplifiers, operating in the wavelength window ranges from the 1565 to 1605 nm, add more room for channels in high-data-rate dense wavelength-division multiplexing (DWDM) systems (Harun et al., 2003). However, the L-band EDFA normally requires a significantly longer doped fiber lengths to allow re-absorption process for L-band amplification. Recently, many efforts have been taken to reduce the fiber length in the amplifier. For instance, double pass technique was deployed to increase the amplification efficiency in the L-band region and thus reduces the required EDF length. Another effort to reduce the fiber length involves the use of high erbium-doping concentration.

In this chapter, efficient and compact L-band EDFAs are demonstrated using two types of highly doped fiber as the gain medium. At first, the fabrication and characterization of the Zirconia-based Erbium co-doped fiber (Zr-EDF) are described. The amplification performance of the Zr-EDF in single and double-pass setups is then demonstrated for L-band region. The effects of pumping wavelength are also investigated. The second part of this chapter discusses about fabrication, characterization and amplification performance of the second active fiber, Hafnium-Bismuth-based Erbium co-doped fiber (HB-EDF). Finally, the performance of both fibers for L-band amplification in double-pass configuration is compared.

### 3.2 Zirconia-Yttria-Alumina-erbium co-doped fiber (Zr-EDF)

#### 3.2.1 Fabrication and optical characterization of the Zr-EDF

The Zr-EDF used in this study was fabricated using the standard modified chemical vapor deposition (MCVD) technique in conjunction with a solution doping (SD) process. The MCVD process is illustrated in Figure 3.1. The preform was fabricated based on zirconia–yttria–alumina–phosphor silica glass with a high doping level of  $ZrO_2$ . The glass formers incorporated by the MCVD process were  $SiO_2$  and  $P_2O_5$  along with the glass modifiers  $Al_2O_3$ ,  $ZrO_2$ ,  $Er_2O_3$  and  $Y_2O_3$ , which were doped into the glass by the SD technique. The SD utilized an alcoholic-water mixture of suitable strength to form the complex molecules of  $ErCl_3 \cdot 6H_2O$ ,  $AlCl_3 \cdot 6H_2O$ ,  $YCl_3 \cdot 6H_2O$  and  $ZrOCl_2 \cdot 8H_2O$ . The inclusion of the  $Y_2O_3$  particulates into the host matrix also serves the additional purpose of slowing down or eliminating changes in the  $ZrO_2$  crystal structure to avoid cracking of the fabricated preform.

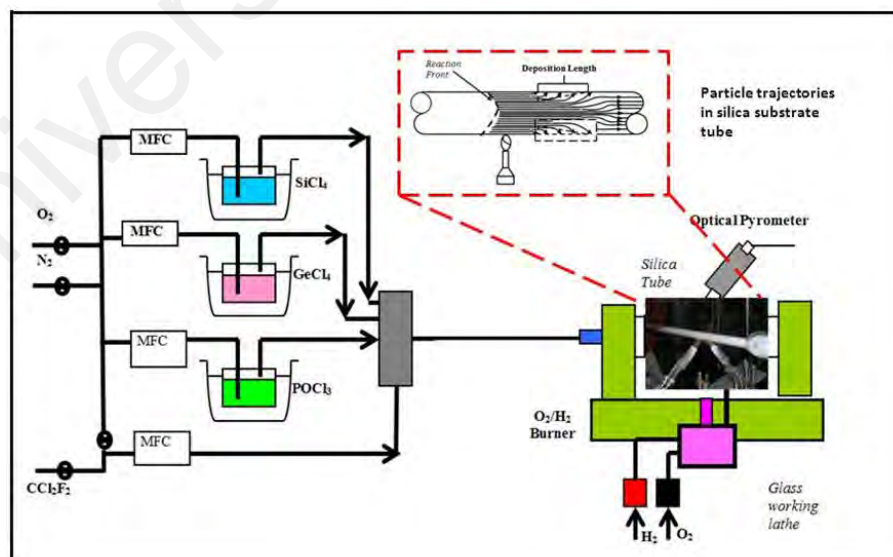
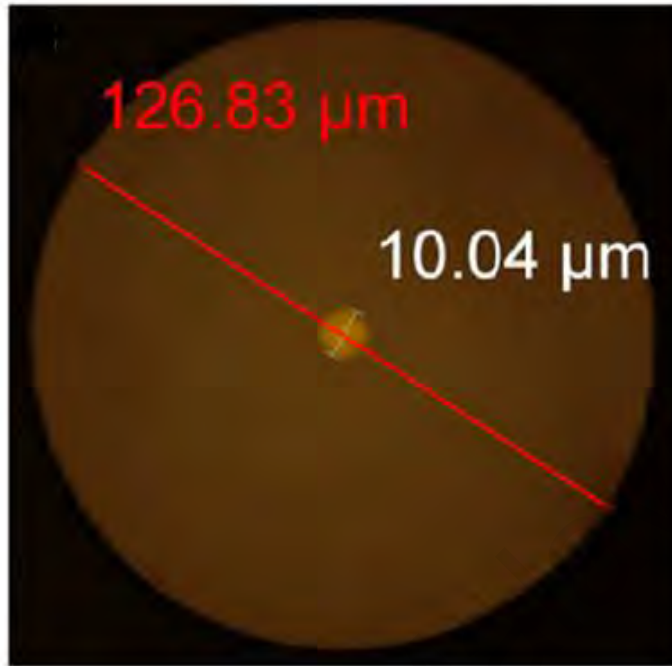
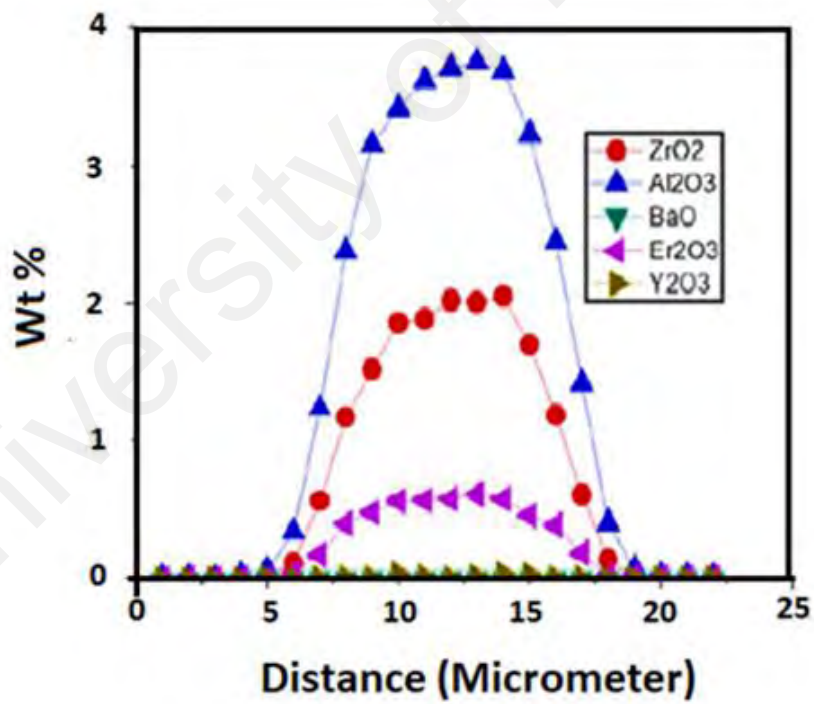


**Figure 3.1:** Setup of the MCVD system used in the doped fiber fabrication.

This is a crucial factor in the fabrication process. After the fabrication of the preform by the MCVD process, it was annealed at 1100 °C for three hours in a closed furnace under heating and cooling rates of 20°C/min to produce Er<sub>2</sub>O<sub>3</sub>-doped ZrO<sub>2</sub> rich nano-crystalline particles inside the core region. The fiber was obtained by drawing at around 2000 °C from the annealed preform and simultaneously coated with resin using fiber drawing tower. The absorption loss of the fiber at 980 nm is found to be 80 dB/m, which can be translated to the erbium ion concentration of 4000 ppm. The doping level within the core region of the fabricated high ZrO<sub>2</sub> co-doped EDF (Zr-EDF) was measured by electron probe micro analysis (EPMA). It is found that the fiber core glass contains around 2 wt% ZrO<sub>2</sub> and 0.6 wt% Er<sub>2</sub>O<sub>3</sub>. Figure 3.2(a) shows the cross-section image of the fabricated Zr-EDF, which indicates the core and cladding diameters of 10.04 and 126.83 μm, respectively. The average dopant distribution along the diameter of the core is shown in Figure 3.2(b). Based on the refractive index (RI) profile which is shown in Figure 3.3(a), the numerical aperture (NA) is calculated to be 0.17. The base loss at 1300 nm was measured to be around 50 dB/km as illustrated in Figure 3.3(b). Doping of Zr ions in silica glass creates nonbridging oxygens in silica network which allow the host glass to accommodate other optically-active in NIR co-dopants such as Erbium ion. Here, with a combination of both Zr and Al ions, we could achieve a high erbium doping concentration of 4000 ppm in the glass host without any phase separations of rare-earth. Zr ions can also be capable to slightly modify the overall core-glass structure, facilitating dispersion of active co-dopants for development of wide-band optical amplifier at near infra-red (NIR) region.



(a)



(b)

**Figure 3.2:** (a) Cross-sectional view and (b) Dopant distribution profile of the fabricated Zr-EDF.

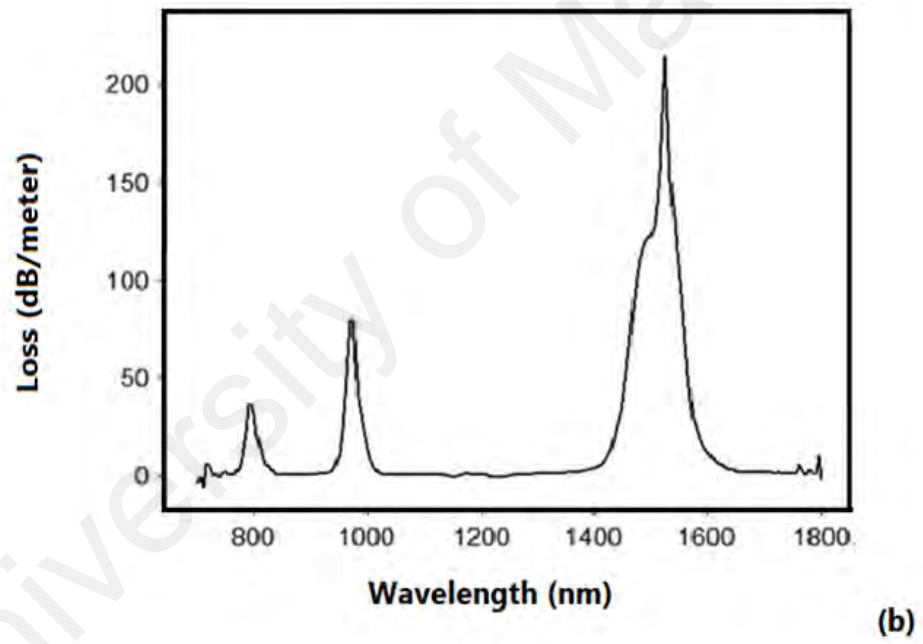
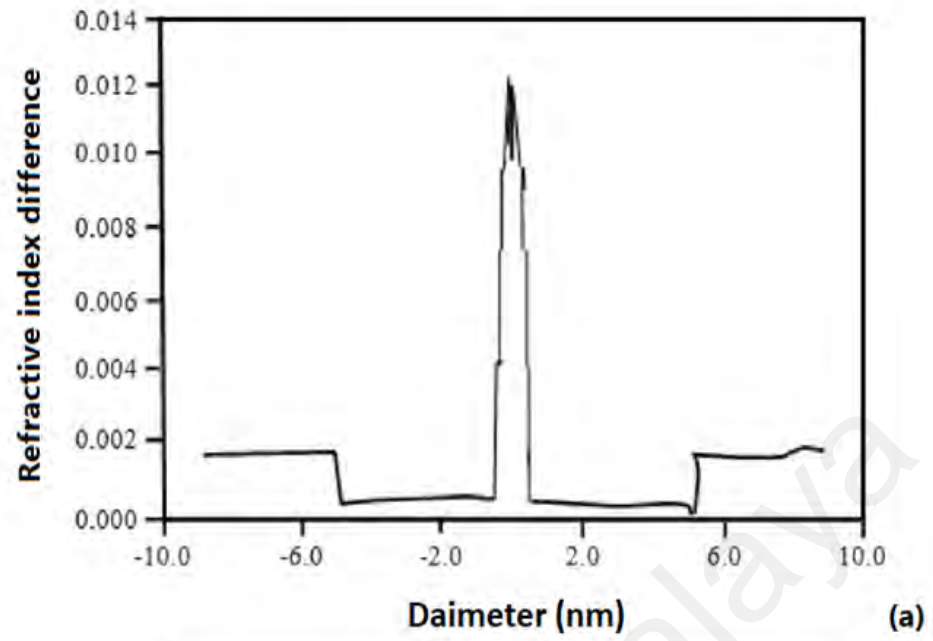


**Figure 3.3:** (a) Refractive index profile and (b) Absorption loss curve of the Zr-EDF.



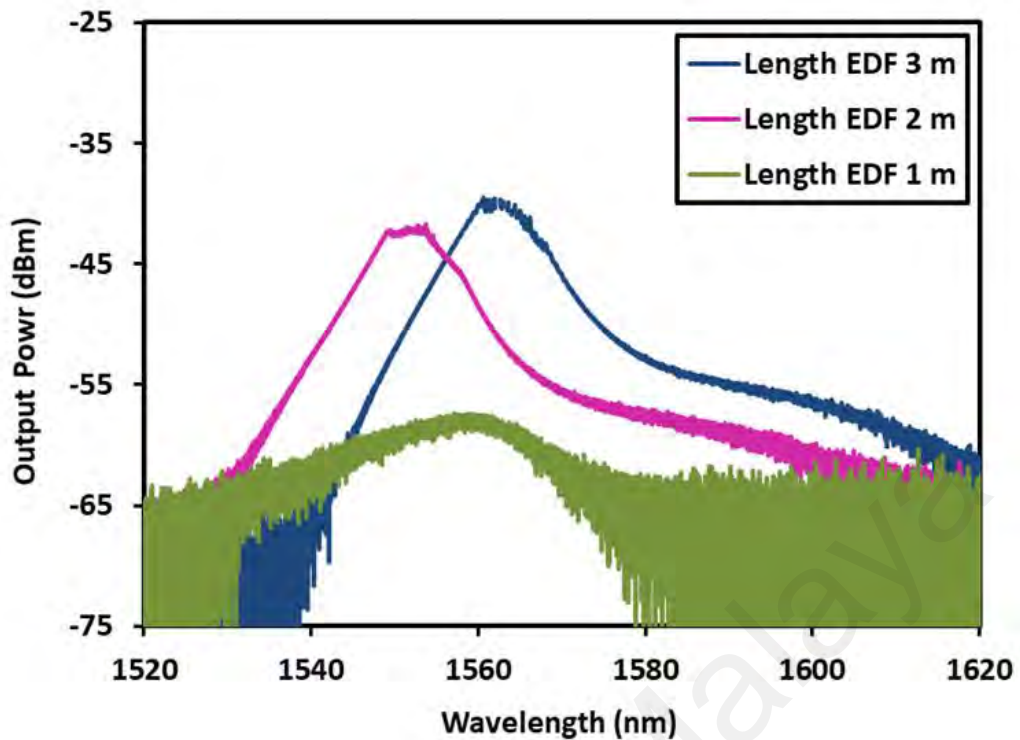
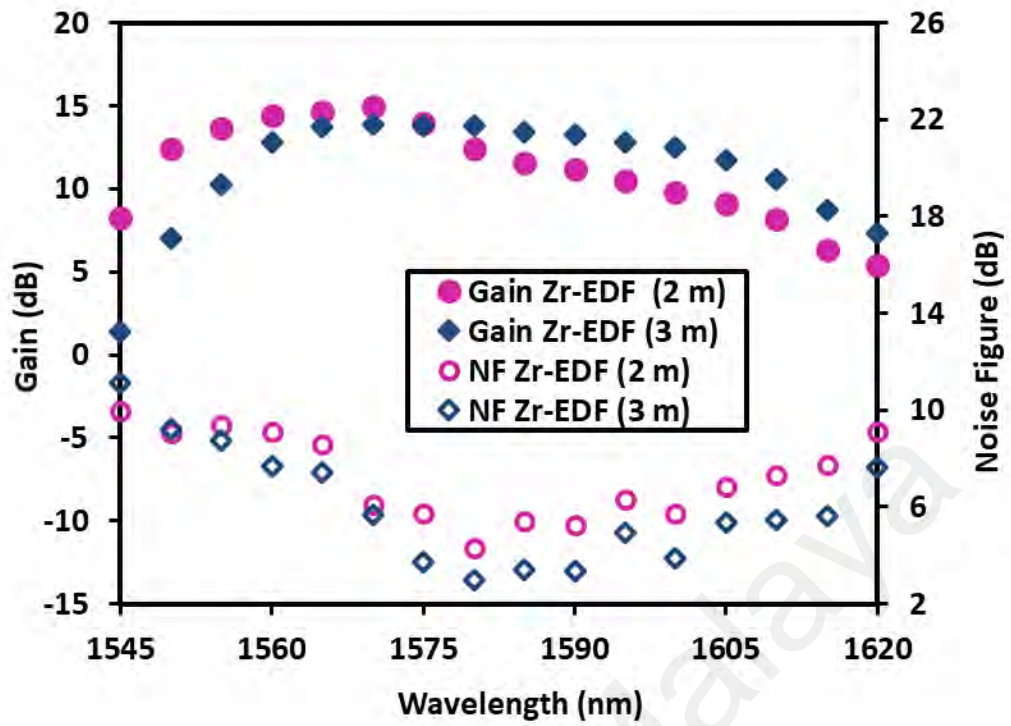


**Figure 3.5:** ASE spectrum for different lengths of Zr-EDF.

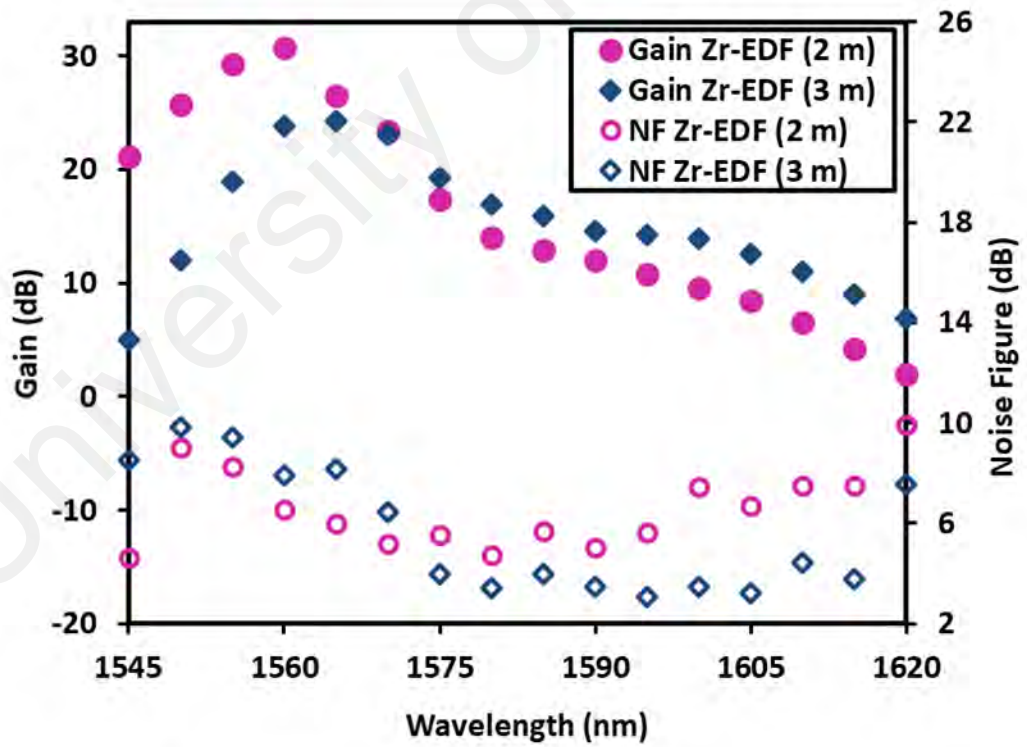
The amplification characteristic of Zr-EDF was then investigated using a Tunable laser source (TLS) in conjunction with an optical spectrum analyser (OSA) as shown in Figure 3.4. The one of the special designs for DWDM applications is TLS which is used to evaluate the optical components and dense wavelength division multiplexing systems. The TLS type of Ando AQ4321D is provide wide wavelength tuning range from (1520 to 1620 nm). The latest version of OSA is AQ6370D from Yokogawa which is provide multiuse wavelength span from 600 to 1700 nm. This range is suitable for telecommunications and general purpose. The programmable optical attenuator (POA, Anristu MN9610B) is used to obtain the accurate input signal power to the amplifier setup. The Zr-EDF amplifier (Zr-EDFA) was based on a single-pass configuration and the performance was optimized for amplification in L-band region. Figure 3.6 shows the gain and noise figure of the L-band Zr-EDFA for two different EDF lengths. The

amplifier performance was characterised at two input signal powers -10 and -30 dBm. The pump power is adjusted for 1480 nm at 170 mW for the experiment. It is clearly seen from Figure 3.6(a) that the length of 3 m obtains the best amplification performance in L-band region at input signal power of -10 dBm. At length of 3 m, a flat gain of 13.3 dB was achieved with gain variance of less than 1 dB within a wide-band wavelength region from 1560 to 1600 nm. This is due to quasi-two-level system amplification process, which enable L-band amplification in the Zr-EDFA. In this process, the shorter wavelengths photons are absorbed to emit at longer wavelengths. The corresponding noise figure varies from 3.8 to 7 dB within the flat gain region. Meanwhile, at length EDF of 2 m, the inefficient amplification in L-band region was observed since the lower gains are obtained especially at wavelengths longer than 1560 wavelength. This is due to the insufficient of Erbium ions to support the population inversion (PI). The noise figure spectrum indicates a relatively higher value with 2 m long of Zr-EDF due to the lower gain.

At low input signal power of -30 dBm, it is found that the 3 m length produces a better amplification performance in the L-band region as shown in Figure 3.6(b). For instance, the maximum gain of 24 dB was obtained at wavelength of 1565 nm. The average gain has improved by 23 % when the length of the HB-EDF increased from 2 m to 3 m within wavelength region from 1565 to 1620 nm. The noise figure was varied from 3 to 8 dB within the L-band region. At the Zr-EDF length of 2 m, the gain reduction was observed in the spectrum especially at the longer wavelength due to the same reason explained. The noise figure spectrum, which are depended on the gain characteristic, are higher.



(a)



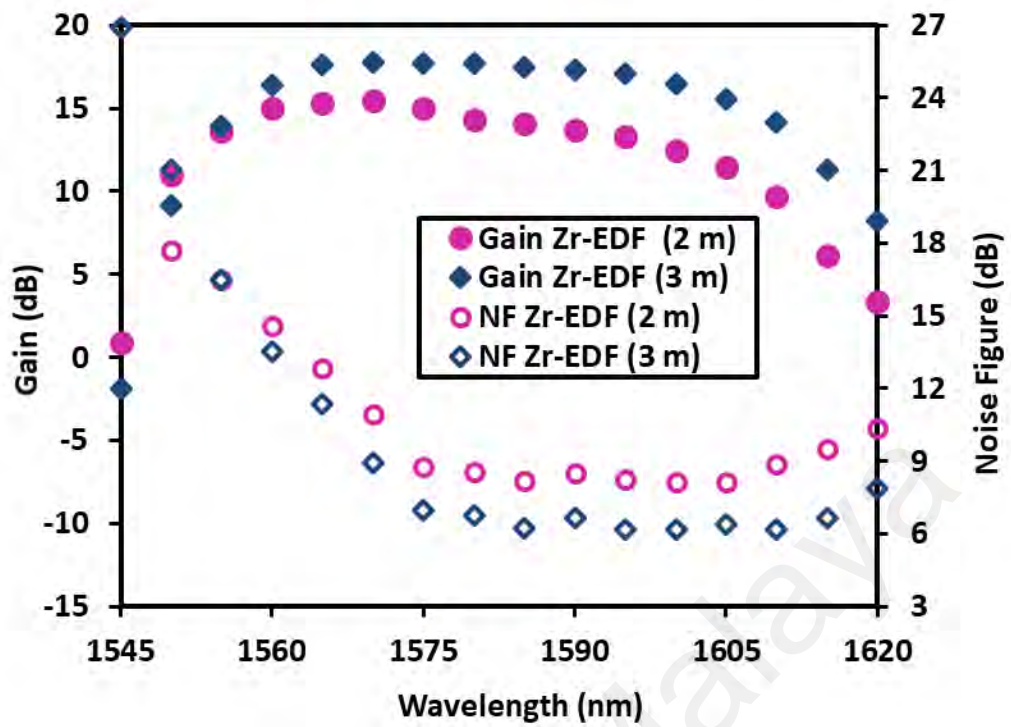
(b)

**Figure 3.6:** Gain and noise figure spectra with two different Zr-EDF length in single-pass setup at input signal powers of (a) -10 dBm and (b) -30 dBm.

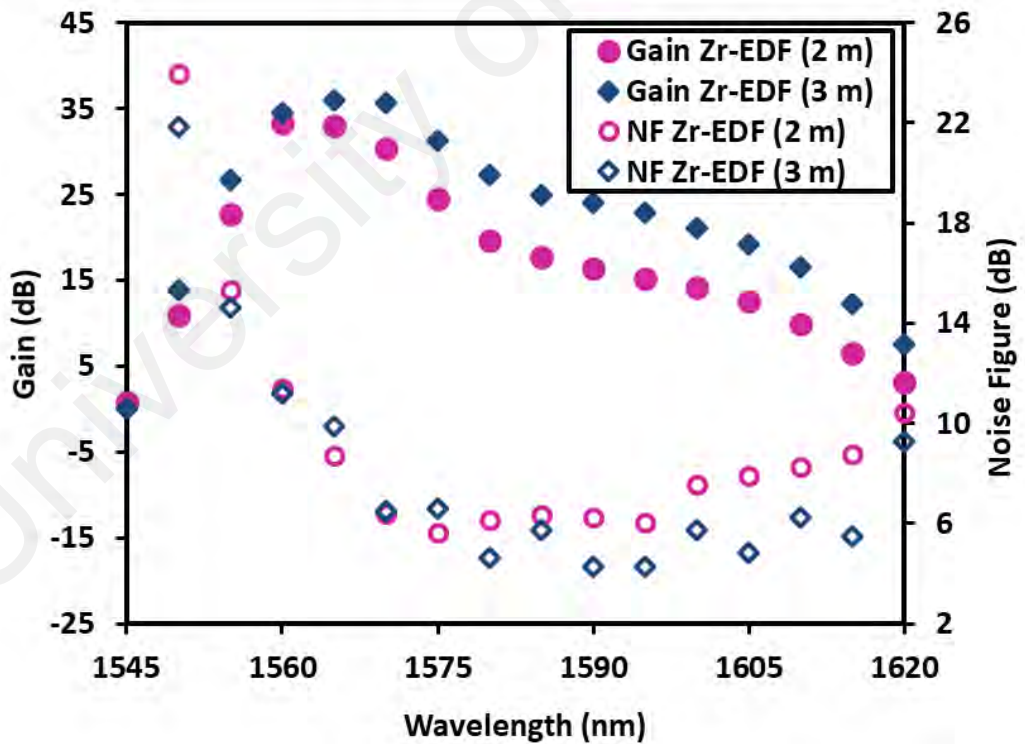


The gain and noise figure performances of the double-pass Zr-EDFA were investigated and the result is shown in Figure 3.8 for two different lengths of active fiber; 2 m and 3 m. The amplifier performance was characterized at two input signal powers of -10 and -30 dBm. In the experiment, the pump wavelength and power were fixed at 1480 nm and 170 mW, respectively. As shown in Figure 3.8(a), at high input power of -10 dBm, the gain spectrum was higher and flatter as the Zr-EDF length is increased from 2 to 3 m. At 3 m long Zr-EDF, the double-pass amplifier produced a flat gain at around 17.1 dB with gain variance of less than 1 dB over wavelength range from 1560 to 1605 nm. This is owing to the reabsorption effect of Erbium ions based on quasi-two-level effect where the C-band photons were absorbed to emit in L-band wavelength region. This effect increases the gains at longer wavelength and thus a flat gain can be easily achieved by optimization of the pump power. At fiber length of 2 m, the gain spectrum at L-band region was more than 14 dB, however; the gain was inclined at longer wavelength region especially beyond 1575 nm.

As shown in Figure 3.8(b), the higher gain spectrum was obtained at low input signal power of -30 dBm. For instance, the maximum gain of 36 dB was obtained at wavelength of 1565 nm. The noise figure was maintained below 9 dB within the L-band region. On the other hand, the lower gain was obtained as the Zr-EDF length was reduced to 2 m. This is attributed to the insufficient of Erbium ions to support population inversion (PI). The noise figure spectrum was observed to be relatively higher with the shorter Zr-EDF (2 m) due to the gain reduction.



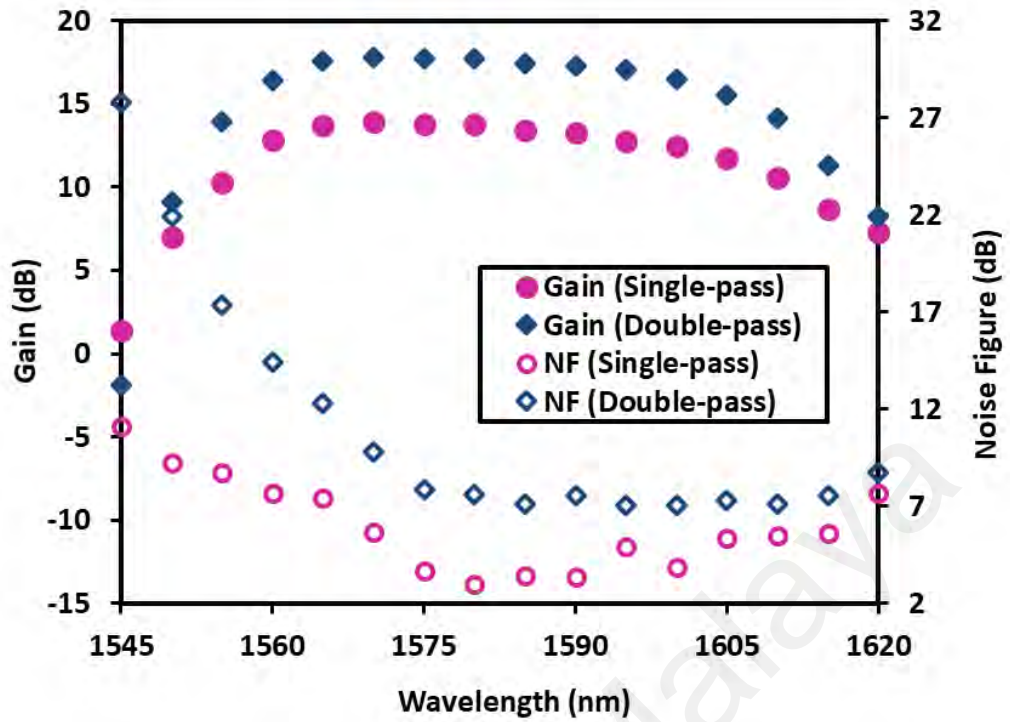
(a)



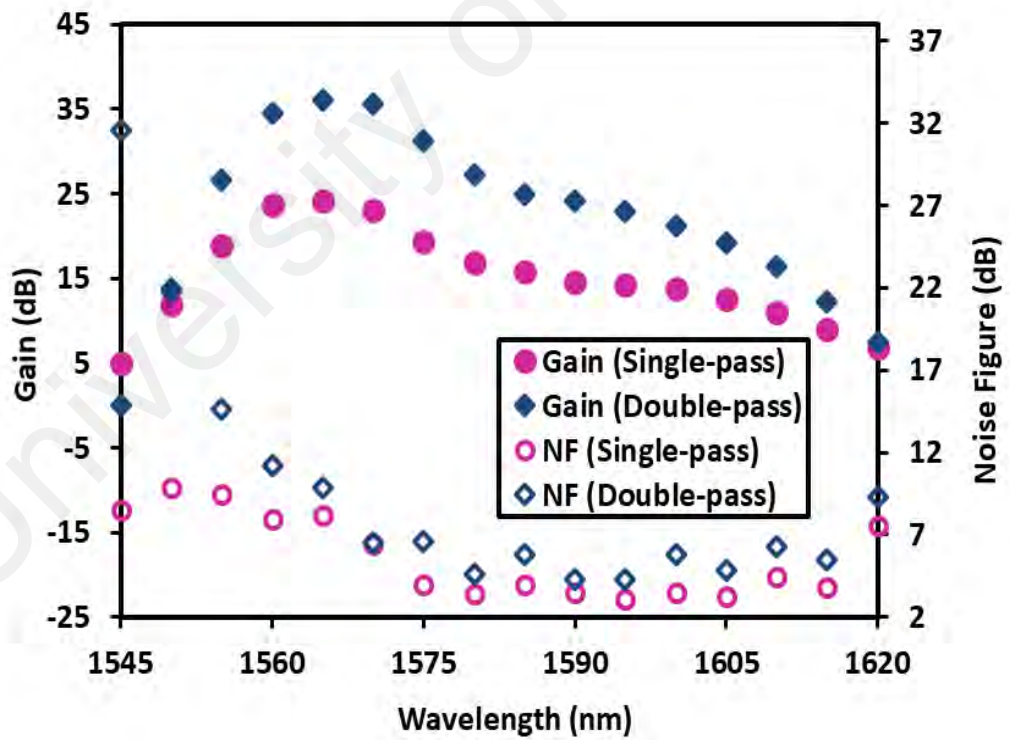
(b)

**Figure 3.8:** Gain and noise figure spectra for the double-pass Zr-EDFA at two input signal powers of (a)-10 dBm and (b)-30 dBm.

The performance of the double-pass Zr-EDFA is also compared to that of the single-pass Zr-EDFA, which was obtained by removing the optical circulators and measuring the amplified signal at the output end of the Zr-EDF. Figure 3.9(a) and (b) illustrate the gain and noise figure performances of L-band amplifier when the input signal power is fixed at -10 and -30 dBm, respectively. In the experiment, the Zr-EDF length was fixed at 3m while the 1480 nm pump power was fixed at 170 mW. At input signal power of -10 dBm, the amplifier's gain was enhanced by about 30% in the double-pass system as compared to that of the single-pass. This is due to the double propagation of the signal in the gain medium, which increases the effective length of the amplifier and thus the gain. As shown in Figure 3.9(a), a flat gain of around 13.1 and 17.1 dB is achieved with gain fluctuation about 1 dB within wavelength region from 1560 to 1605 nm for single and double-pass, respectively. As depicted in Figure 3.9(b), the gain is also higher in the double-pass Zr-EDFA compared to that of single-pass at input signal power of -30 dBm. This is due to same reason as explained earlier. The peak gains of 24.2 and 36 dB are obtained at 1565 nm for single and double-pass configurations, respectively. On the other hand, the noise figure is higher in the double-pass configuration compared to that of the single-pass. This is attributed to the increased backward propagating ASE power at the input part of the amplifier, which reduces the population inversion. The noise figure is relatively higher at the shorter wavelength which is attributed to the lower gain and higher loss characteristics associated with the shorter wavelength.



(a)

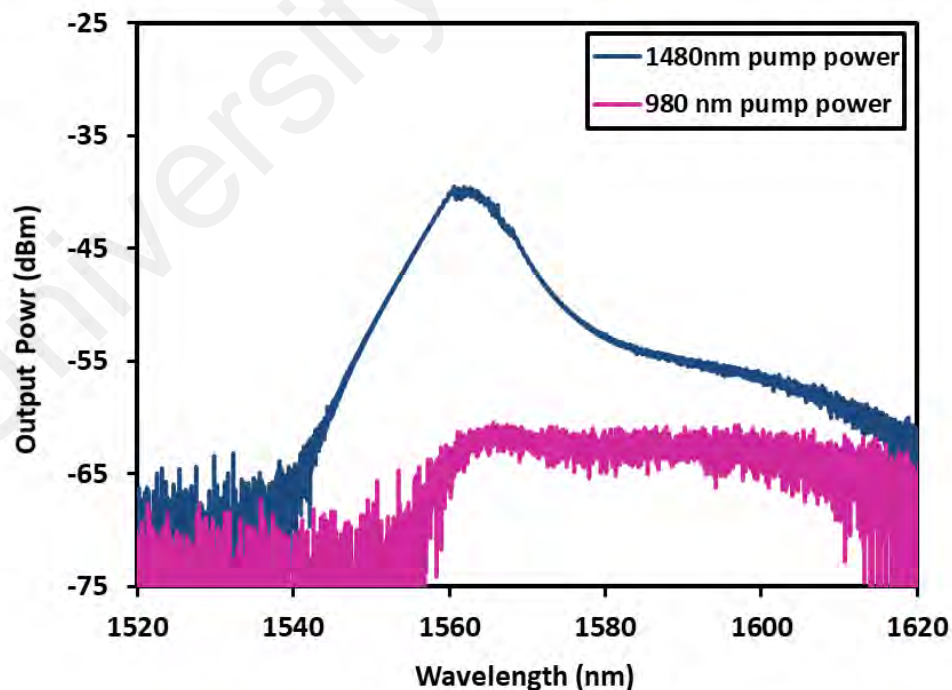


(b)

**Figure 3.9:** Gain and noise figure spectrum of the single and double-pass Zr-EDFA configured with 3 m long Zr-EDF at input signal powers of (a) -10 dBm and (b) -30 dBm.

### 3.2.4 Effect pumping wavelength on the performance of the double-pass Zr-EDFA

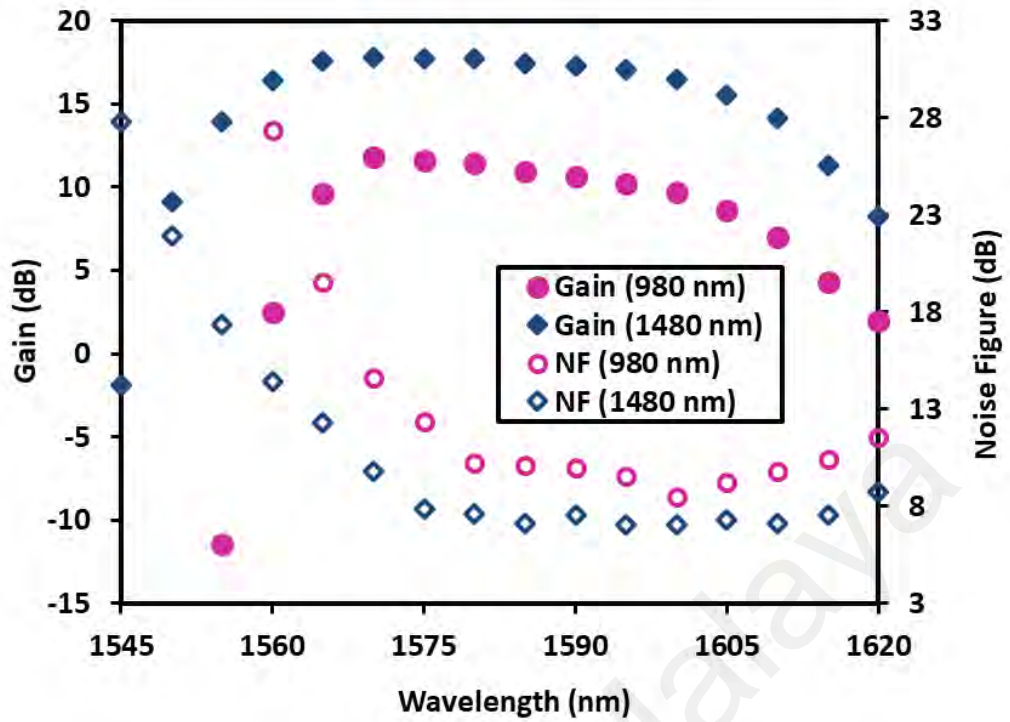
Since the double-pass configuration provides higher gain spectrum, this scheme is used to study effect of the laser diode pump wavelength on the performance of the Zr-EDFA. The Zr-EDF length is fixed at 3 m in the experiment. At first, the ASE spectrum of the Zr-EDF is investigated for two pumping schemes; 1480 nm and 980 nm based on forward pumping scheme in a single-pass arrangement. Figure 3.10 compares the ASE spectra when both LD pumps are fixed at 170 mW. As depicted in the figure, the power level of the ASE is higher with 1480 nm pumping. This is attributed to the higher optical power conversion efficiency at 1480 nm pumping due to the single photon conversion process of erbium amplification. 980 nm pumping involves three level energy transition and thus some energy is wasted for non-radiation transition, which reduces the efficiency of the ASE generation.



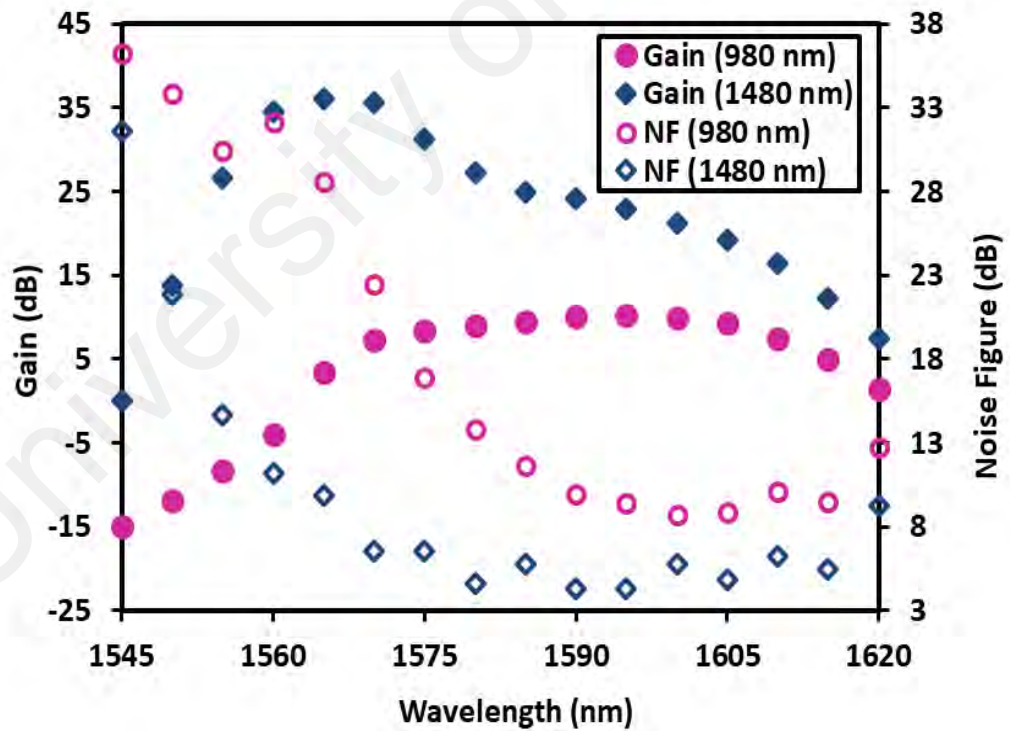
**Figure 3.10:** Comparison of ASE characteristics for the Zr-EDF at two pumping wavelengths.

Figure 3.11 compares the gain and noise figure performances of the Zr-EDFA in double-pass configuration between two pumping wavelengths, 980 nm and 1480 nm pump wavelength. In the experiment, the power for both LD pumps was adjusted at 170 mW. At input signal power of -10 dBm, the amplifier's gain with 1480 nm pumping is higher than that of 980 nm pumping as shown in Figure 3.11(a). The gain improvement is attributed to the efficient use of 1480 nm pump power with a long gain medium. A flat gain of around 17.1 dB is obtained with fluctuation of around 1 dB within spectral bandwidth from 1560 to 1605 nm when EDF was pumped at 1480 nm. The corresponding noise figure of the amplifier pumped at 1480 nm is lower compared to that one pumped at 980 nm. The noise figure of less than 14 dB is obtained within the flat gain region.

Figure 3.11(b) illustrates the Zr-EDFA performance at input signal power of -30 dBm for two different pumping wavelengths. The 1480 nm pumping provides better gain spectrum with the maximum gain improvement of 19.4 dB is observed in the L-band region as compared to 980 nm pumping. The gain improvement is attributed to the efficient use of 1480 nm pump power with a long gain medium. Furthermore, the 1480 nm pumping provides a greater amplification bandwidth ranging from 1545 to 1620 nm. The noise figure of the amplifier pumped at 1480 nm is also lower compared to that one pumped at 980 nm. On the other hand, the noise figure is relatively higher at a shorter wavelength region (shorter than 1560 nm) as shown in the figure. This is attributed to the lower gain and higher loss characteristic associated with shorter wavelength region.



(a)



(b)

**Figure 3.11:** The gain and noise figure of the double-pass Zr-EDFA at two different pump wavelengths when the input signal is fixed at (a) -10 dBm and (b) -30 dBm.

### 3.2.5 Effect of Erbium dopant concentration on the performance of the Zr-EDFA

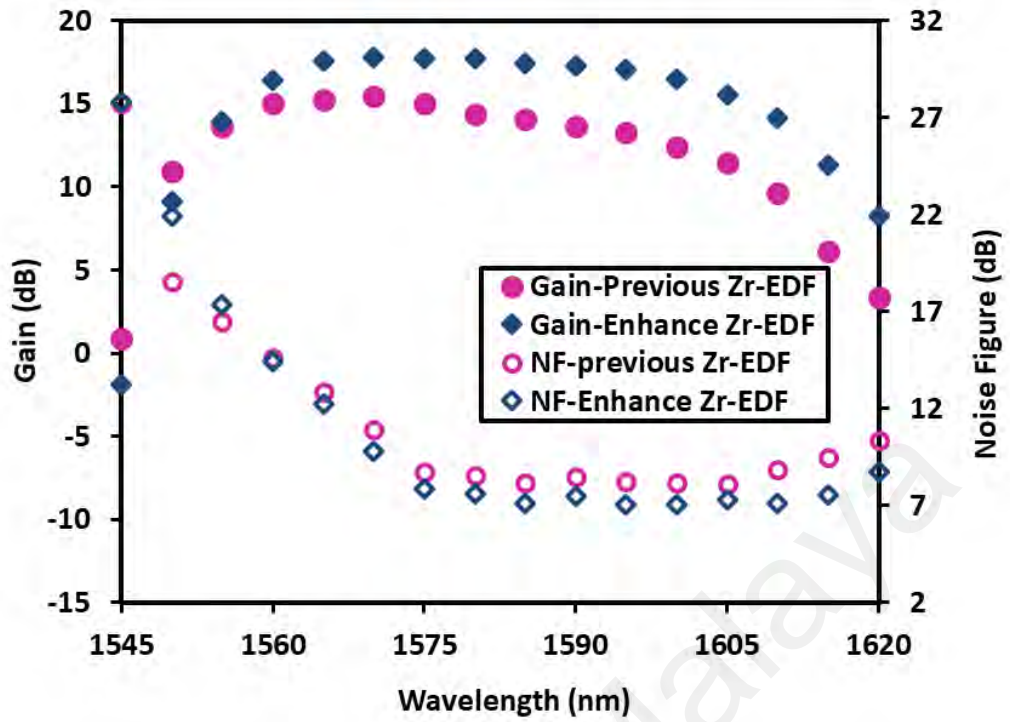
In this section, the performance of the Zr-EDFA is compared for two active fibers with different Erbium ion concentration. Since the 1480 nm pump wavelength provides higher gain spectrum in double-pass configuration, this laser diode is used to compare the performance of Zr-EDFA. In this work, the double-pass configuration is deployed. The performance of the newly developed Zr-EDF is compared with the conventional Zr-EDF with a lower Erbium ion concentration. Table 3.1 compares the specification of the conventional and the newly developed fiber Zr-EDF, which will be used throughout this study. The conventional Zr-EDF was fabricated through the similar process as the current fiber.

**Table 3.1:** Specification comparison between the newly developed and the previous (conventional) Zr-EDF

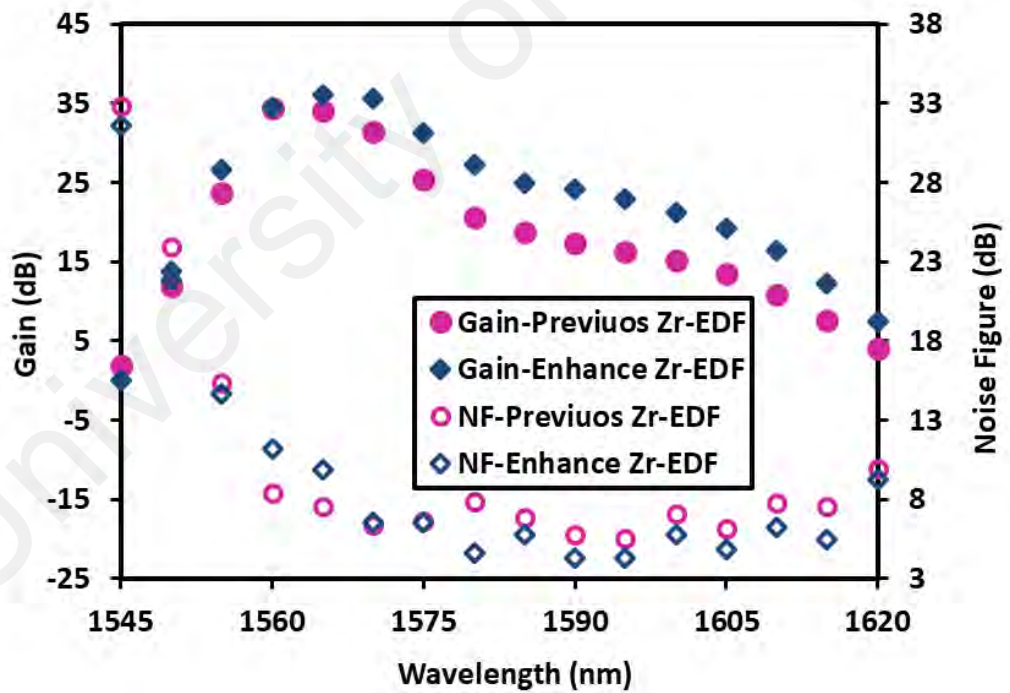
<b>Performs</b>	<b>Newly improved Zr-EDF</b>	<b>Conventional Zr-EDF</b>
Er doped ion concentration	4000 ppm	2800 ppm
Absorption loss at 980 nm	80 dB/m	14.5 dB/m
Core & Clad diameter	Core: 10 Clad: 126.83	Core: 10.5 Clad: 125
Numerical Aperture	0.17	0.17
Background loss at 1300 nm	50 dB/km	145 dB/km

It was obtained from a fiber preform, which was fabricated in a ternary glass host, zirconia-yttria-aluminum co-doped silica fiber using a MCVD (Paul et al., 2010b). Doping of Er<sub>2</sub>O<sub>3</sub> into zirconia-yttria-aluminosilicate-based glass was done through a solution doping process. Small amounts of Y<sub>2</sub>O<sub>3</sub> and P<sub>2</sub>O<sub>5</sub> were added, where both Y<sub>2</sub>O<sub>3</sub> and P<sub>2</sub>O<sub>5</sub> serve as a nucleating agent to create the phase separation with generation of Er<sub>2</sub>O<sub>3</sub>-doped micro crystallites into the core matrix of optical fiber preform. A fiber of 125 μm in diameter was drawn from the fabricated preform at a temperature of around 2000 °C using the conventional fiber drawing technique. The peak absorption loss of the Zr-EDF at 978 nm is found to be 14.5 dB/m, which translates to the erbium ion concentration of 2800 wt.ppm. The fabricated Zr-EDF has an NA of 0.17, a core diameter of 10.5 μm, and a background loss of 0.11 dB/m at 1300 nm.

In the experiment, the comparison was performed at two input signal powers of -10 and -30 dBm where the pump power was fixed at 170 mW. The Zr-EDF length is fixed at the optimum length of 3 m and 4 m for the new and the conventional fiber, respectively. Figure 3.12(a) and (b) shows the gain and noise figure spectra at input signal power of -10 and -30 dBm, respectively. As shown in Figure 3.12(a), at input signal power of -10 dBm, the proposed Zr-EDFA configured with a higher concentration of Erbium achieves a relatively higher and flatter gain especially at L-band region as compared with the conventional Zr-EDFA. This is attributed to the population inversion which is higher in the shorter length of Zr-EDF as well as the efficient use of pump power with a shorter gain medium. A high and flat gain of about 17.1 dB is achieved within region from 1560-1605 nm for the new Zr-EDFA, while a slightly lower flat gain of about 15 dB is achieved for the previous Zr-EDFA within same wavelength region. On other hand, the noise figures of the new Zr-EDFA are lower compared to those of the previous Zr-EDFA. This is attributed to the higher gain and lower loss characteristics of the shorter gain medium.



(a)



(b)

**Figure 3.12:** Comparison of the gain and noise figure spectra between enhanced Zr-EDFA (ER-3) and the conventional Zr-EDFA (NER-6) at input signal power of (a) -10 dBm and (b) -30 dBm.

The Zr-EDFA shows higher gain at input signal power of -30 dBm as compared to gain of the previous Zr-EDFA within L-band region as depicted in Figure 3.12(b). The average gain enhancement of about 21% is observed with Zr-EDFA of higher concentration, within region from 1560 to 1600 nm. This improvement is owing to a considerably higher concentration of erbium ions in the Zr-EDF and therefore increases the population inversion. The enhance Zr - EDFA's noise figure is slightly lower than the conventional amplifier in the L-band region. This is due to the ions populated in upper level were mainly used for amplification and thus decreases the ASE level and therefore decreases the noise level.

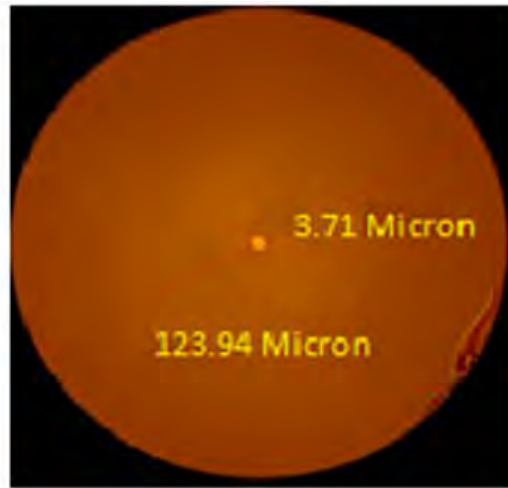
### **3.3 Hafnium bismuth erbium co-doped fiber (HB-EDF)**

#### **3.3.1 Fabrication and Characterization**

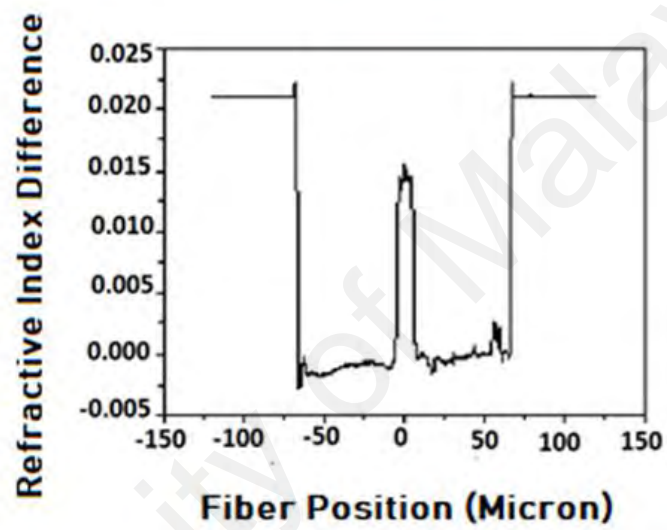
The HB-EDF was obtained from Hafnium Bismuth Erbium co-doped Yttria-Alumina-Silica glass based preform. The preform was fabricated through deposition of porous silica layer at around 1500 °C temperature by the modified chemical vapor deposition (MCVD) followed by the solution doping (SD). Suitable strength of  $\text{Al}(\text{NO}_3)_3 \cdot 9\text{H}_2\text{O}$ ,  $\text{HfCl}_3$ ,  $\text{Bi}(\text{NO}_3)_3 \cdot x\text{H}_2\text{O}$ ,  $\text{Y}(\text{NO}_3)_3 \cdot 6\text{H}_2\text{O}$  and  $\text{ErCl}_3 \cdot x\text{H}_2\text{O}$  were used for soaking of the porous layer for a period of one hour in the SD process to incorporate all the co-dopants such as  $\text{Al}_2\text{O}_3$ ,  $\text{HfO}_2$ ,  $\text{Bi}_2\text{O}_3$ ,  $\text{Y}_2\text{O}_3$  and  $\text{Er}_2\text{O}_3$ . All the halide and nitrate salts retain into porous layer after draining out of the solution followed by air drying with the flow of  $\text{N}_2$  gas at room temperature. Such salts were converted to their respective oxides through an oxidation process with a flow of  $\text{O}_2$  gas at around 800–900 °C temperature. Sintering of the porous layer containing such oxides was done by gradually increasing temperature from 1300 to 1900 °C to form a transparent glass. The glass was converted to a solid preform by collapsing stages where it was over-cladded with a thick silica tube

to reduce the core diameter. The final fiber was drawn from the preform by a conventional way using a fiber drawing tower, at  $\sim 2000$  °C.

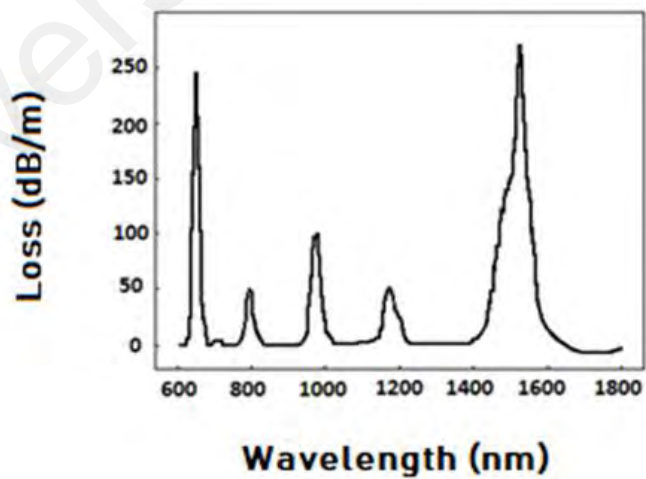
The doping level within the core region of the fabricated fiber was measured by electron-probe micro-analysis (EPMA). It is found that the fiber core glass contains 6.0 wt%  $\text{Al}_2\text{O}_3$ , 1.23 wt%  $\text{Er}_2\text{O}_3$ , 2.2 wt%  $\text{HfO}_2$  and 0.035 wt%  $\text{Bi}_2\text{O}_3$ . The fiber cross sectional view and the refractive index profile of the fabricated fiber is shown in Figure 3.13(a) and (b) respectively. As shown in both figures, the core and cladding diameters of the fiber are 3.71 and 123.94  $\mu\text{m}$ , respectively. Based on the refractive index profile, the numerical aperture is calculated to be 0.21. The spectral attenuation curve of the fiber is shown in Figure 3.13(c). The absorption loss at 980 nm is found to be 100 dB/m, which is equivalent to 12500 wt ppm of  $\text{Er}_2\text{O}_3$ . The high erbium ion concentration was possible due to the co-doping with Hafnium and Aluminum ions, which reduces the ions clustering effects.



(a)



(b)



(c)

**Figure 3.13:** HB-EDF characteristics: (a) Microscopic view (b) Refractive index profile, and (c) Absorption loss curve.

### 3.3.2 ASE characteristics

The observation of the ASE spectra at various length of gain medium of the amplifier was performed at a maximum pump power of 170 mW as shown in Figure 3.14. The length of HB-EDF was fixed at 0.5 m, 1 m and 1.5 m respectively, and they were forward pumped at 1480 nm pump wavelength in the single pass configuration. As illustrated in the figure, both HB-EDFA with a gain medium length of 1 m and 1.5 m provide emissions in the L-band region range from 1560nm to 1620nm. However, the emission wavelength shifted to a longer range when the length of the HB-EDF increased to 1.5 m. The ASE level of the HB-EDFA with 1.5 m length of HB-EDF was around 5 dBm higher compared to the HB-EDF with 1 m length of gain medium. This is attributed to the enhancement of the population inversion of the Erbium ions in the fiber, which increases with the EDF length. As the HB-EDF length decreases to 0.5 m, the operating wavelength shifts to the C-band region due to insufficient Erbium ions to provide reabsorption process in the active fiber.

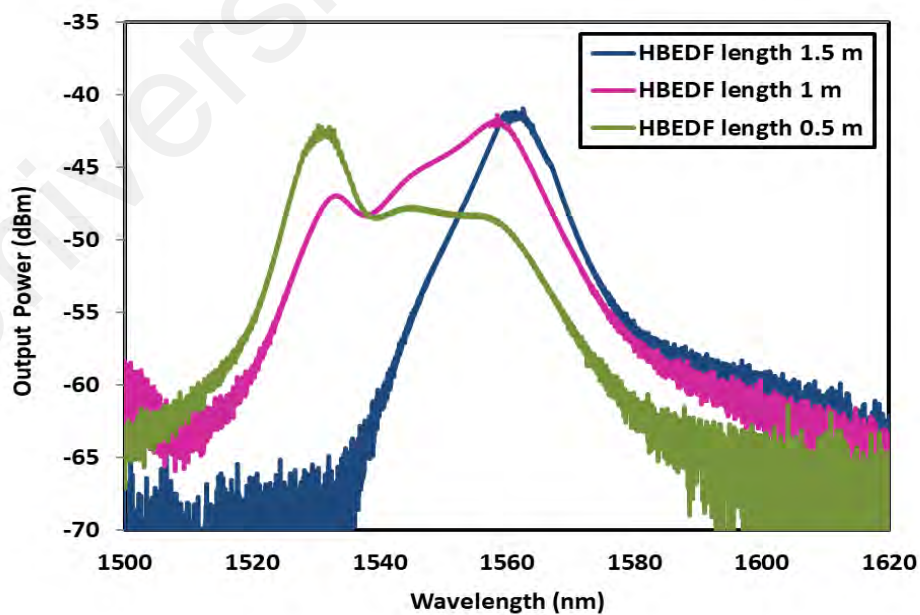
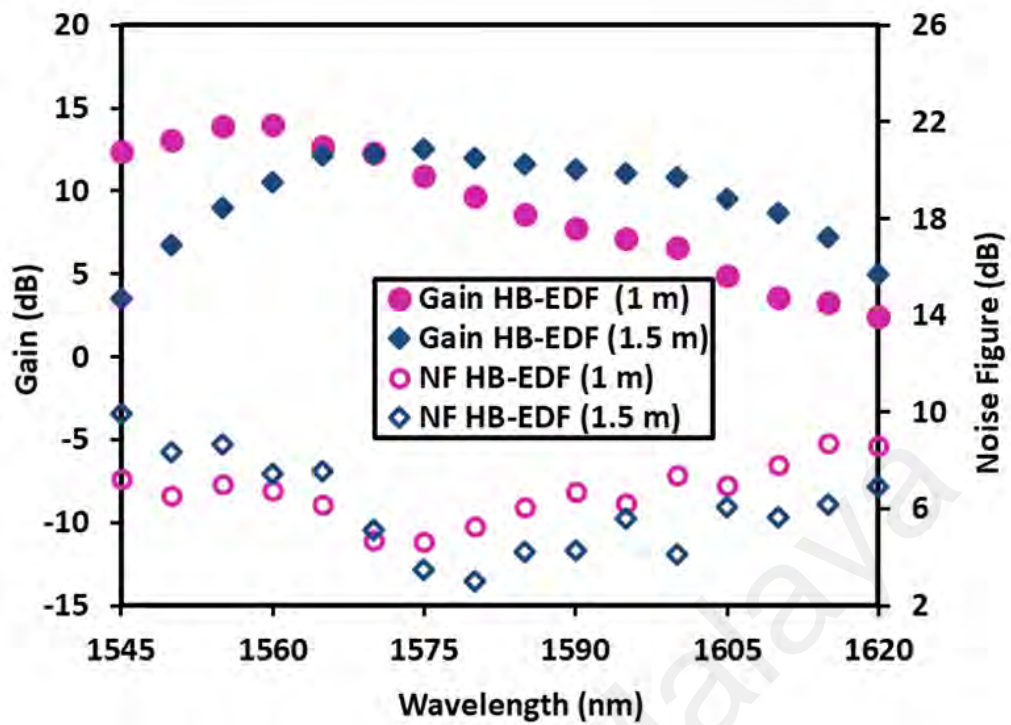


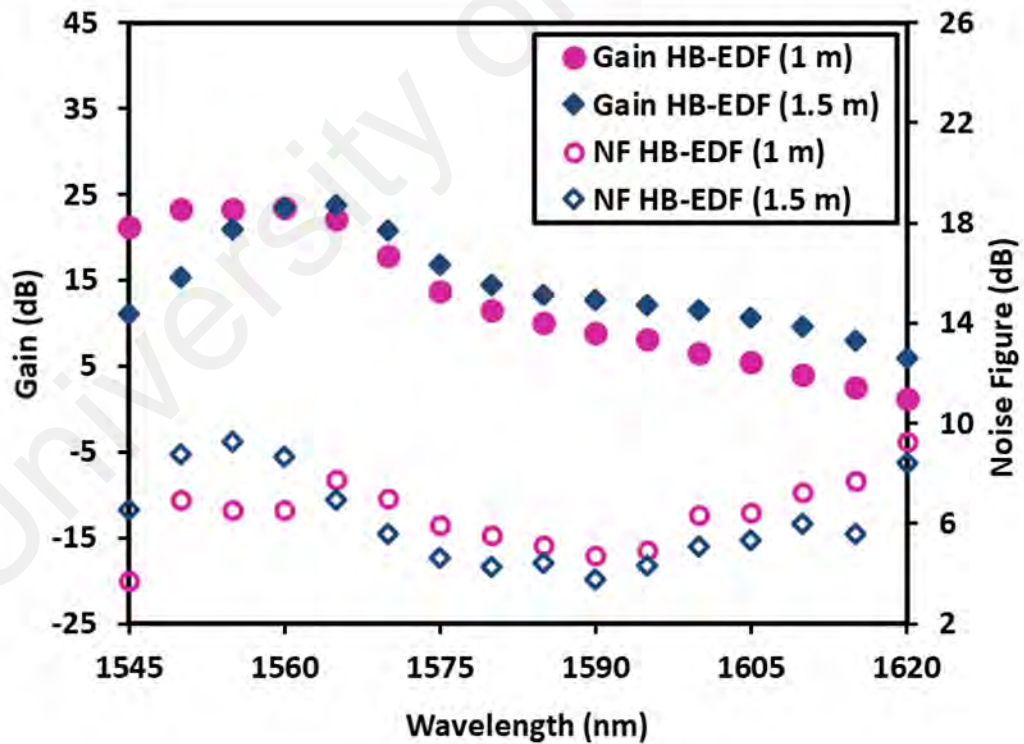
**Figure 3.14:** ASE spectrum for various lengths of HB-EDF as they were pumped at 170 mW using 1480 nm LD in single pass configuration.

### 3.3.3 Amplification performances in single-pass and double-pass set-up

The gain and noise figure performances of the single pass HB-EDFA was investigated at two various lengths of HB-EDF, 1 m and 1.5 m as shown in Figure 3.15. This is done by replacing the piece of Zr-EDF with the HB-EDF in Figure 3.5. The two HB-EDFs were forward pumped by a 1480 nm laser diode at the pump power of 170 mW. It is clearly seen from Figure 3.15(a) that the length of 1.5 m obtains the best amplification performance in L-band region at input signal power of -10 dBm. The average gain has improved by 34 % when the length of the HB-EDF increased from 1 m to 1.5 m within wavelength region from 1565 to 1620 nm. At HB-EDF length of 1.5 m, a flat gain of 10 dB was obtained with gain variance of around 1 dB within a wide-band wavelength region from 1555 to 1605 nm. This is due to quasi-level system process in HB-EDFA whereby the shorter wavelengths photons are absorbed to emit at longer wavelengths. The corresponding noise figure was varied from 3.8 to 9 dB within the flat gain region. However, the noise figure is relatively higher at the shorter wavelength due to the lower gain and higher loss characteristics associated with the shorter wavelength region. On other hand, a flat gain of about 11.1 dB was obtained at HB-EDF length of 1 m within L-band wavelength region. At low input signal power of -30 dBm, it is found that the length of 1.5 m obtains the best amplification performance in L-band region as shown in Figure 3.15(b). For instance, the maximum gain of 23.7 dB was obtained at wavelength of 1565 nm. The average gain has improved by 42 % when the length of the HB-EDF increased from 1 m to 1.5 m within wavelength region from 1565 to 1620 nm. The noise figure was varied from 3.7 to 8 dB within the L-band region. However, at the length of 1 m, the inefficient gain spectrum was obtained at longer wavelength but with lower values. This is attributed to the insufficient the EDF length to support population inversion (PI). The noise figure spectrum is relatively higher with 1 m long of Zr-EDF due to the gain reduction.



(a)

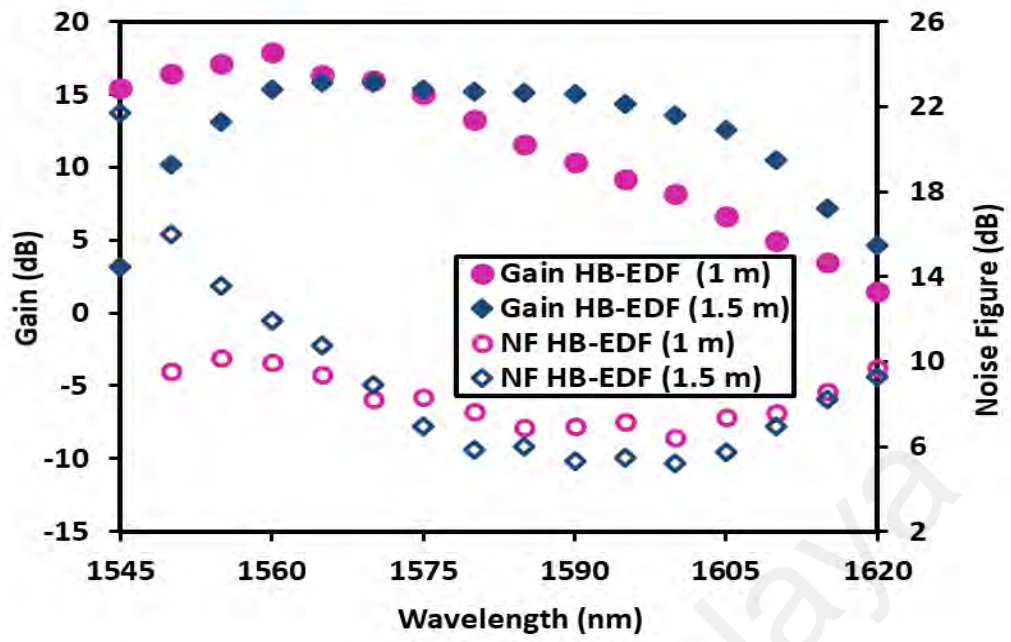


(b)

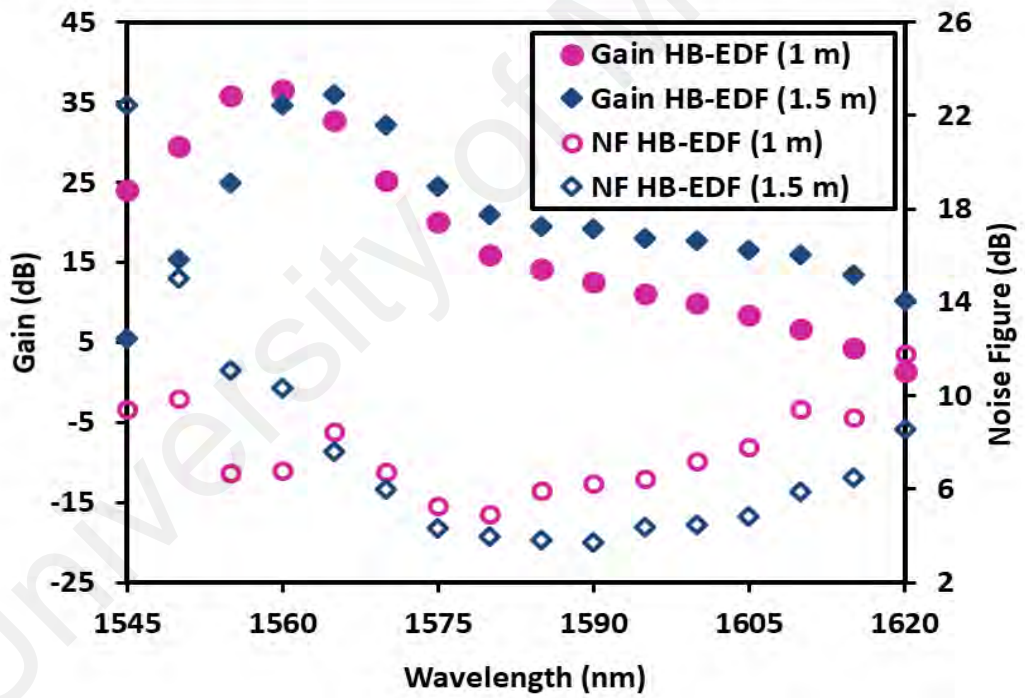
**Figure 3.15:** Gain and noise figure performances with different length of HB-EDF in single-pass setup at input signal power of (a) -10 dBm and (b) -30 dBm.

The gain and noise figure performance of the double-pass HB-EDFA was then investigated at two various lengths of HB-EDF, 1 m and 1.5 m as shown in Figure 3.16. This is done by replacing the piece of Zr-EDF with the HB-EDF in Figure 3.7. The two HB-EDFs were forward pumped by a 1480 nm laser diode at the pump power of 170 mW. At high input power of -10 dBm, the gain spectrum was relatively higher and flatter when the length fiber increased from 1 to 1.5 m especially at L-band region as shown in Figure 3.16(a). For instance, gain flatness around 15 dB is investigated for 1.5 m long EDF with gain variance around 1 dB over wavelength area from 1560 to 1605 nm. This is owing to quasi-two-level system where the C-band photons were absorbed to emit in L-band wavelength region as well as the optimization of the pump power can achieve a flat gain operation for this region. At fiber length of 1 m, the gain of more than 15 dB was achieved, however; the gain was inclined at L-band wavelength region especially beyond 1575 nm.

At low input signal power of -30 dBm, the use of longer HB-EDF length (1.5 m) provides a higher gain especially at L-band region as shown in Figure 3.16(b). For instance, the maximum gain of 36 dB was obtained at wavelength of 1565 nm. The noise figure was maintained below 9 dB within the L-band region. However, at a shorter length of 1 m, the maximum gain of 36 dB was obtained at shorter wavelength of 1560 nm. In addition, the gain spectrum was also inclined at longer wavelength region especially beyond 1580 nm. The inefficient gain spectrum is attributed to the insufficient of Erbium ions to support population inversion (PI) and thus the longer wavelength gains cannot be increased through the quasi-two-level absorption process. The noise figure spectrum is relatively higher with 1 m long of HB-EDF due to the gain reduction.



(a)

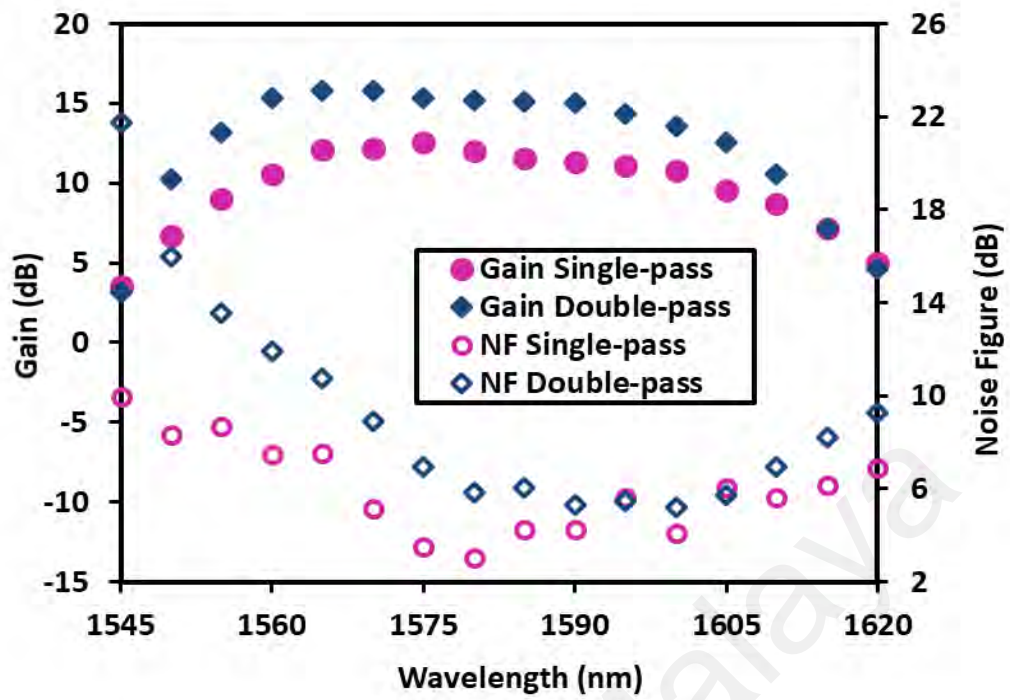


(b)

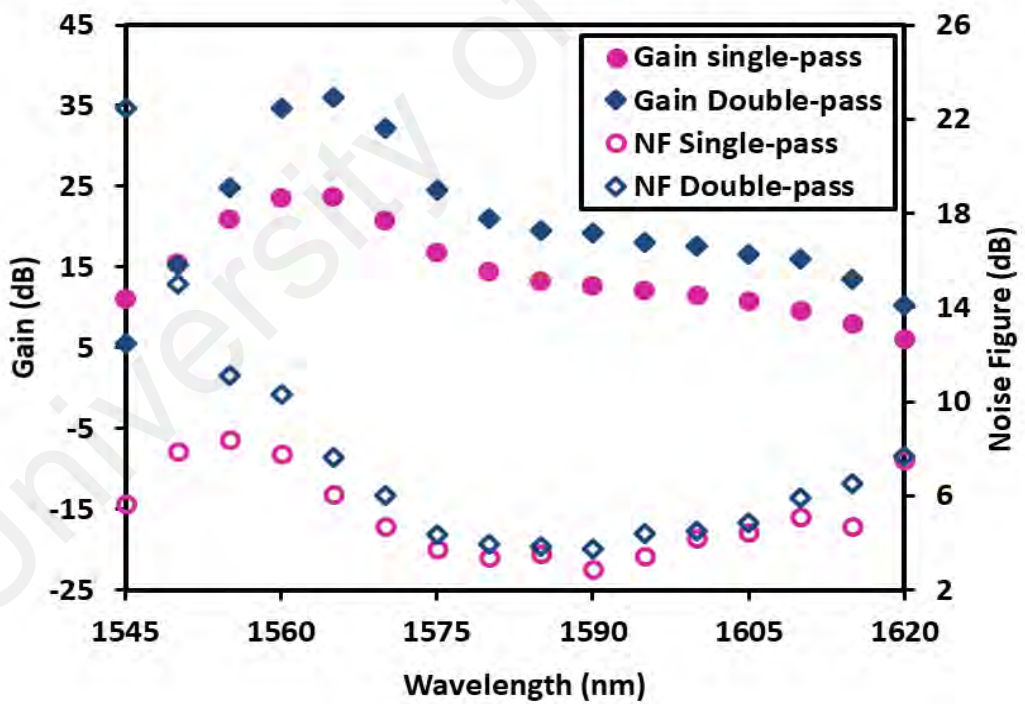
**Figure 3.16:** Gain and noise figure performances with different length of HB-EDF in double-pass setup at input signal power of (a) -10 dBm and (b) -30 dBm.

Since the use of 1.5 m long HB-EDF provided a better amplification L-band region, this length was used in the experiment to compare the performance of the single-pass and double-pass HB-EDFA. The comparison is illustrated in Figure 3.17(a) and (b), which were carried out at input signal powers of -10 and -30 dBm, respectively. In the experiment, the pump power was fixed at 170 mW. At input signal of -10 dBm as illustrated in Figure 3.17(a), the gain enhancement of 27% in double-pass as compared to that of the single-pass due to the double propagation of the signal in the gain medium, which increases the effective length of the amplifier and thus the gain. For instance, a higher flat gain of 10.3 and 15 dB were obtained with small gain fluctuation of about 1 dB within wavelength region from 1560 to 1605 nm for single and double-pass HB-EDFA, respectively. On the other hand, the higher noise figure was obtained with double-pass HB-EDFA compared to that of single-pass due to the increased backward propagating ASE power at the input part of the amplifier, which reduces the population inversion.

At input signal of -30 dBm, the gain was higher in double-pass HB-EDFA compared to that of single-pass as illustrated in Figure 3.17(b). The gain enhancement of 38% is obtained in double-pass setup as compared to that of the single-pass. The maximum gain of 24 dB and 35 dB were achieved at 1565 nm for single and double-pass configurations, respectively. This is attributed to doubly propagated the signal through the gain medium, which increased the population inversion resulting in the increment of gain in the proposed double-pass setup. The noise figure was raised of about 0.24 dB in double-pass as compared single-pass at L-band region due to the increased backward propagating ASE power at the input part of the amplifier, which reduces the population inversion. However, the noise figure is relatively higher at the shorter wavelength which is attributed to the lower gain and higher loss characteristics associated with the shorter wavelength.



(a)

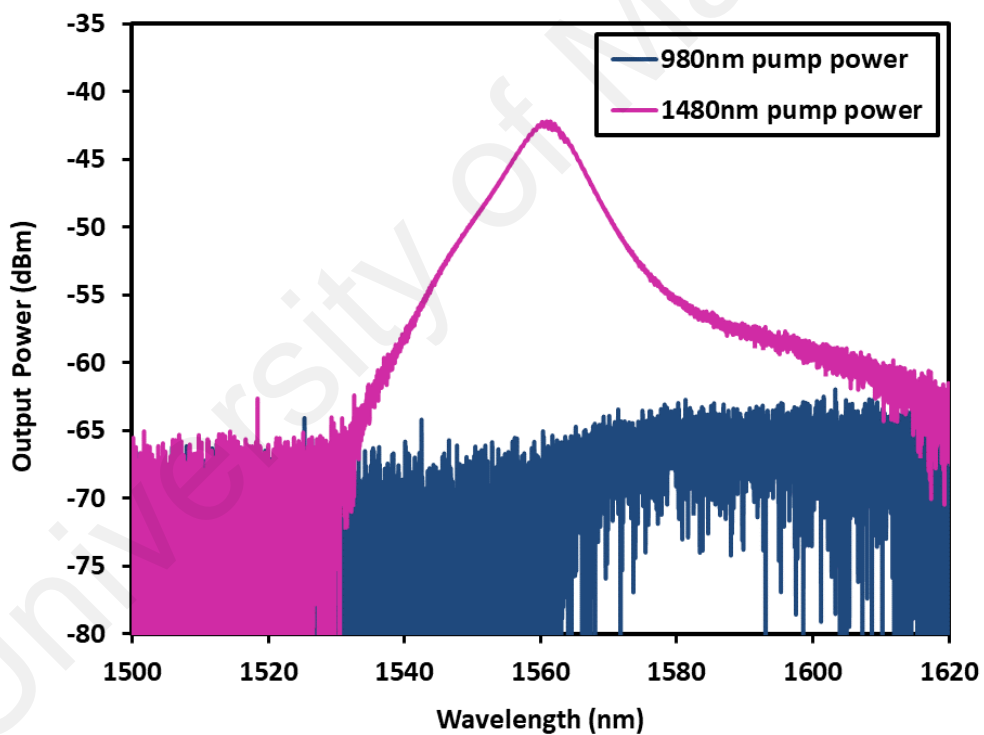


(b)

**Figure 3.17:** Gain and noise figure spectrum of single and double-pass of the 1.5 m long HB-EDFA at input signal power of (a) -10 dBm and (b) -30 dBm.

### 3.3.4 Effect of pumping wavelength

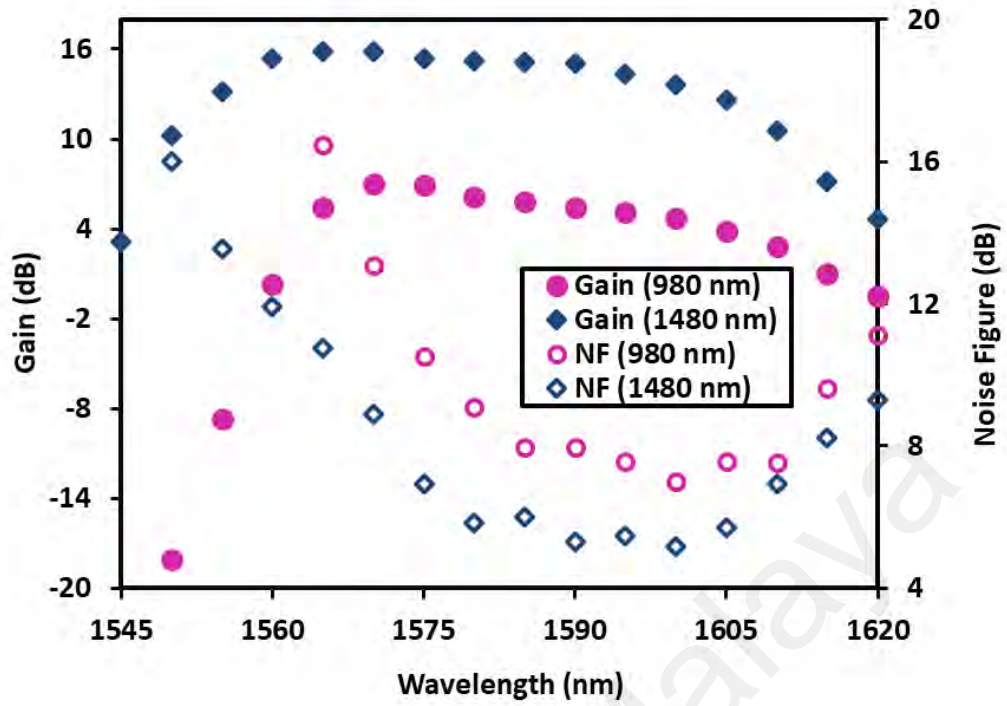
The effect of the laser diode pump wavelength was tested on the performance of the HB-EDFA within erbium fiber length of 150 cm. The EDF was forward pumped by 1480 nm then the experiment was repeated with pumping 980 nm to compare the amplified spontaneous emission (ASE) in single-pass configuration. The pump powers were fixed at 170 mW for both pump wavelengths. As depicted in Figure 3.18, the power level of the ASE was higher at 1480 nm pumping. This is attributed to the higher optical power conversion efficiency at 1480 nm pumping due to the single photon conversion process of erbium amplification.



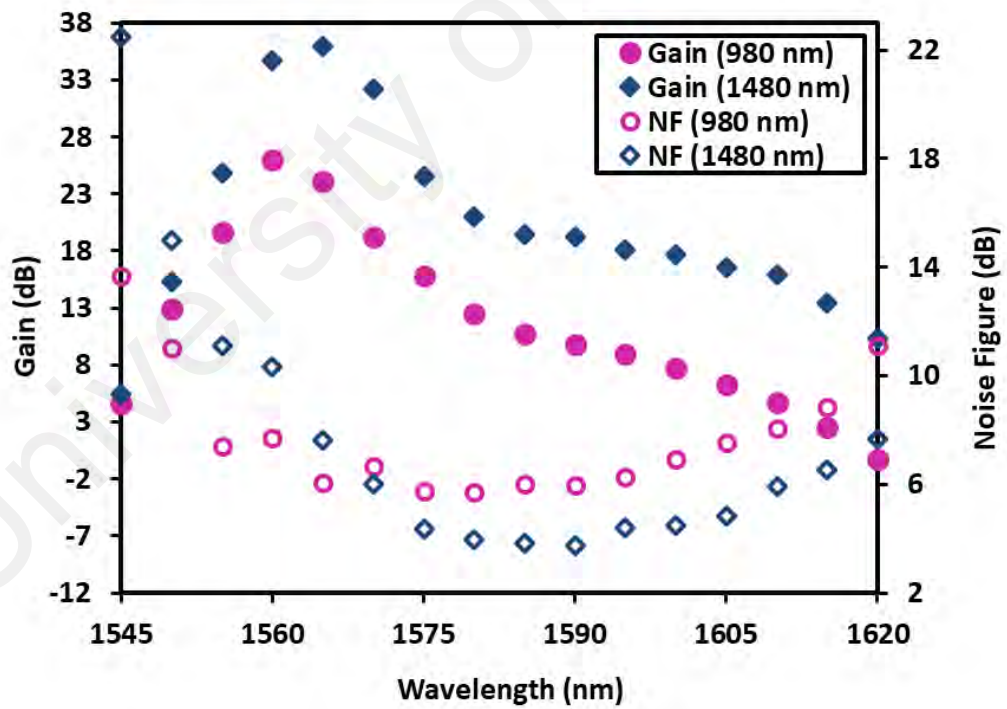
**Figure 3.18:** Comparison the characteristics of amplified spontaneous emission for HB-EDFA at two pumping wavelengths.

Figure 3.19 shows the comparison of the gain and noise figure performances of the HB-EDFA in double-pass configuration between two pumping wavelengths, 980 nm and 1480 nm pump wavelength. In the experiment, the power for both LD pumps was adjusted at 170 mW. At input signal power of -10 dBm, the gain of the amplifier that pumped at 1480 nm are higher as compared to that the one pumped at 980 nm as shown in Figure 3.19(a). The gain improvement is attributed to the efficient use of 1480 nm pump power with a long gain medium. Gain flatness around 15 dB is investigated with gain variance around 1 dB within bandwidth area from 1560 to 1605 nm when EDF pumped at 1480 nm. The corresponding noise figure of the amplifier pumped at 1480 nm is lower compared to that one pumped at 980 nm. The noise figure is continued under 10 dB within the flat gain region.

Figure 3.19(b) illustrates the EDFA performance at input signal power of -30 dBm. The average improvement of the gain about 10.1 dB is observed in L-band region when the amplifier pumped at 1480 nm. The gain improvement is attributed to the efficient use of 1480 nm pump power with a long gain medium. For instance, the maximum gain of about 25 and 36 dB at wavelength of 1560 and 1565 nm when the amplifier pumped at 980 and 1480, respectively. Furthermore, the HB-EDF that pumped at 1480 nm is provided a greater amplification bandwidth ranging from 1545 to 1620 nm. The noise figure of the amplifier pumped at 1480 nm is also lower compared to that one pumped at 980 nm. On the other hand, the noise figure is relatively higher at shorter wavelength less than 1560 nm as shown in the figure. This is attributed to the lower gain and higher loss characteristics associated with shorter wavelength region.



(a)



(b)

**Figure 3.19:** The HB-EDF amplifier characteristics in term of gain and noise figure for different pump wavelengths at two input signal powers.

### 3.3.5 Performance comparison with Zr-EDFA

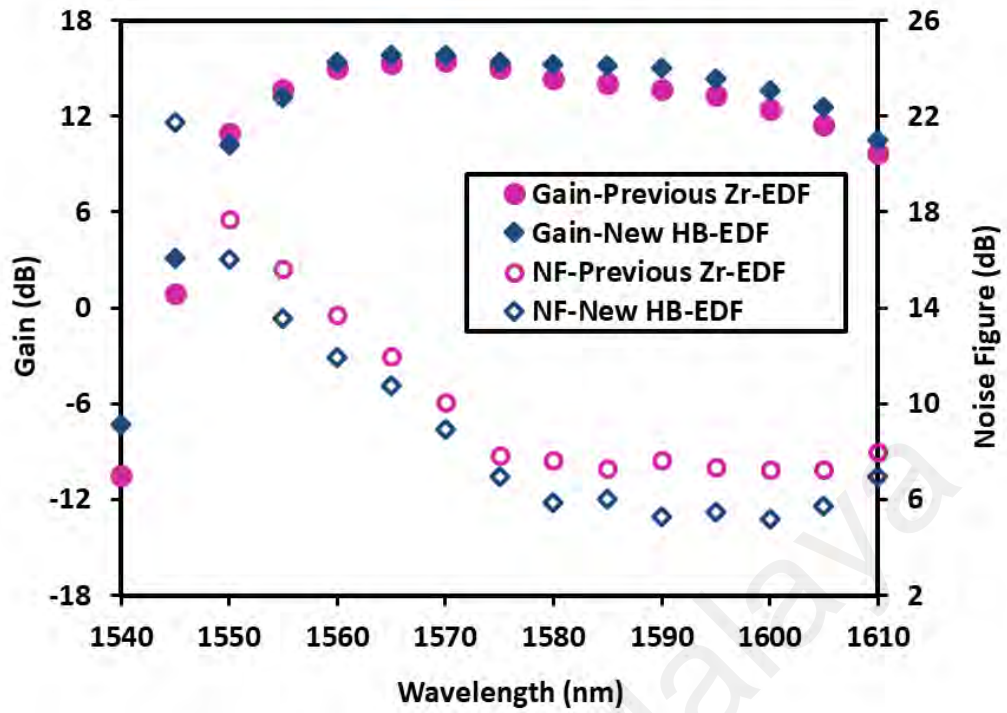
In this sub-section, the performances of HB-EDFA are compared with the Zr-EDFA. In this experiment, the 1480 nm pumping scheme was used in conjunction with double-pass configuration based on the previous finding. At first, the HB-EDFA is compared with Zr-EDFA configured with the conventional gain medium with lower concentration. The Zr-EDF has an erbium ion concentration of 2800 ppm and the optimal length for L-band amplification is 4 m. Table 3.2 illustrate the specification comparison between the conventional Zr-EDF and the new HB-EDF. In the experiment, the 1480 nm pump power was fixed at 170 mW for two input signal powers of -10 and -30 dBm. The active fiber length is fixed at optimum length of 1.5 m and 4 m for the HB-EDFA and Zr-EDFA, respectively.

**Table 3.2:** Specification comparison between the previous Zr-EDF and HB-EDF

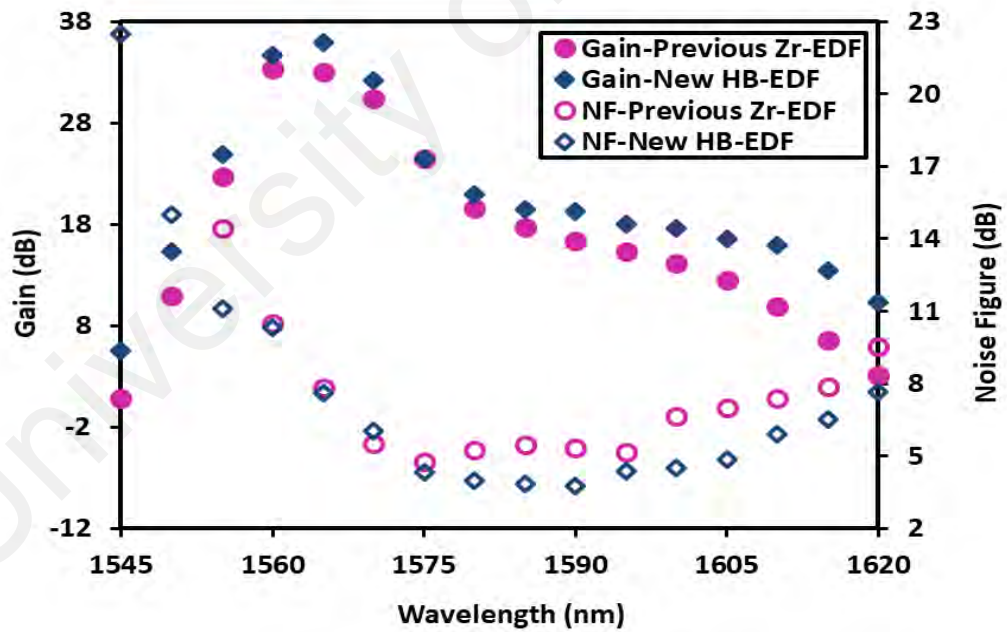
Type of fiber	The HB-EDF	Conventional Zr-EDF
Er doped ion concentration	12500 ppm	2800 ppm
Absorption loss at 980 nm	100 dB/m	14.5 dB/m
Core & Clad diameter	Core: 3.71 Clad: 123.94	Core: 10.5 Clad: 125
Numerical Aperture	0.21	0.17

At input signal power of -10 dBm, as compared with the previous Zr-EDFA, the proposed amplifier has a better gain and noise figure performances as shown in Figure 3.20(a) even though the gain medium length used is only about quarter of the Zr-EDF length. This is attributed to the population inversion which is higher in the shorter length of HB-EDF as well as the efficient use of pump power with a shorter gain medium. A high and flat gain of about 15 dB is achieved with gain fluctuation of about 1 dB within region from 1560-1605 nm for HB-EDFA. On other hand, the noise figures of the new HB-EDFA are lower compared to those of the previous Zr-EDFA. This is attributed to the higher gain and lower loss characteristics of the shorter gain medium.

At input signal power of -30 dBm shown in Figure 3.20(b), the proposed HB-EDFA has comparable performance with the conventional Zr-EDFA. However, the gain of the proposed HB-EDFA is improved at a longer wavelength. The gain was improved by about 20% at a longer wavelength region with the use of HB-EDF as the gain medium. This is attributed to the higher erbium concentration in this fiber, which increases the gain bandwidth of the amplifier to cover longer wavelength region. On the other hand, the noise figure is shown lower with the proposed HB-EDFA. This is due to the use of shorter length of EDF, which reduces the loss and thus reduces the noise figure.



(a)



(b)

**Figure 3.20:** Comparison of the gain and noise figure spectra between HB-EDFA and the conventional Zr-EDFA at input signal power of (a) -10 dBm and (b) -30 dBm.

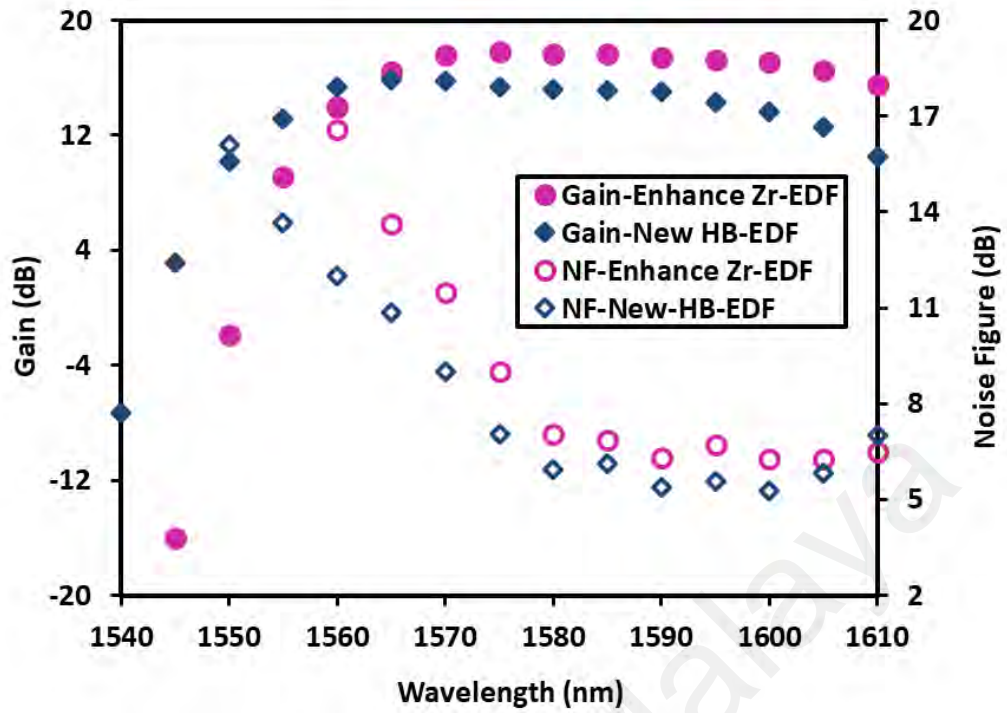
The performance of the double-pass HB-EDFA is then compared with the new Zr-EDF with a higher concentration at the optimized length of gain medium. The Zr-EDF has an erbium ion concentration of 4000 ppm and the optimal length for L-band amplification is 3 m. The HB-EDF is fixed at the optimized length of 1.5m in this experiment. Table 3.3 illustrate the specification comparison between the enhance Zr-EDF and the HB-EDF. In the experiment, the 1480 nm pump power and an input signal power were fixed at 170 mW for both amplifiers. The amplification is accomplished at two input signal powers of -10 and -30 dBm.

**Table 3.3:** Specification comparison between Enhance Zr-EDF and HB-EDF

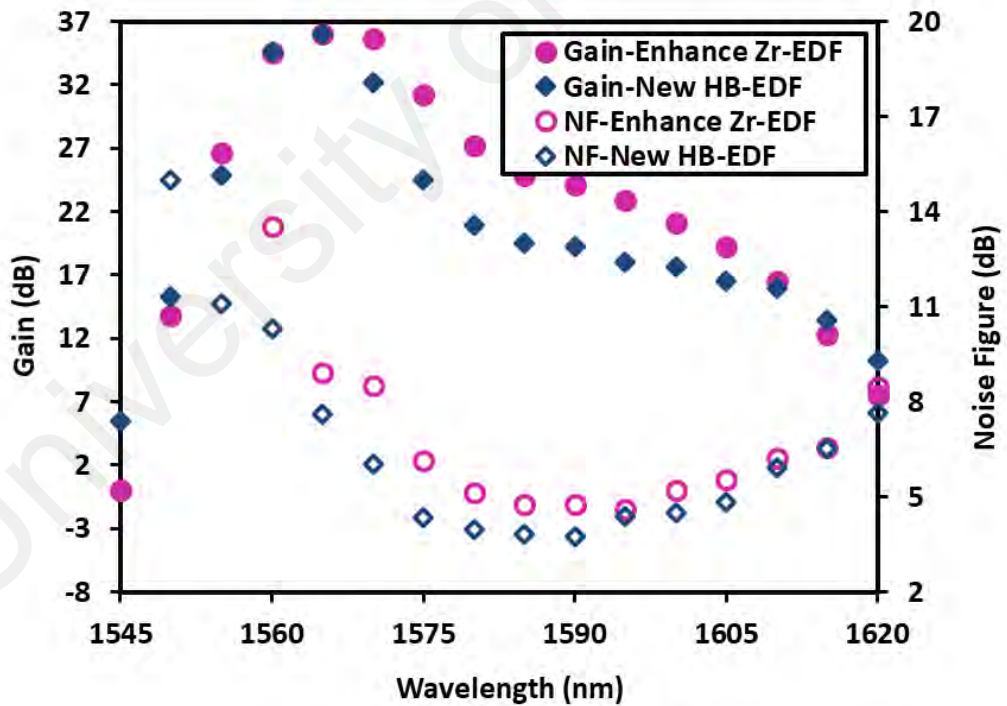
<b>Types of active fiber</b>	<b>The HB-EDF</b>	<b>Enhance Zr-EDF</b>
<b>Er doped ion concentration</b>	12500 ppm	4000 ppm
<b>Absorption loss at 980 nm</b>	100 dB/m	80 dB/m
<b>Core &amp; Clad diameter</b>	Core: 3.71 Clad: 123.94	Core: 10 Clad: 126.83
<b>Numerical Aperture</b>	0.21	0.17

As depicted in Figure 3.21(a), the Zr-EDFA has relatively higher gain as compared to that of HB-EDFA over wavelength region from 1565 to 1610 nm at input signal power of -10 dBm. However, a shorter length of 1.5 m was used for the proposed amplifier which is half of the Zr-EDF length due to high erbium ion concentration of the proposed fiber. As well, the HB-EDFA provided wider bandwidth amplification started from 1545 nm. The corresponding noise figure of the proposed HB-EDFA was lower as compared to that of Zr-EDFA. This is most probably due to the balance between the stimulated emission and energy transfer from C-band to L-band in proposed HB-EDFA.

At lower input signal power of -30 dBm, the Zr-EDFA produces a relatively higher gain as compared to that of HB-EDFA over wavelength region from 1570 to 1605 nm as shown in Figure 3.21(b). However, a shorter length of 1.5 m was used for the proposed amplifier which is half of the Zr-EDF length due to high erbium ion concentration of the proposed fiber. In addition, the HB-EDFA provides a higher gain at C-band region. For instance, the gain of HB-EDFA is higher by more than 5 dB at wavelength of 1545 nm. The corresponding noise figure of the proposed HB-EDFA was lower as compared to that of Zr-EDFA. The average spectrum of the noise figure was decreased by 15% with HB-EDFA as compared with those of Zr-EDFA.



(a)



(b)

**Figure 3.21:** Comparison of the gain and noise figure spectra between HB-EDFA and the enhanced Zr-EDFA at input signal power of (a) -10 dBm and (b) -30 dBm.

### 3.4 Summary

Experimentally, efficient L-band amplifiers were successfully achieved using two types of new Erbium-doped fiber; Zr-EDF and HB-EDF as a gain medium. Both fibers have a significantly high Erbium ions concentration and were fabricated by using MCVD in conjunction with SD process. For instance, the enhanced Zr-EDF has an absorption loss 80 dB/m, which can be translated to the erbium ion concentration of 4000 ppm. The HB-EDF, on the other hand, has an absorption loss 100 dB/m, which equivalents to the erbium ion concentration of 12500 ppm. Both fibers are suitable for L-band amplification application. It is found that the optimum length for L-band operation was 3 m and 1.5 m for the Zr-EDFA and HB-EDFA, respectively.

Both EDFs were provided higher and flatter gain in double-pass amplification as compared with single-pass amplification. For enhance Zr-EDF, a significant flat gain of about 13.3 dB was achieved with gain variance of less than 1 dB within band over 40 nm wavelength region for single-pass setup at input power of -10 dBm. However, the double-pass enhance Zr-EDFA was provided a higher and flatter gain of 17.1 dB with gain variance less than 1 dB with same wavelength region as compared with those of single-pass. The noise figure for double-pass was provided higher spectrum as compared with single-pass where, the noise figure was varied from 6 to 10 dB at high input signal power within flat region. Single-pass and double-pass Zr-EDFA comparison shows that the double pass HB-EDFA produces a better gain spectrum. The effect of changing pump wavelength on the performance of enhance Zr-EDFA were investigated. It is clearly seen that the gain of the amplifier that pumped at 1480 nm are higher as compared to that the one pumped at 980 nm for both input signal power. As compared this performance with the previous fiber which is the conventional Zr-EDF, the enhance one provided better and higher gain and lower noise figure at L-band region. The conventional Zr-EDF has an Erbium ions concentration of 2800 wt. ppm and the absorption loss at 980 nm is 14 dB/m.

It is observed that the enhance Zr-EDFA provided higher and flatter gain of about 17.1 dB while a slightly flat gain of about 15 dB was achieved with the conventional Zr-EDFA within L-band wavelength region.

For new HB-EDF, an efficient flat gain of about 15 dB was achieved at gain variance of around 1 dB over wavelength area from 1560 to 1605 nm in double-pass configuration. At low input signal power of -30 dBm, the maximum gain of 36 dB was obtained at wavelength of 1565 nm for double-pass HB-EDFA. The noise figure was maintained below 9 dB within the L-band region. The effect of changing pump wavelength on the performance of HB-EDFA were investigated. It is clearly seen that the gain of the amplifier that pumped at 1480 nm are higher as compared to that the one pumped at 980 nm for both input signal power. As compared HB-EDFA performance with the previous Zr-EDFA, the proposed amplifier which is used length reach to quarter of the Zr-EDF length, has slightly comparable performance. On other hand, the noise figures of the new HB-EDFA are lower compared to those of the previous Zr-EDFA.

Finally, the performance of HB-EDFA was compared with enhance Zr-EDFA performance in double-pass configuration. Both EDFs were pumped by 1480 nm laser diode and the maximum pump power is fixed at 170 mW. The comparison observed that the Zr-EDFA has relatively higher gain as compared to that of HB-EDFA over wavelength region from 1565 to 1610 nm at input signal power of -10 dBm. However, a shorter length of 1.5 m was used for the HB-EDF amplifier which is half of the Zr-EDF length due to high erbium ion concentration of the HB-EDF. As well, the new HB-EDFA provided wider bandwidth amplification started from 1545 nm. The corresponding noise figure of the proposed HB-EDFA was lower as compared to that of Zr-EDFA.

## CHAPTER 4: WIDE-BAND AND FLAT GAIN ERBIUM DOPED FIBER AMPLIFIER USING PARALLEL CONFIGURATION

### 4.1 Introduction

The tremendous growth of the internet and data traffic has created an enormous demand for transmission bandwidth of dense wavelength-division-multiplexed (DWDM) optical communication systems (Lopez-Amo et.al. 1993; Mochida et.al. 2002). This has led to the development of compact wide-band amplifiers with a very short gain medium length (Hamzah et.al. 2011; Harun et.al. 2010; Long et.al. 2011; Paul et.al. 2010; Qui et.al. 2010). The active fiber with high concentration doping of erbium ions is used to compensate for the short gain medium length. However, a high concentration erbium ion may result in a pair induced quenching effect, which potentially reduces the pump power conversion efficiency and increase the noise figure for an Erbium-doped fiber amplifier (EDFA). Several techniques have been proposed and demonstrated by using different glass hosts such as telluride (Ohishi et.al. 1998; Yang et.al. 2010), bismuth (Cheng et.al. 2009; Hayashi et.al. 2006; Ohara et.al. 2008), and ytterbium (Li et. al. 2009; Harun et. al. 2006; Vienne et. al. 1998; Wysocki et. al. 1996), to increase the limit of erbium doping concentration while maintaining the transmission capacity. In the previous chapter, new efficient and flat gain optical amplifiers operating in long-wavelength band (L-band) region were proposed and demonstrated using two types of highly doped Erbium-doped fibers; Zirconia Erbium co-doped fiber (Zr-EDF) and Hafnium Bismuth Erbium co-doped fiber (HB-EDF) as a gain medium.

On the other hand, a wide-band amplifier is normally constructed by cascading two amplifiers, where the multiplexing (WDM) coupler, amplified by amplifiers that are suitable for the corresponding wavelength band, and finally multiplexed again with another WDM coupler. In this chapter, wide-band and flat gain optical amplifiers are

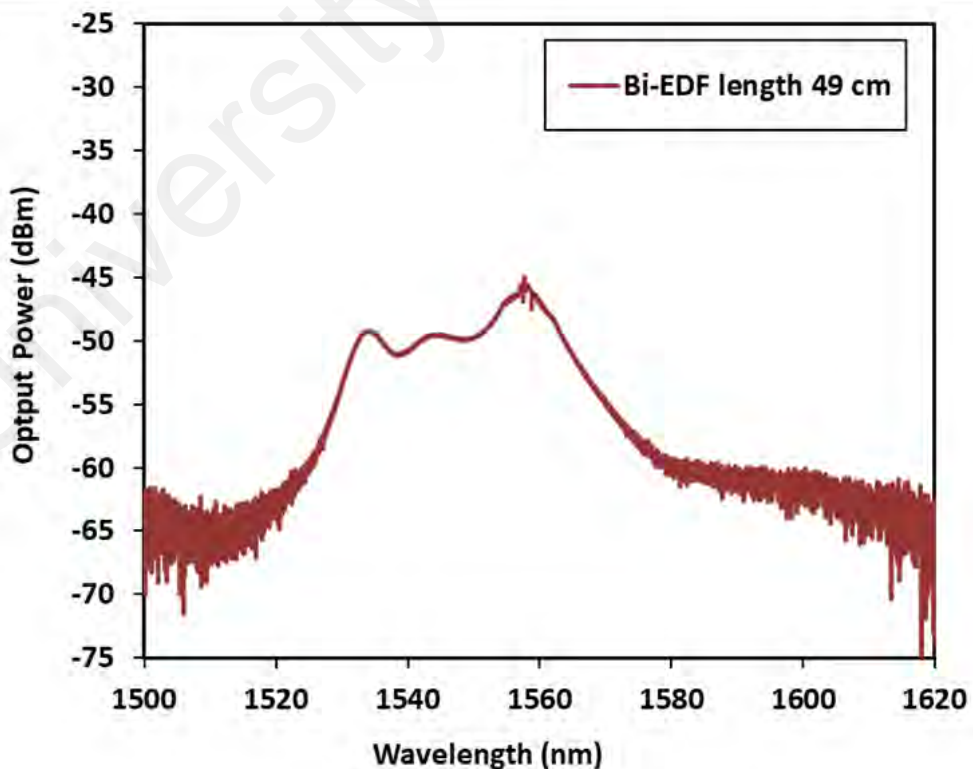
demonstrated using dual-stage erbium doped fiber amplifier (EDFA) based on parallel configuration. The amplifier employs the previously developed Zr-EDF and HB-EDF, which were optimized for L-band operation in conjunction with a commercial Lanthanum Erbium co-doped fiber, which was fabricated in Bismuth oxide ( $\text{Bi}_2\text{O}_3$ ) glass host (Bi-EDF) operating in conventional band (C-band) region. At first, an efficient C-band EDFA is developed using a 49 cm long Bi-EDF as the gain medium. The wide-band optical amplifier is then developed by combining the C-band Bi-EDF amplifier (Bi-EDFA) with the L-band HB-EDF amplifier (HB-EDFA) in parallel configuration. The performance of the hybrid wide-band amplifier is also investigated by replacing the Bi-EDF or HB-EDF with Zr-EDF for C-band and L-band stage, respectively. Finally, the experiment is repeated using only Zr-EDF for both C-band and L-band stages for comparison purpose.

#### **4.2 Development of efficient Bi-EDFA**

Many researchers have focused on high silica glass in the choice of glass host due to its proven reliability and compatibility with conventional fiber-optic components. However, the commercial Bi-EDF used in this study was fabricated by co-doping Lanthanum and Erbium ions into a  $\text{Bi}_2\text{O}_3$  glass host using melting and casting method. The single mode fiber has a cladding diameter of 125  $\mu\text{m}$ , which was protected by a plastic coating. The core of the fiber has erbium and lanthanum ions concentration of 3250 wt.ppm and 4.4 wt%, respectively. The absorption loss of the fiber was at rate of 0.55 dB/m and 141 dB/m at 980 and 1480 nm, respectively. The mode field diameter and the refractive index at 1550 nm were set to be 6.21  $\mu\text{m}$  and 2.03, respectively. The numerical aperture (NA) of the fiber were 0.20. However, this type of fiber cannot be spliced with a standard single-mode fiber (SMF) using the standard splicing machine owing to the difference in melting temperature. In this work, the Bi-EDF was fusion-spliced to high

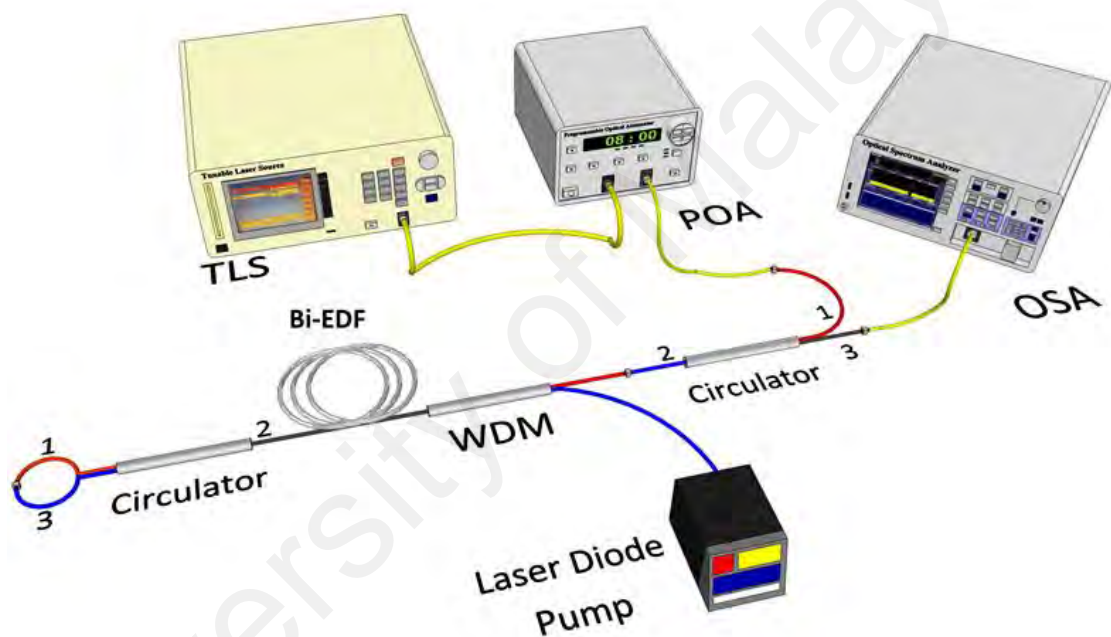
NA fibers (Corning HI980) using a special fusion-splicer and the average splice loss was estimated to be less than 0.5 dB/point. Angled-cleaving and splicing were applied to suppress the reflection due to the large refractive index difference between the Bi-EDF and silica fiber. Mixed angle which satisfies Snell's law was also adopted to reduce the coupling loss ( $6^\circ$  for Bi-EDF,  $8^\circ$  for silica fiber).

At first, the amplified spontaneous emission spectrum (ASE) of the Bi-EDF is investigated. In the experiment, the 49 cm long fiber was forward pumped with a 1480 nm laser diode. The 1480 nm pump wavelength was used since the cut-off wavelength of the Bi-EDF was 1440 nm to maintain the single-mode propagation inside the fiber. Due to this reason, 1480 nm pumping provides a higher efficiency compared to that of 980 nm pumping. Figure 4.1 shows the ASE for the Bi-EDFA at 1480 nm pump power of 170 mW. As shown in figure, the ASE spectrum operates efficiently within a wavelength region from 1520 nm to 1580 nm. The peak power is observed at 1555 nm.



**Figure 4.1:** ASE spectrum for the Bi-EDFA at 170 mW pump power.

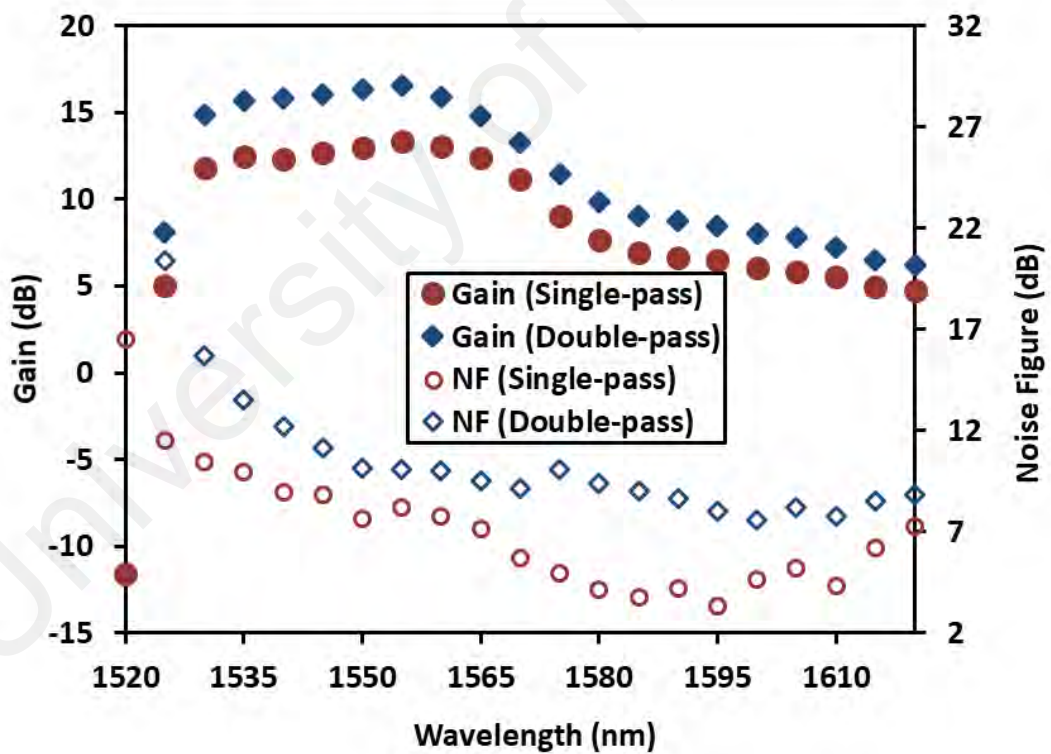
Figure 4.2 shows the experimental setup for the double-pass Bi-EDFA. This configuration is used to investigate the gain performance of the Bi-EDFA due to its advantages as discussed in the previous chapter. The performance of the double-pass Bi-EDFA is also compared to that of the single-pass Bi-EDFA, which was obtained by removing the optical circulators and measuring the amplified signal at the output end of the EDF.



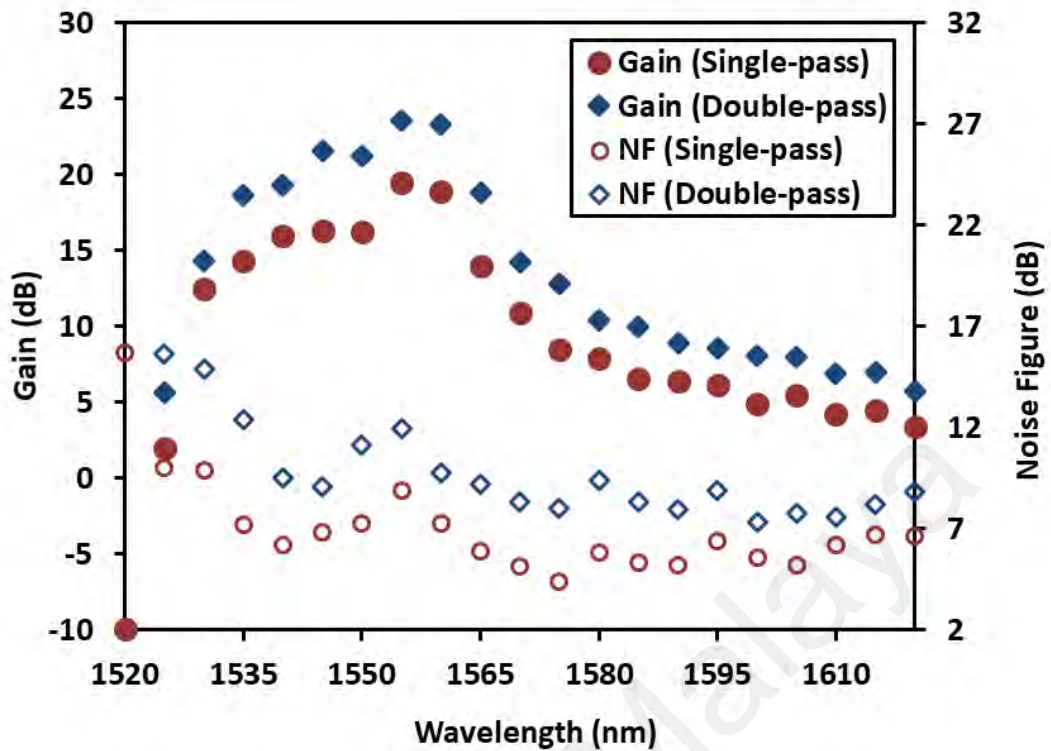
**Figure 4.2:** Double-pass configuration for Bi-EDFA.

Figure 4.3(a) and (b) illustrate the gain and noise figure performances of Bi-EDFA with 49 cm at two input signal power of -10 and -30 dBm, respectively. In the experiment, the 1480 nm pump power is fixed at 170 mW. At input signal power of -10 dBm, the gain enhancement of 24% in double-pass as compared to that of the single-pass due to the double propagation of the signal in the gain medium, which increases the effective length of the amplifier and thus the gain. As shown in Figure 4.3(a), a flat gain around 12.4 and

15.4 dB are achieved with gain fluctuation about 1 dB within wavelength region from 1530 to 1570 nm for single and double-pass, respectively. As depicted in Figure 4.3(b), the gain is higher in the double-pass Zr-EDFA compared to that of single-pass at input signal power of -30 dBm due to same reason as explained earlier. On the other hand, the noise figure is higher in the double-pass configuration compared to that of the single-pass. This is attributed to the increased backward propagating ASE power at the input part of the amplifier, which reduces the population inversion. The noise figure is relatively higher at the shorter wavelength which is attributed to the lower gain and higher loss characteristics associated with the shorter wavelength.



(a)



(b)

**Figure 4.3:** Single and double-pass comparison for Bi-EDFA at two input signals power of (a) -10 dBm and (b) -30 dBm.

Figure 4.4 shows the gain and noise figure performances against pump power for both input signals power of -30 dBm and -10 dBm. In the experiment, the TLS is fixed at 1550 nm and the pump power is varying from 10 to 170 mW. In order to obtain saturation state, the input signal power of -10 dBm requires high pump power as compared to input signal power of -30 dBm. As shown in Figure, the saturation gain occurs when the pump power is increased beyond 80 and 170 mW at low input signal power of -30 dBm. However, the saturation gain occurs when the pump power is increased beyond 110 mW at high input signal power of -10 dBm.

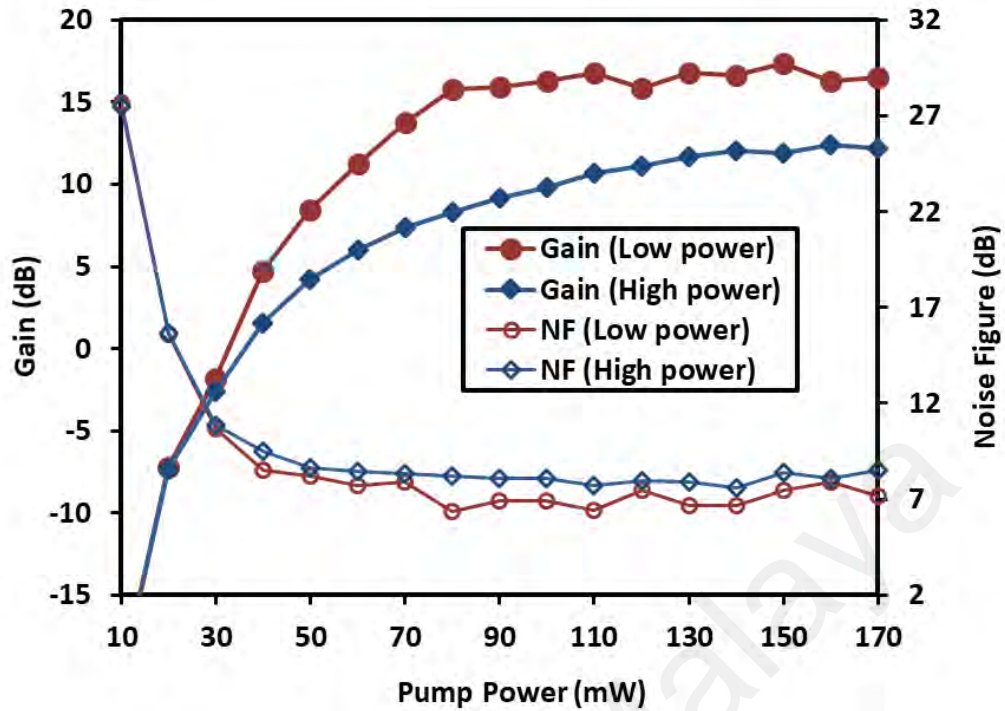


**Figure 4.4:** Gain and noise figure performances of Bi-EDFA against pump power at two input signals power of -30 dBm and -10 dBm.

### 4.3 Wide-band and flat gain optical amplifier using a hybrid gain medium

Figure 4.5 shows the proposed hybrid amplifier which utilizes Bi-EDF and HB-EDF as gain media in double-pass parallel configuration. The HB-EDF has an erbium ion concentration of 12500 ppm. Table 4.1 summarizes the optical characteristics for Bi-EDF and HB-EDF. The 49 cm long of Bi-EDF and 150 cm long of HB-EDF were placed in first and second stage to provide the amplification in C- and L-band region, respectively. Both fibers were forward pumped by 1480 nm via wavelength division multiplexing (WDM) coupler. A C/L-band coupler was used to separate/combine both C- and L-band signals into/from first and second stage, respectively. Three optical circulators were used in the proposed configuration. The first one was act as isolator to prevent reverse direction of amplified spontaneous emission (ASE). In addition, it was used to forward the input

signal into the C/L band coupler and rotate the amplified signal into the optical spectrum analyser (OSA). The second and third circulators were used to act as mirrors and thus allow double propagation of the amplified signal in the gain medium. By jointing port 3 of the circulator with port 1, the light launched into the device is forced to return into port 2. A tunable laser source (TLS) was used to launch an input signal to the amplifiers while a programmable optical attenuator (POA) was used to obtain the accurate power of the input signal. All outputs were measured using the OSA.

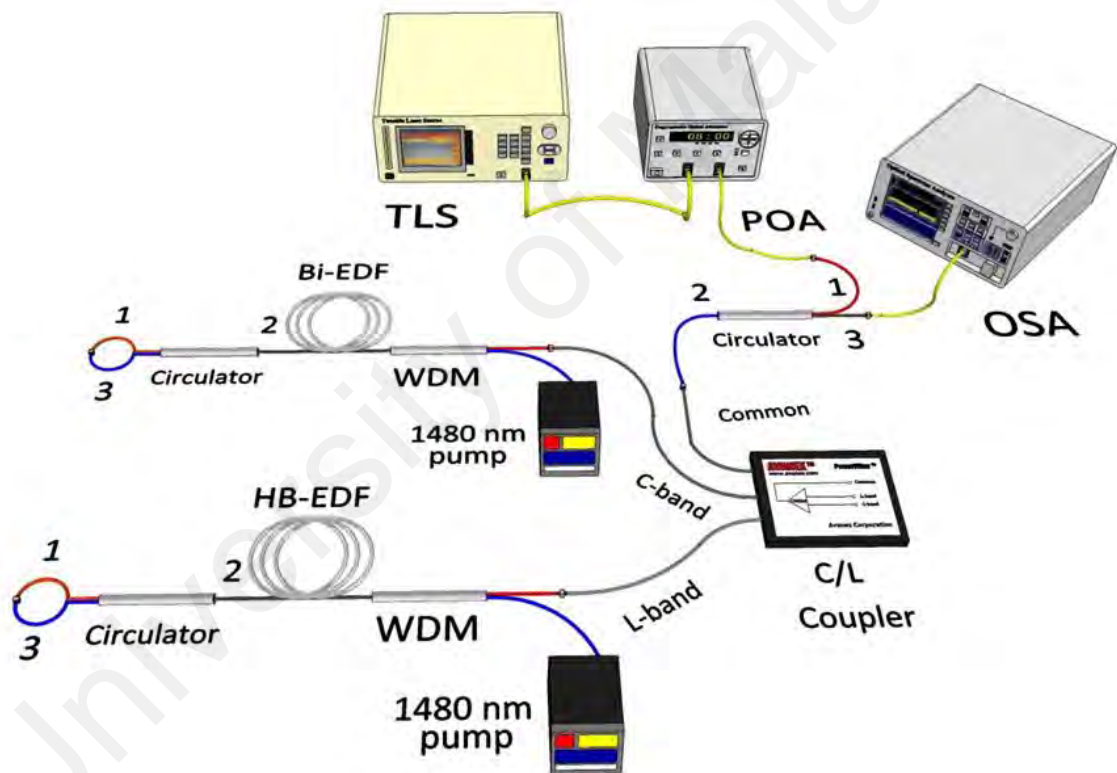


**Figure 4.5:** Dual-stage configuration for the proposed hybrid amplifier.

**Table 4.1:** The specification of the Bi-EDF and HB-EDF

<b>Parameters</b>	<b>Bi-EDF</b>	<b>HB-EDF</b>
<b>Core diameter</b>	1.72 $\mu\text{m}$	3.71 $\mu\text{m}$
<b>Numerical aperture</b>	0.20	0.23
<b>MFD</b>	6.21 $\mu\text{m}$	4.5 $\mu\text{m}$
<b>Cut-off wavelength</b>	1440 nm	1050 nm
<b>Erbium ion concentration</b>	3250 wt. ppm.	12500 wt. ppm

Figure 4.6 shows the gain and noise figure performances of the proposed wide-band amplifier for three different lengths of HB-EDF (100, 150 and 200 cm) at the L-band stage when the Bi-EDF of the C-band stage was fixed at 49 cm. In the experiment, the input signal power was fixed at -10 dBm. As shown in the figure, the optimum length of the HB-EDF was around 150 cm since a higher flat gain was observed at wider wavelength region ranging from 1535 nm to 1605 nm. At 100 cm length of HB-EDF, the gain spectrum was shifted to C-band region. For instance, the gain decreased from 14 dB to 11.4 dB at 1585 nm when the length was changed from 150 to 100 cm. This is due to decrease in the number of erbium ions in the gain medium which in turn reduce the population inversion and thus, decrease the gain for the L-band region. The gain spectrum was not significantly reduced at 200 cm long HB-EDF due to insufficient pump power to support population inversion with a longer gain medium. However, a flat gain of 6.3 dB was obtained within wavelength region from 1570 to 1610 nm with the use of 200 cm long HB-EDF. The gain spectrum of the C-band was unchanged due to the fixed length

of Bi-EDF. On the other hand, the highest noise figure was obtained at 200 cm which is attributed to the lower gain and higher loss characteristic at the L-band region. However, the noise figure spectrum was maintained below 9 dB for the L-band operation at 150 cm.

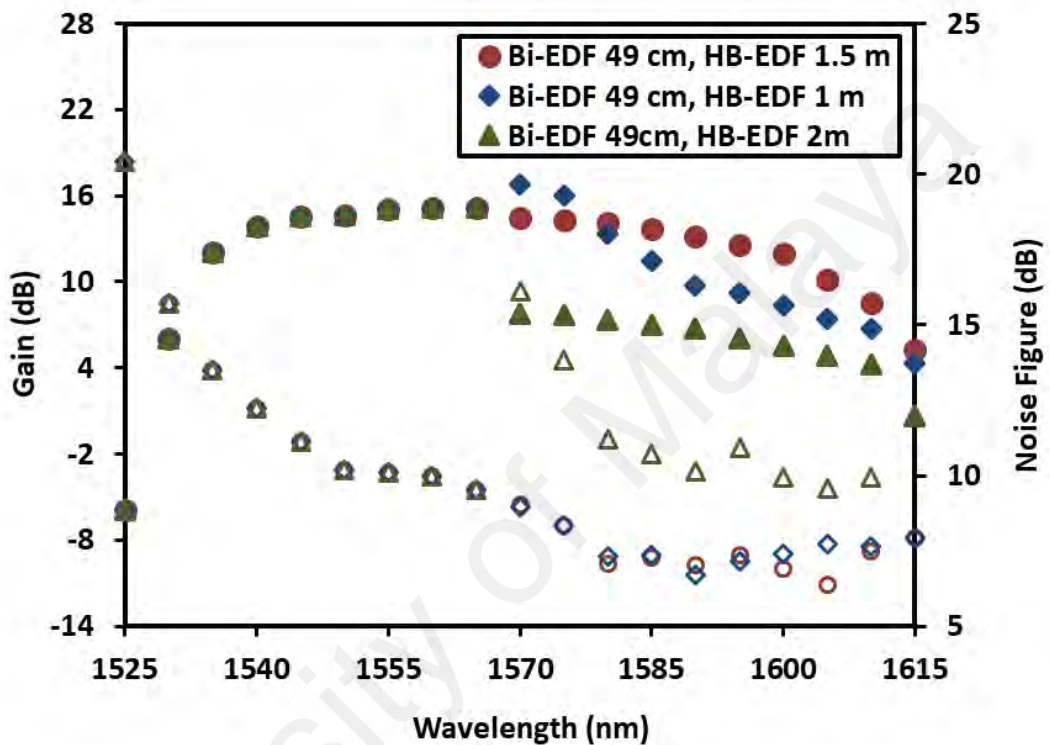


**Figure 4.6:** Gain (solid symbol) and noise figure (hollow symbol) performances of the parallel amplifier at different length of HB-EDF for L-band region at input signal power of -10 dBm.

Since the optimum length for the wide-band amplification is obtained at 49 and 150 cm for Bi-EDF and HB-EDF, respectively; this amplifier was measured at two input signals power -10 dBm and -30 dBm as illustrated in Figure 4.7. Both fibers were forward pumped by 1480 nm laser diodes which were set at powers of 90 and 170 mW for the first and second stages, respectively. For input signal power of -30 dBm, a wide-band amplification from 1535 to 1590 nm was demonstrated with gain variation from 13 to 27

dB. The gain was suddenly jumped to 27 dB at wavelength of 1560 nm due to the shift in the amplification medium from Bi-EDF to HB-EDF. At input signal power of -10 dB, a flat gain of about 14 dB was investigated with small gain fluctuation of less than 1.5 dB over 75 nm wavelengths from 1535 to 1605 nm. As depicted in the figure, the corresponding noise figures were maintained below 12 dB over wide-band region for both input signal powers.

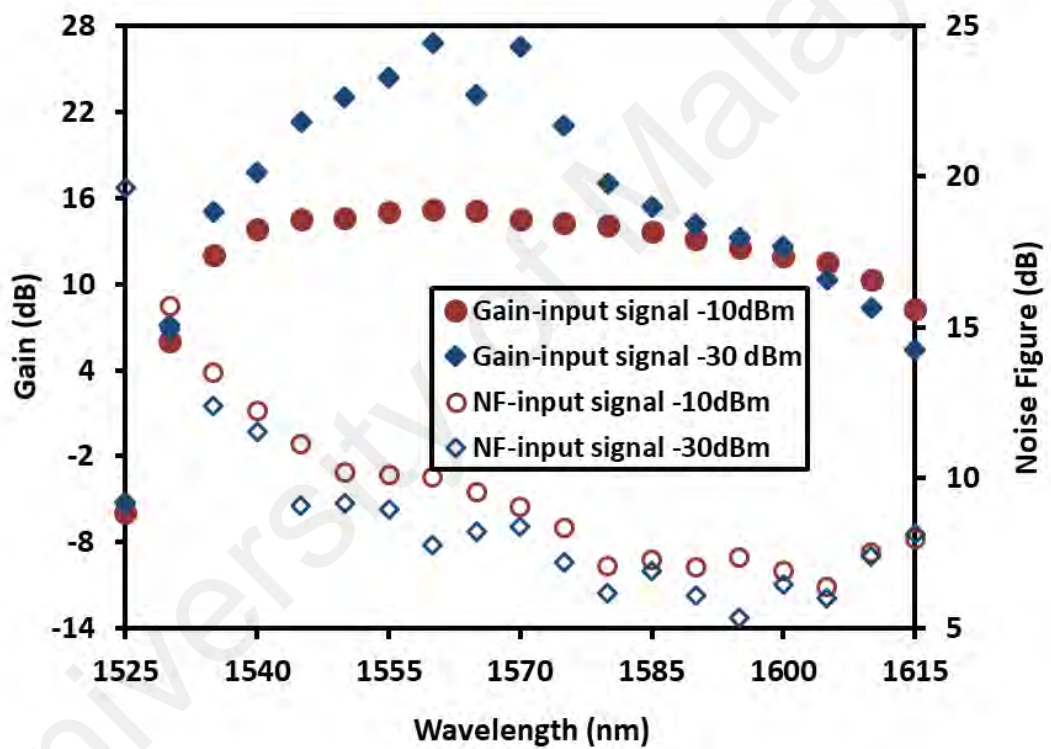
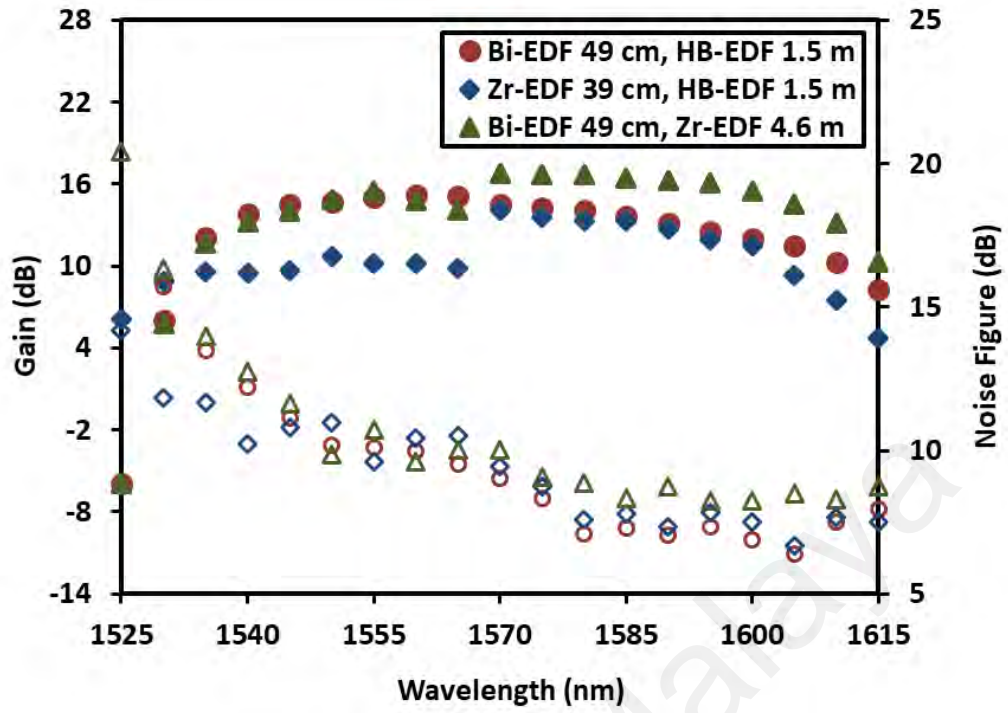


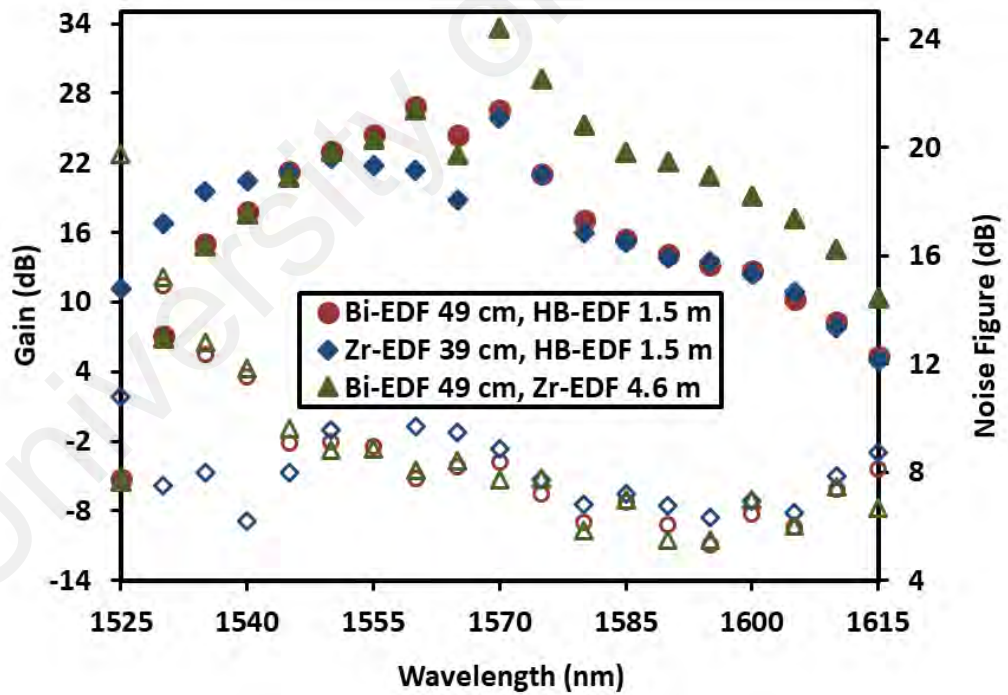
**Figure 4.7:** Gain and noise figure spectrum characteristics for the proposed wide-band amplifier with parallel configuration at two different input signal powers of -30 and -10 dBm.

For comparison purpose, the experiment is repeated by replacing either Bi-EDF or HB-EDF with Zirconia Erbium co-doped fiber (Zr-EDF). The Zr-EDF is also a highly concentrated EDF and it has an erbium ion concentration of 4000 ppm, which is slightly higher than Bi-EDF. The core diameter and NA of the Zr-EDF are 10.04  $\mu\text{m}$  and 0.17, respectively. The fiber has absorption losses of 120 dB/m and 80 dB/m at 1480 nm and 980 nm, respectively. For fair comparison, at first, the 49 cm long of Bi-EDF was replaced with 39 cm long of Zr-EDF. Later, the 1.5 m long HB-EDF was replaced with 4.6 m long of Zr-EDF. All fibers are forward pumped by 1480 nm laser diode at the optimum pump power. The pump powers are optimum at 90 and 170 mW for C- and L-band stages, respectively.

Figure 4.8 illustrates the performance comparison of these hybrid amplifiers over 70 nm wavelength span at two input signal powers of -10 and -30 dBm. At input signal power of -10 dBm (see Figure 4.8(a)), the amplifier with a combination of Bi-EDF and Zr-EDF for C- and L-band stages, respectively; shows a high flat gain of about 15 dB with gain fluctuation of less than 2 dB within wavelength region from 1540 nm to 1610 nm. This amplifier is using a hybrid gain medium with total length of 5.1 m. Another amplifier uses a shorter length of gain medium by combining Zr-EDF and HB-EDF for C- and L-band stages, respectively. Even though the number of Erbium ions is almost similar to the previous hybrid amplifier, this amplifier produces a lower flat gain of about 11.3 with gain variation of 2 dB over wavelength region from 1535 nm to 1605 nm. The gain reduction is attributed to inefficient Erbium ions doping in the Zr-EDF compared to the Bi-EDF. The clustering of Erbium ions in this fiber may reduce the population inversion and thus the gain for C-band region.



(a)



(b)

**Figure 4.8:** Gain (solid symbol) and noise figure (hollow symbol) performances of different parallel hybrid amplifier at input signal power of (a) -10 dBm and (b) -30 dBm.

In the third configuration of the hybrid amplifier, which combines 49 cm long Bi-EDF and 1.5 m long HB-EDF for C- and L-band stages, respectively, a flat gain of 14 dB was achieved within 75 nm wavelength span. This amplifier uses only 1.99 m long of hybrid gain medium, but producing an efficient, flat and wide gain spectrum. This result shows that the increase of Erbium ion concentration in a gain medium slightly reduces the efficiency of the population inversion.

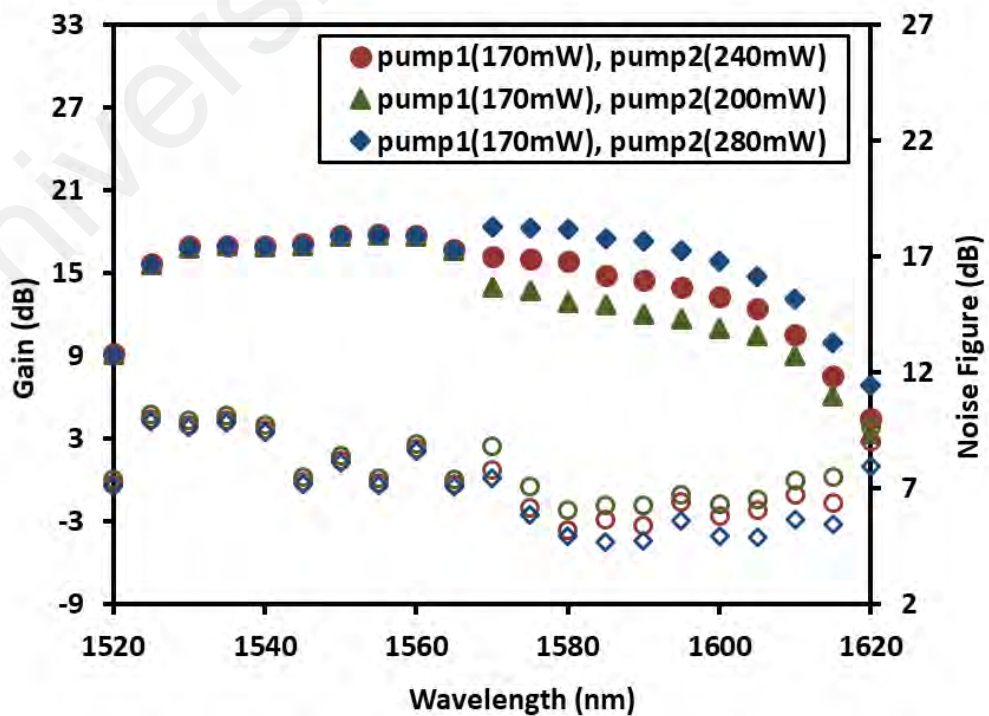
Figure 4.8(b) shows the performance of the hybrid amplifiers at low input signal power of -30 dBm. In the experiment, the pump powers are fixed at 90 and 170 mW for C- and L-band stages, respectively. The gain and noise figure of these amplifiers were investigated at 75 nm wavelength region. The highest gain spectrum was obtained with the use of Bi-EDF and Zr-EDF as the hybrid gain medium. This is attributed to both active fibers, which have a relatively lower Erbium concentration and thus improves the amplification performance especially at L-band region. However, the gain spectrum for the hybrid amplifier is slightly flatter with the combination of Bi-EDF and HB-EDF. An average gain of 19 dB is obtained at wide-band wavelength region from 1535-1610 nm in this amplifier. At 1570 nm, the gain is suddenly increase to high level due to shift in the amplification medium from short to long fiber length. Table 4.2 summarizes the performance comparison of these hybrid amplifiers.

**Table 4.2:** Summary of the amplification performance of the hybrid amplifiers.

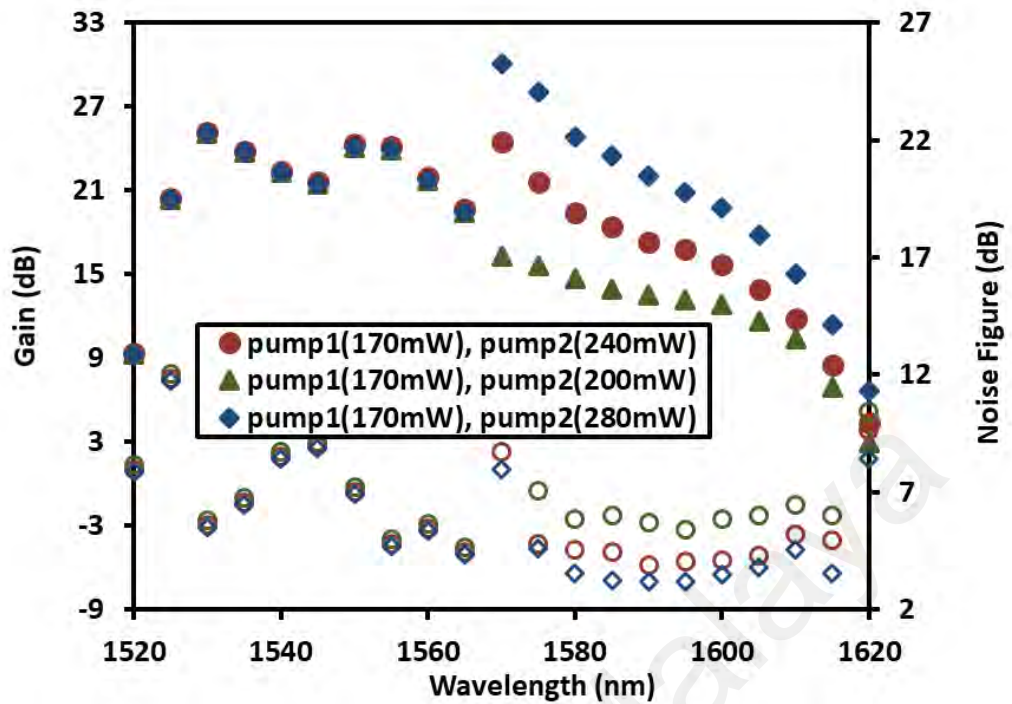
Amplifiers	At high input signal power of -10 dBm	At low input signal power of -30 dBm
A combination of Bi-EDF and Zr-EDF	Total length= 5.1 m. Flat gain= 15 dB Gain fluctuation= 1.8 dB Wavelength span= 75 nm. Wide-band=1540-1610 nm. NF= varied from 8-13 dB.	Maximum gain= 33.6 dB at 1570 nm. Higher gain spectrum is observed at L-band region. Wide-band operation from 1530-1620 nm.
A combination of Zr-EDF and HB-EDF	Total length= 1.86 m. Flat gain= 11.3 dB Gain fluctuation= 2.1 dB Wavelength span= 75 nm. Wide-band=1535-1605 nm. NF= varied from 6.6-12 dB.	maximum gain= 25.8 dB. High gain spectrum is observed at C-band region. Wide-band operation from 1530-1620 nm.
A combination of Bi-EDF and HB-EDF	Total length= 1.99 m. Flat gain= 14 dB. Gain fluctuation= 1.5 dB. Wavelength span= 75 nm. Wide-band=1535-1605 nm. NF= varied from 6-12 dB.	Maximum gain= 26.59 dB. Slightly high gain spectrum is observed at C- and L-band regions. Wide-band operation from 1530-1620 nm

#### 4.4 Wide-band and flat gain using enhanced Zr-EDF as gain medium

In this section, an efficient wide-band flat gain EDFA is demonstrated using two pieces of Zr-EDFs as a gain medium, with total length of 3.5 m in double-pass dual-stage parallel configuration. In order to improve the flatness of the gain spectrum, the pump power of second stage, which controlling the L-band gain is varied while the pump power of the first stage is fixed at 170 mW. Figure 4.9 shows the performance of the proposed amplifier at various pump powers for input signal powers of -10 and -30 dBm. At input signal of -10 dBm, the gain of L-band region is slightly improved about 2.2 dB when the pump power increases from 200 to 280 mW. For instance, at 1570 nm, the gain increases from 13.9 to 18.3 dB as the pump change from 200 to 280 mW. The small gain variation is due to the saturation effect. The optimum pump power for flat gain operation is observed to be around 280mW as shown in Figure 4.9(a). A wide-band and flat gain of 17.2 dB is obtained with gain fluctuation less than 1.5 dB within wavelength region from 1525 to 1600 nm as well as the noise figure is maintained below 10 dB within this region.



(a)



(b)

**Figure 4.9:** Gain (solid symbol) and noise figure (hollow symbol) spectrum of single and double-pass of the 3 m long Zr-EDFA at input signal power of (a) -10 dBm and (b) -30 dBm.

At input signal power of -30 dBm, the L-band gain also increases when the pump power increases from 200 to 280 mW as shown in Figure 4.9(b). Furthermore, the noise figure spectrum decreases when the pump power increases from 200 to 280 mW. As illustrate from the figure, it is found that the average gain is achieved at approximately 25 dB within a wide-band wavelength region from 1525 to 1600 nm at the optimum pump power of 280 mW. However, the gain suddenly increases to 30 dB at wavelength 1570 nm. This is attributed to the shift in amplification medium from the short length of 0.5 m to the longer length of 3 m. The noise figure is maintained below 12 dB with that wavelength region. Figure 4.10 shows the gain and noise figure performances of the proposed amplifier at three different lengths of Zr-EDF (0.5, 1 and 2 m) at the first stage, which controlling the C-band gain while the Zr-EDF of the second stage, which

controlling L-band was fixed at 3 m. In the experiment, the input signal power was fixed at -10 dBm. The optimum Zr-EDF length for the first stage was observed to be around 0.5 m whereas the higher and flatter gain was observed over 75 nm wavelength span as shown in Figure 4.10. As also seen in the figure, the 1550 nm gain decreased from 17.6 dB to 9.4 dB when the fiber length increased from 0.5 to 2 m. At the active fiber length of 2 m, the gain spectrum is shifted to longer wavelength and reduces the C-band gain significantly. This is due to insufficient pump power to support population inversion with a longer gain medium. The gain spectrum of the L-band was unchanged due to fixed length of 3 m for Zr-EDF. On the other hand, the highest noise figure was obtained at 2 m which is attributed to the lower gain and higher loss characteristics associated with the shorter wavelength. However, the noise figure spectrum was maintained below 9 dB for the C-band operation at 0.5 m.

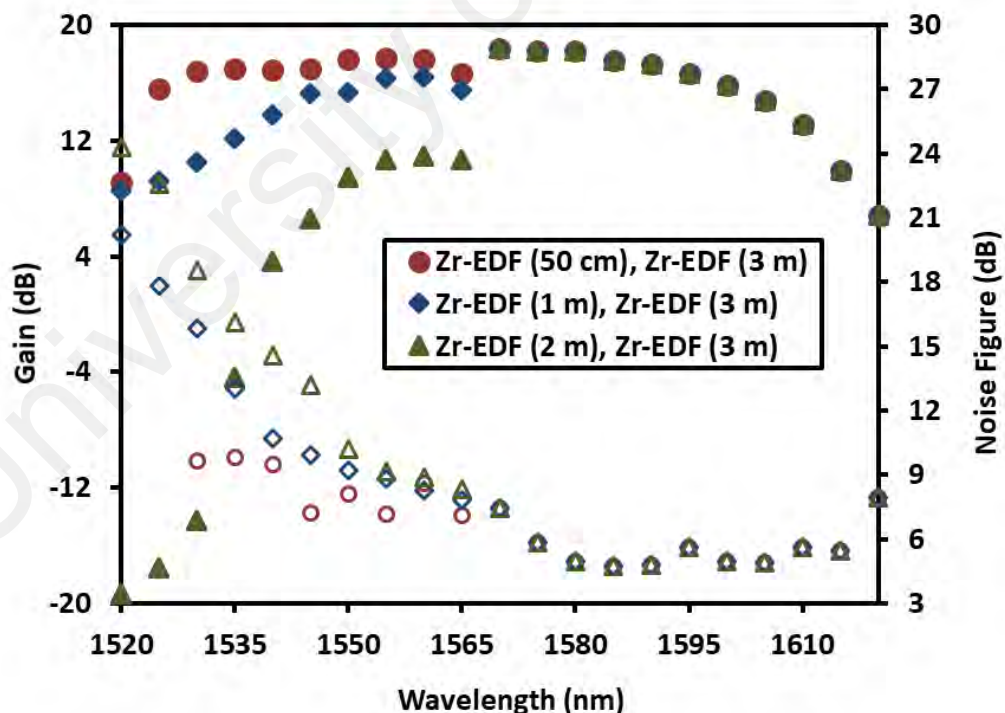


**Figure 4.10:** Gain (solid symbol) and noise figure (hollow symbol) performances of the parallel amplifier at different length of Zr-EDF for C-band region at input signal power of -10 dBm.

## 4.5 Summary

A flat gain wavelength throughout wide-band window was successfully accomplished using dual-stage EDFA in parallel configuration. An efficient hybrid amplifier with wide-band and flat gain characteristics was demonstrated using a combination of Bi-EDF and HB-EDF with total optimal length of 1.99 m in double-pass parallel configuration. In the experiment, the 1480 nm optimum pump powers were fixed at 90 and 170 mW for C- and L-band wavelength region, respectively. As compared to other hybrid amplifier, a combination of Bi-EDF and HB-EDF provided flat gain of 14 dB with gain fluctuation less than 1.5 dB over 75 nm wavelengths from 1535 to 1605 nm at high input power of -10 dBm. For input signal power of -30 dBm, a wide-band amplification from 1535 to 1590 nm was demonstrated within gain verification from 13 to 27 dB. On the other hand, the corresponding noise figures were maintained below 12 dB over wide-band region for both input signal powers.

An efficient wide-band EDFA operating in C- and L- band wavelength region was also obtained using two pieces of Zr-EDFs as gain media for both stages, with total length of 3.5 m in double-pass parallel configuration. In the experiment, the optimum pump powers were fixed at 170 and 280 mW for C- and L-band wavelength region, respectively. The proposed amplifier also provided a wide-band and high flat gain of 17.1 dB with gain fluctuation less than 1.5 dB within wavelength region from 1525 to 1600 nm at input signal power of -10 dBm. Table 4.3 summarized the achievement of the amplifiers with parallel configuration, which consisted of two pieces of Zr-EDF or combination of Bi-EDF and HB-EDF as hybrid gain medium.

**Table 4.3:** Summary of the performance comparison for two types of parallel EDFAs.

<b>Merit</b>	<b>Parallel configuration using two pieces of Zr-EDF</b>	<b>Parallel configuration using hybrid gain medium (Bi-EDF + HB-EDF)</b>
<b>Laser diode and pump power</b>	980 nm laser diodes with optimum pump powers of 170 and 280 mW for C- and L-band stages, respectively.	1480 nm laser diodes with optimum pump powers of 90 and 170 mW for C- and L-band stages, respectively.
<b>Total length of fiber</b>	3.5 m Zr-EDF= 0.5 m for C-band stage. Zr-EDF= 3 m for L-band stage.	1.99 m Bi-EDF=0.49 m for C-band stage. HB-EDF=1.5 m for L-band stage.
<b>Gain (G) achievement</b>	At high input signal of -10 dBm: A higher flat gain of 17.1 dB is investigated with gain fluctuation less than 1.5 dB within wavelength region from 1525 to 1600 nm.  At low input signal of -30 dBm: A wide-band amplification from 1520 to 1615 nm was	At high input signal of -10 dBm: A flat gain of 14 dB is investigated with gain fluctuation less than 1.5 dB over 75 nm wavelengths from 1535 to 1605 nm.  At low input signal of -30 dBm: A wide-band amplification from 1530 to 1615 nm was

**Table 4.3**, continued

<b>Merit</b>	<b>Parallel configuration using two pieces of Zr-EDF</b>	<b>Parallel configuration using hybrid gain medium (Bi-EDF + HB-EDF)</b>
	demonstrated within gain verification from 11 to 30 dB.	demonstrated within gain verification from 5 to 27 dB.
<b>Noise Figure (NF) achievement</b>	low noise figure is varied from 4.7-9.8 dB within flat gain region.	The noise figure is varied from 7-12 dB within flat gain region.

University of Malaysia

## **CHAPTER 5: FLAT GAIN AND WIDE-BAND PARTIAL DOUBLE-PASS ERBIUM CO-DOPED FIBER AMPLIFIER WITH HYBRID GAIN MEDIUM**

### **5.1 Introduction**

The rapid penetration of new technologies in modern society has led to explosive growth in demand for fast broadband connectivity. The dense wavelength division multiplexed (DWDM) transmission system which offers wide-band operation is a key technology to meet this requirement (Cheng et al., 2009; Emami et al., 2010). From the last decades, the DWDM communication system has progressively growth especially in long-haul transmission system. In the previous works, L-band EDFAs have received more attention in terms of gain enhancement, flatness-improvement and gain clamping (Qureshi et al., 2012; Shen, Lee, & Huang, 2009; J. Yang et al., 2016). A dual-stage EDFA with a flat gain of 17 dB and noise figure of less than 6.7 dB, was demonstrated (Yusoff et al., 2012). However, this amplifier has two drawbacks; it requires high pump power and long EDF. The pump power and the total EDF length were 600 mW and 27 m, respectively. Furthermore, this amplifier works only in 35 nm of the L-band wavelength region. In (Liaw et al., 2008), a series type of hybrid amplifier with wide amplification bandwidth of 65 nm (1530–1595 nm), was reported. The proposed amplifier achieved a lower gain variation of less than 0.5 dB. However, to get the low gain variation, a complicated array of fiber Bragg grating mirrors was employed, which results in a complex design and costly amplifier. (B. Hamida et al., 2016) proposed a wideband amplifier, by using a combination of the zirconia erbium-doped fiber (Zr-EDF) with silica erbium-doped fiber (Si-EDF) as an effective gain medium in parallel and serial configurations. However, the total length of EDFs used was 11m which is very long. Besides, the amplifier based on series configuration could not achieve a flat gain over the wideband operation region.

Wide-band and flat gain optical amplifiers were demonstrated in the previous chapter by using dual-stage EDFA based on parallel configuration. In this chapter, wide-band and flat gain optical amplifiers are demonstrated using a dual-stage EDFA based on series configuration. At first, the partial double-pass EDFA is proposed and demonstrated. The partial double-pass amplifier employs HB-EDF and Zr-EDF in the first and second stage, respectively; as the gain media. The performance of the proposed amplifier is investigated for various arrangements of pump power and active fiber length. Then, the triple-pass hybrid EDFA using a novel dual-stage configuration is presented and demonstrated. The proposed amplifier uses Bi-EDF and HB-EDF as the gain medium for the first and second stage, respectively. Furthermore, the triple-pass EDFA has been enhanced by utilizing distribution pumping scheme in the configuration. This improvised configuration minimized the cost of the amplifier yet having the comparable performance with the dual-pump configuration.

## **5.2 Partial double-pass amplifier**

In this section, a partial double-pass optical amplifier is proposed and demonstrated for wide-band operation. Figure 5.1 shows the proposed amplifier, which is based on two stages amplifier using both HB-EDF and Zr-EDF as the gain medium. Both active fibers were drawn from the over cladded perform using fiber drawing technique at a temperature of 2000 °C as described in Chapter 3. The HB-EDF and Zr-EDF has an erbium ion concentration of 12500 and 2800 wt. ppm, respectively. Table 5.1 summarizes the optical characteristics for Zr-EDF and HB-EDF. As shown in Figure 5.1, a 1m long HB-EDF and 2m long Zr-EDF were placed in the first and second stage of the amplifier separately. Both EDFs were forward pumped by 1480 nm and 980 nm laser diode (LD), respectively via wavelength division multiplexing (WDM) coupler. For the HB-EDF, a 1480 nm pumping wavelength was used since it can provide a higher gain and lower noise figure as compared to other pumping wavelength of 980 nm as discussed

in the previous chapters (Almukhtar et al., 2019; Jung et al., 2012). This is attributed to the higher optical power conversion efficiency at 1480 nm pumping due to the single photon conversion process of erbium amplification. An optical circulator (C1) was used to isolate both stages. It prevents the transmission of the backward ASE from the Zr-EDF into the 1<sup>st</sup> stage of the amplifier but allows the amplified signal from the HB-EDFA to be transmitted to the 2<sup>nd</sup> stage through port 1 to port 2 of C1. The transmitted signal will be amplified again in the 2<sup>nd</sup> stage of the amplifier. Another optical circulator (C2) was used to reflect the signal for double pass operation in the 2<sup>nd</sup> stage of the amplifier. The amplified signal from Zr-EDFA will be extracted via port 2 to port 3 of circulator C1 and measured by an optical spectrum analyzer (OSA).

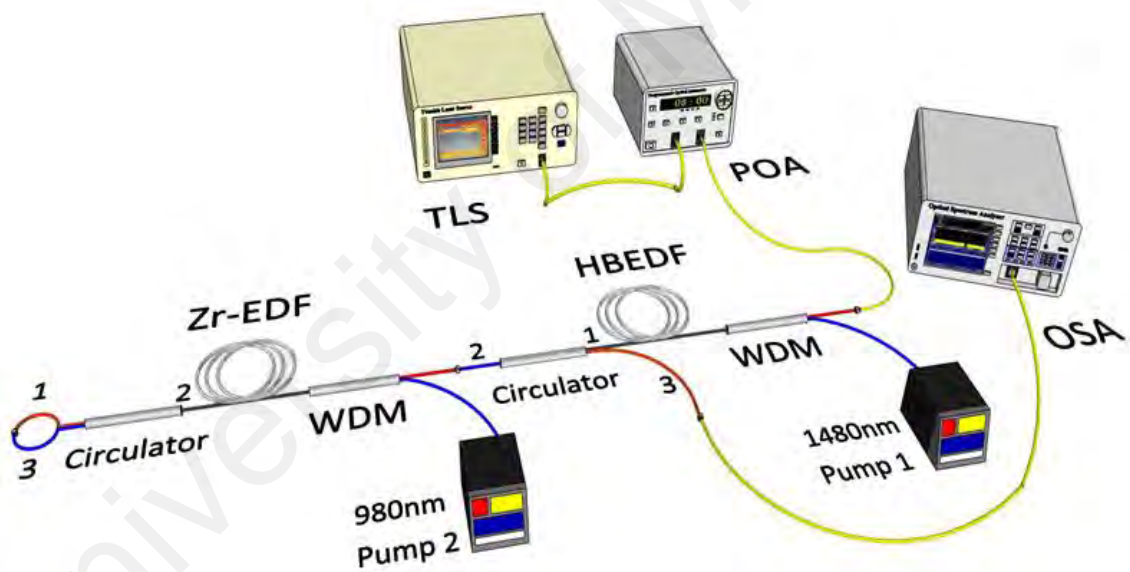


**Figure 5.1:** The experimental setup for partial double-pass amplifier.

**Table 5.1:** The optical characteristics of the Zr-EDF and HB-EDF

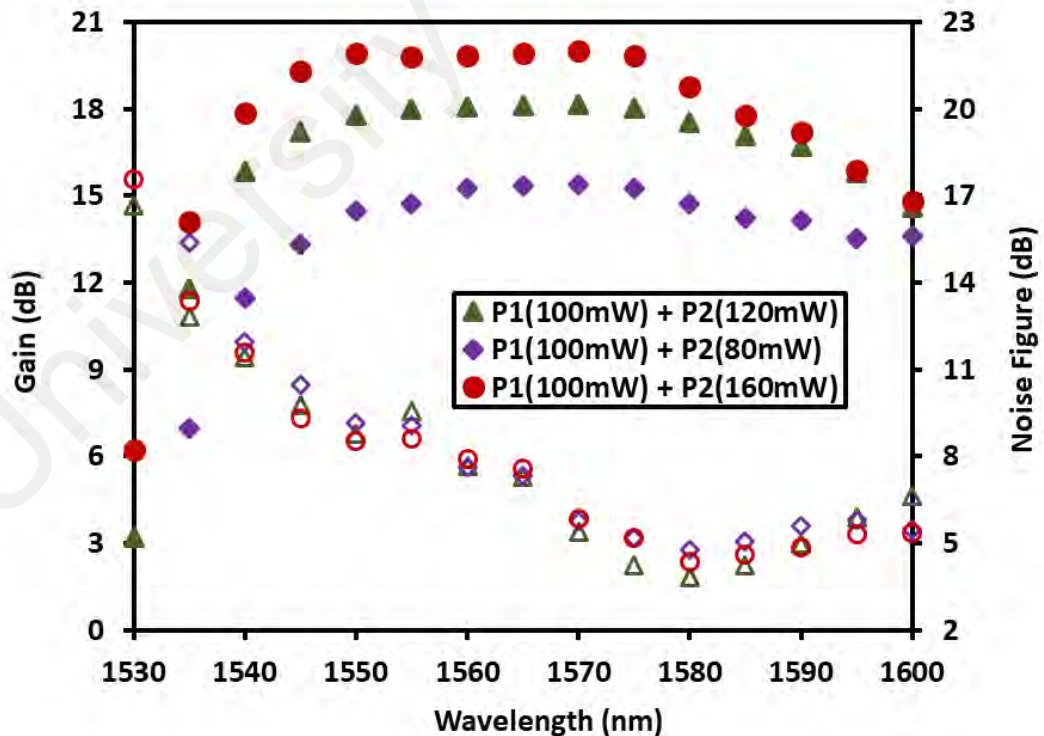
<b>Merit</b>	<b>Zr-EDF</b>	<b>HB-EDF</b>
<b>Core diameter</b>	10.5 $\mu\text{m}$	3.71 $\mu\text{m}$
<b>Numerical aperture</b>	0.17	0.23
<b>MFD</b>	11.25 $\mu\text{m}$	4.5 $\mu\text{m}$
<b>Cut-off wavelength</b>	1875 nm	1050 nm
<b>Erbium ion concentration</b>	2800 wt. ppm.	12500 wt. ppm

### 5.2.1 The effect of changing pump power

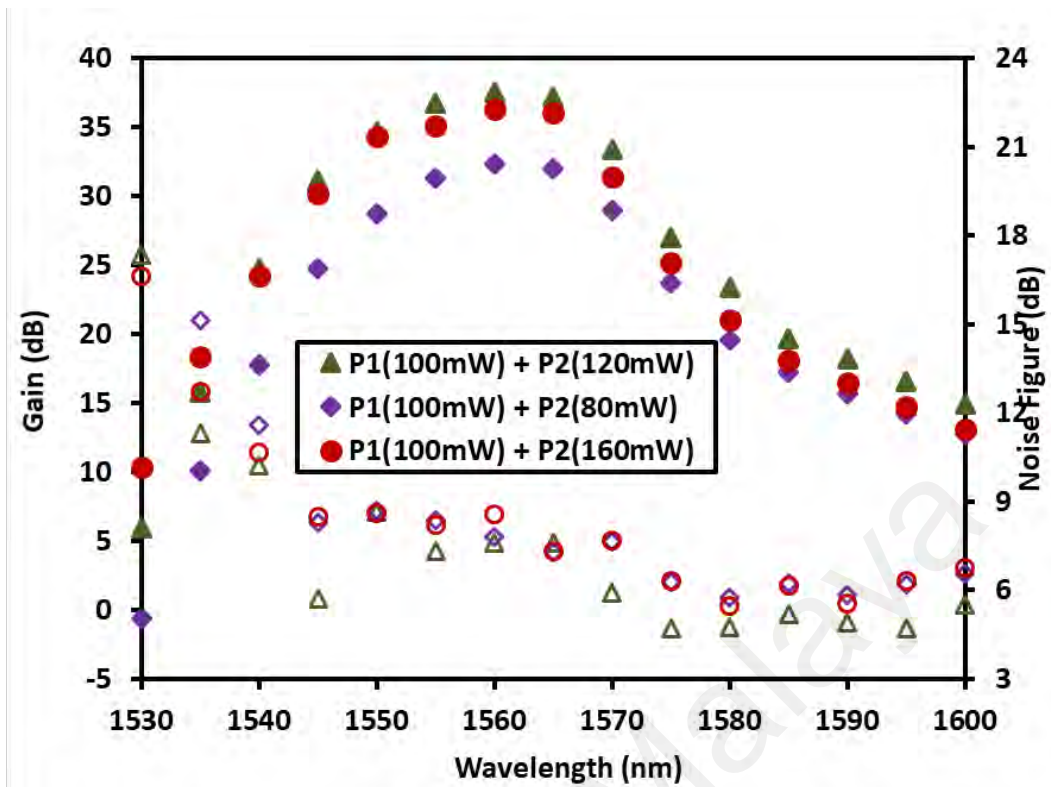
Figure 5.2 shows the gain and noise figure characteristics of the hybrid amplifier at various LD pump powers at two input signals power of -10 dBm and -30 dBm. In this experiment, the pump power for the HB-EDF (P1) is fixed at 100 mW while the pump power for Zr-EDF (P2) is increased from 80 mW to 160 mW. The gain spectrum of the proposed amplifier rises with the increase of P2. For instance, at input signal wavelength of 1575 nm, the gain increases from 15.3 dB to 18.0 dB and 20.0 dB as the pump power changes from 80 mW to 120 mW and 160 mW respectively. Nevertheless, the gain enhancement declines especially at input signal wavelength longer than 1575 nm when P2 increases from 120 to 160 mW due to the saturation effect. It is also worthy to note that no significant changes in the gain spectrum was observed with the increment of P1 from 100 mW to 140 mW while P2 remains at 120 mW. The flat gain spectrum is obtained at a combination of pump power of 100 mW and 120 mW for P1 and P2 respectively.

The noise figure is seen to be unaffected by the change of both pump powers. The noise figure values vary from 4.7 to 9.5 dB within the wide-band span from 1550 to 1600 nm.

At input signal power of -30 dBm, the gain spectrum of the partial double-pass amplifier with a hybrid gain medium is significantly enhanced when the pump power of P2 is changed from 80 to 120 mW as illustrated in Figure 5.2(b). For instance, the gain is improved by 5.5 dB at operating wavelength of 1560 nm. Meanwhile, the gain spectrum slightly decreases as the P2 pump power is further increased from 120 to 160 mW while maintaining the P1 power at 100 mW. For instance, the gain reduces by 1.3 dB for 1560 nm signal. The peak gain of 37.5 dB is observed at 1560 nm when the pump power of P1 and P2 are fixed at 100 and 120 mW, respectively. Therefore, the optimum pump powers for obtaining a flat gain and wide-band operation are 100 mW for HB-EDF and 120 mW for Zr-EDF, in the first and second stage, respectively.



(a)



(b)

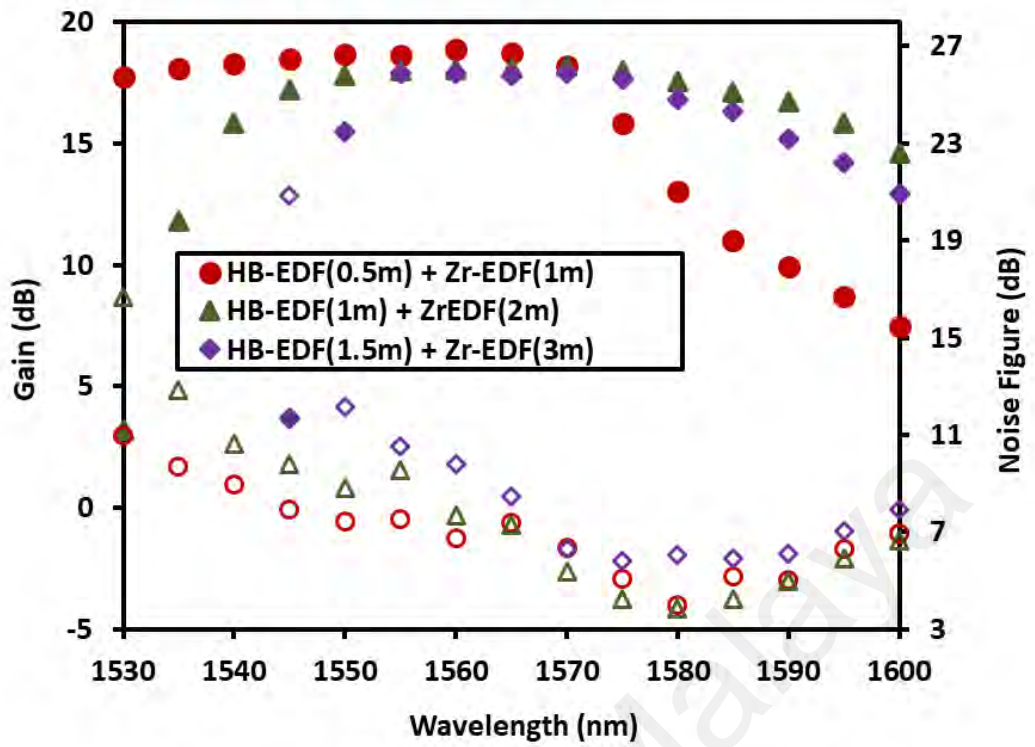
**Figure 5.2:** Gain (solid symbol) and noise figure (hollow symbol) performances at various LD pump powers for input signal power of (a) -10 dBm and (b) -30dBm.

It is clearly seen that the noise figure is higher at shorter wavelength and reduces gradually when it goes to longer wavelength region at both input signal powers. This is owing to the decrement in the erbium absorption to emission cross section as it goes from shorter to longer wavelength region. The noise figure could be brought to a low level with higher gain amplifier and lower loss characteristics. The standard level of noise figure is more than 3 dB for single-pass EDFA, and it is reasonably higher with double-pass EDFA. This is owing to the higher propagation ASE at the input part of the amplifier, which reduces the population inversion and thus increases the noise figure.

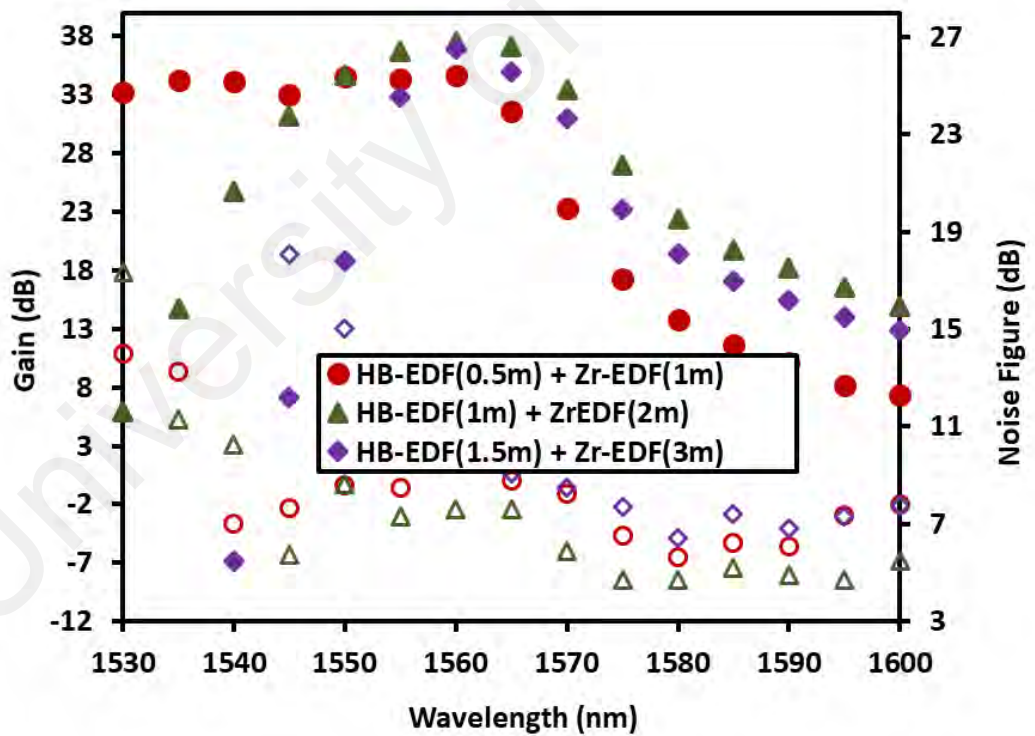
### 5.2.2 The effect of changing EDF lengths

In the previous sub-section, the optimum pump powers are shown at 100 and 120 mW for P1 and P2 respectively. In this sub-section, the performance of the proposed amplifier is investigated for various lengths of HB-EDF and Zr-EDF and the result is shown in Figure 5.3. The gains and noise figures were measured at two input signal powers of -10 dBm and -30 dBm. As shown in the Figure 5.3(a), a flat gain spectrum across 1540 nm to 1600 nm is obtained when the lengths of HB-EDF and Zr-EDF are 1 m and 2 m respectively. The average gain is 17.1 dB with a variation of 2.3 dB within the bandwidth. Nevertheless, the gain spectrum shifts to C-band region when the HB-EDF and Zr-EDF lengths are reduced to 0.5 m and 1 m respectively. It seems that as the length of the gain medium decreases, the operating wavelength shifts to the C-band region. However, at a combination of 1.5 m of HB-EDF and 3 m of Zr-EDF, the gain spectrum shifts to a longer wavelength and starts to reduce at input signal wavelength beyond 1575 nm. This is attributed to the pump attenuation along the gain medium since some portion of the EDF will be pumped below the inversion threshold and thus the signal is reabsorbed.

At lower input power of -30 dBm, the higher gain spectrum is observed of the hybrid gain amplifier especially when the lengths of HB-EDF and Zr-EDF are fixed at 1 m and 2 m, respectively as depicted in Figure 5.3(b). For instance, the peak gain of 37.5 dB is obtained at 1560 nm with the optimum fiber's lengths. Nevertheless, the gain spectrum shifts to C-band region when the HB-EDF and Zr-EDF lengths are reduced to 0.5 m and 1 m respectively. At a combination of 1.5 m and 3 m, for HB-EDF and Zr-EDF, respectively, the gain spectrum shifts to a longer wavelength and starts to reduce beyond the input signal wavelength of 1575 nm.



(a)



(b)

**Figure 5.3:** Comparison of gain (solid symbol) and noise figure (hollow symbol) among three hybrid lengths of gain medium at input signal power of -10 dBm.

In the proposed amplifier, the noise figure is relatively high at shorter wavelength span (1530 to 1540 nm). However, it is gradually reduced above 1540 nm to be less than 3.6 dB at 1585 nm wavelength. This is most likely due to the decrement in the erbium absorption-to-emission cross section ratio as the amplification shifts from shorter to longer wavelengths region. As the lengths of the EDFs are adjusted to cover amplification at longer wavelength, the noise figure reduces as shown as Figure 5.3. At the optimized length, the noise figure is maintained below 11 dB and 9 dB for input signal power of -10 and -30 dBm, respectively at input signal wavelength longer than 1540 nm.

### 5.2.3 Amplification characteristics of each stages and the combined stages

In this subsection, the amplification characteristics of each stages are investigated and compared with the combined stages. In the experiment, the HB-EDF (first stage) and Zr-EDF (second stage) are fixed at the optimum lengths of 1 and 2 m, respectively while the gain and noise figure characteristics are investigated at two different input signal powers; -10 dBm and -30 dBm.

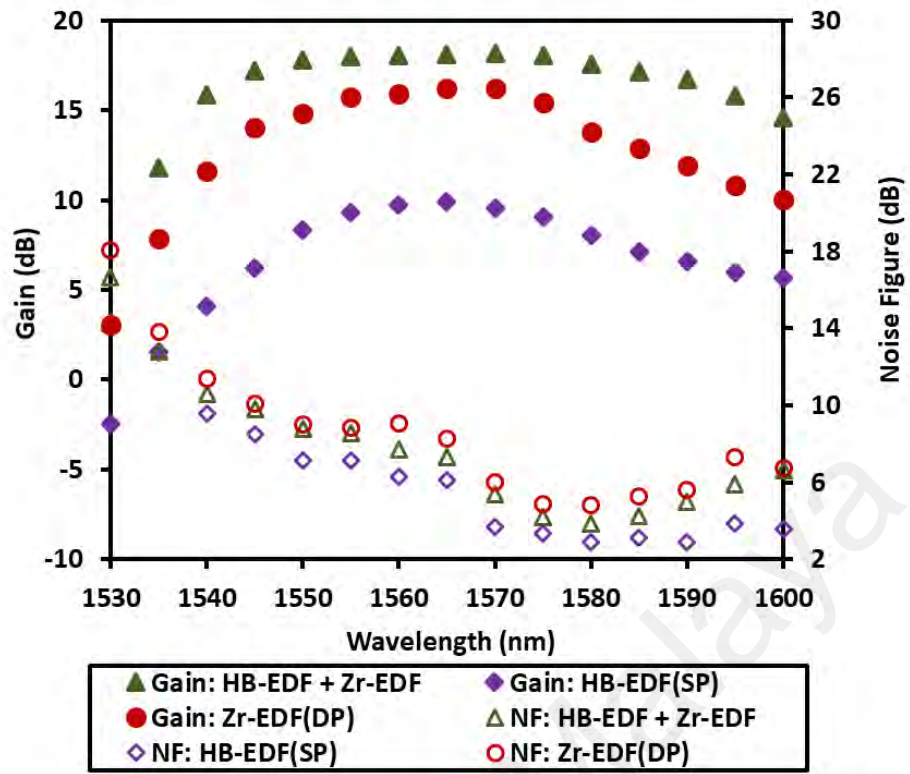
Figure 5.4 compares the separate performance of three types of amplifiers; single-pass (SP) HB-EDFA, double-pass (DP) Zr-EDFA and the combined amplifiers. During the experiment, both HB-EDF and Zr-EDF were forward pumped by 1480 nm and 980 nm laser diode at the optimum pump power of 100 mW and 120 mW, respectively. The gain and noise figures were measured across C- and L-band wavelength region. It is obvious that the amplifiers' gain is higher at lower input signal power of -30 dBm as compared to the that at high input signal power of -10 dBm. This indicates that the effect of the population inversion is larger at smaller input signal powers, whereas the high input signal power suppressed the population inversion and thus reduce the attainable gain.

At input signal of -10 dBm, a flat gain of around 17.2 dB is obtained for the combined amplifier with a gain fluctuation of less than 2.3 dB within the 55 nm wavelength region from 1540 to 1595 nm as shown in

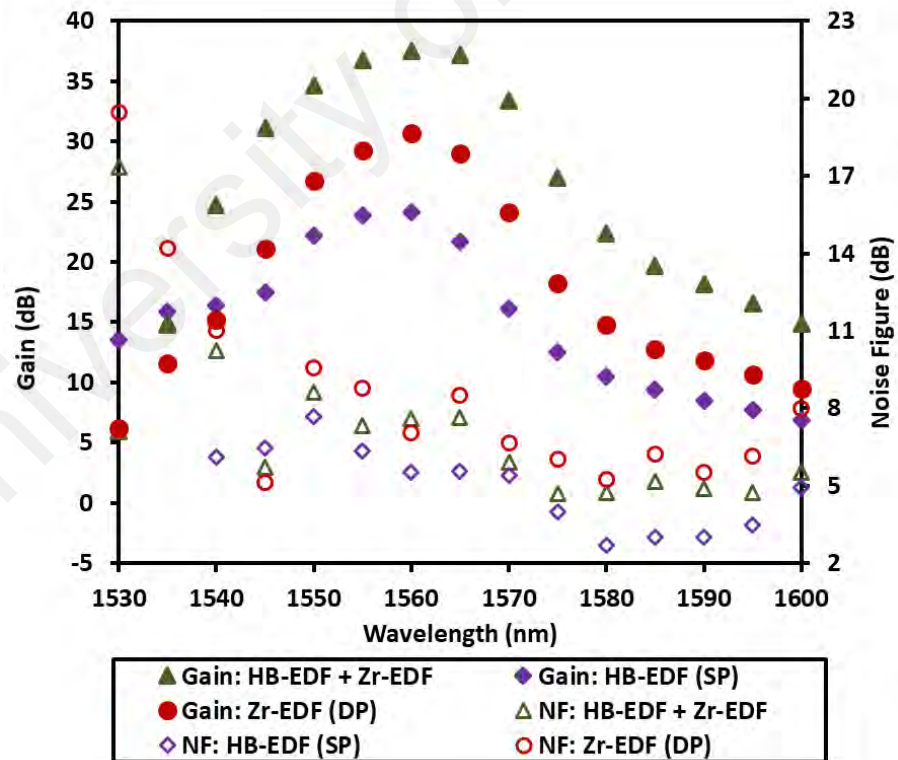
Figure 5.4(a). Within this region, the gain spectrum of the proposed amplifier is also higher than the ones shown by the single pass HB-EDFA and double pass Zr-EDFA. The corresponding noise figure varies from 3.8 dB to 10.6 dB. The relatively lower noise figure at longer wavelength is attributed to the higher gain and lower loss characteristics at the longer wavelength.

As shown in

Figure 5.4(b), the hybrid amplifier achieves a maximum gain of 37.5 dB at 1560 nm region with an input signal power of -30 dBm. This is 6.8 dB and 19.7 dB higher than the gain of double pass Zr-EDFA and single pass HB-EDFA at the same wavelength, respectively. The gain improvement is due to the combination of both stages of EDFA which increases the effective EDF length of the amplifier and thus the gain. At high input signal power of -30 dBm, the gain of the proposed amplifier varies from 15.0 dB to 37.5 dB, but the corresponding noise figure is less than 10.2 dB within the wavelength region from 1540 nm to 1600 nm.



(a)

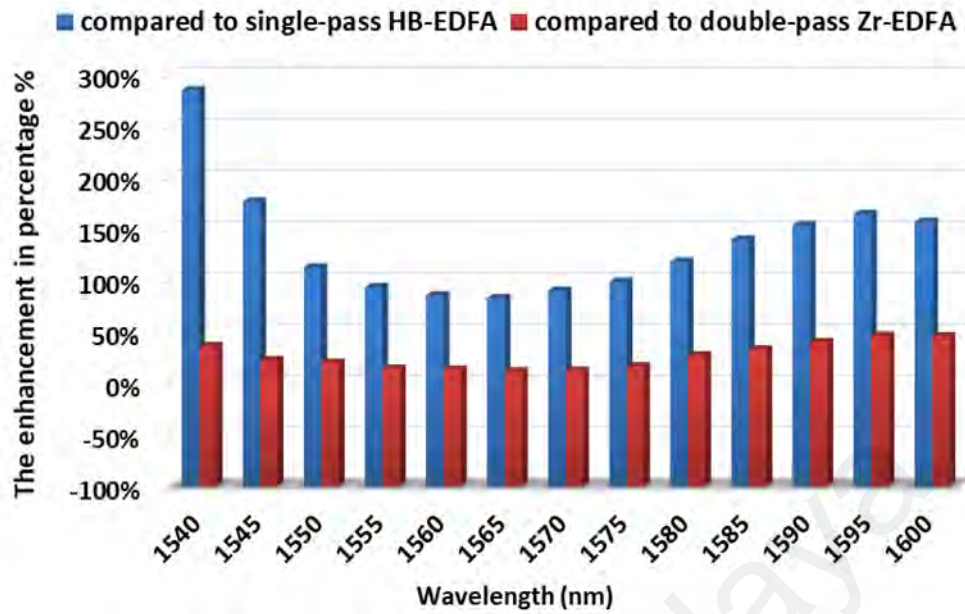


(b)

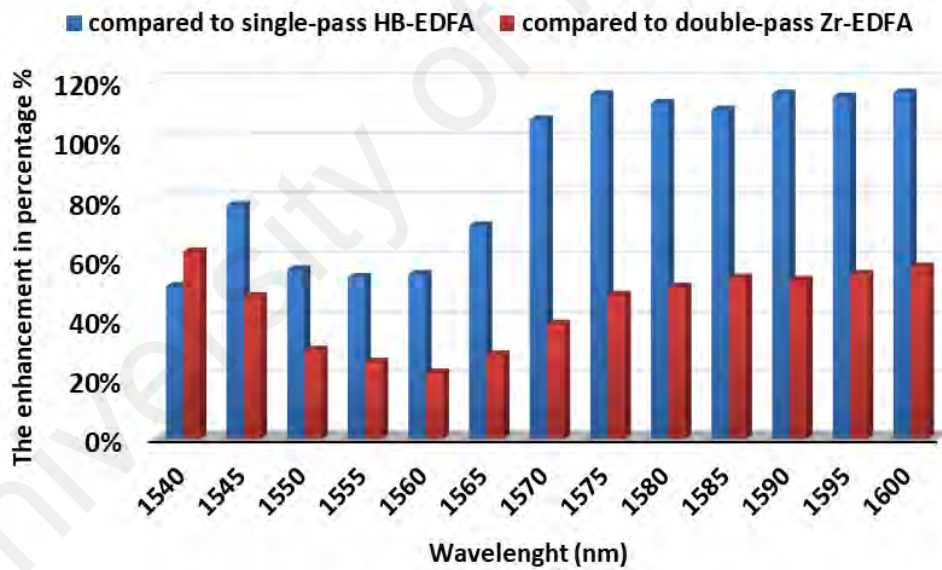
Figure 5.4: Gain and noise figure performances of the hybrid amplifier at input signal power of (a)-10 dBm (b) -30 dBm.

It can be inferred that both fibers have high erbium ions concentration which is important for realizing a compact EDFA device. If the ion concentration of the erbium fibers increase, a shorter erbium fiber can be used. The 1 m long HB-EDF works in the L-band wavelength region while the 2 m long Zr-EDF works in the middle between C- and L-band wavelength regions. However, both fibers could not achieve a wide-band amplification and flat gain characteristic. The proposed hybrid amplifier that consists both fibers achieved a higher gain and flat gain ranging from 1540 to 1600 nm. The hybrid fiber amplifiers are designed to enhance the bandwidth, provide sufficient increase in overall signal gain and enhance the pump conversion efficiency (PCE) (Ali et al., 2014). On other hand, using longer fiber with single-stage configuration lead to shift the amplification to the L-band region. As the length of the gain medium increases, the operating wavelength shifts to the L-band region due to a quasi-two-level absorption effect.

Figure 5.5 illustrates the gain improvement percentage of the hybrid gain amplifier as compared to that of the single-pass HB-EDFA and the double-pass Zr-EDFA, separately. At input signal power of -30 dBm that shown in Figure 5.5(b), the average gain for the hybrid amplifier enhanced by 44% and 89% within wavelength span from 1540 to 1600 nm as compared to that of single-pass HB-EDFA and the double-pass Zr-EDFA, respectively. Overall, the proposed configuration obtains lower noise figure as compared to that of double-pass configuration. This is attributed to the placement of the circulator (C1) in midst of the two stages, which prevents the backward ASE of Zr-EDF from propagating into the HB-EDF, and thus, the noise figure could be kept low.



(a)



(b)

**Figure 5.5:** The gain improvement percentage of the hybrid gain amplifier as compared to that of the single-pass HB-EDFA and the double-pass Zr-EDFA.

### 5.3 Triple-pass hybrid EDFA using a novel dual-stage configuration

In this section, a new triple-pass hybrid EDFA is proposed and demonstrated based on dual-stage serial configuration. Figure 5.6 shows the experimental setup of the triple-pass hybrid amplifier, which comprises of 2 stages of EDFA. The HB-EDF and Bi-EDF are used in the first and second stage, respectively; as the gain medium. In the experiment, the first stage amplifier obtains double-pass amplification, according to the amplified signal that returns back into first stage while, the second stage amplifier provides single-pass amplification. The Bi-EDF used is a commercial fiber that contains 4.4 wt% concentration of Lanthanum co-doped  $\text{Bi}_2\text{O}_3$ . This fiber was fabricated from a perform that was prepared by a melting method. The absorption loss of Bi-EDF is found to be 0.55 dB/m, which is equivalent to 3250 wt.ppm of Erbium ion concentration. The detail specification of the fiber was explained in the previous chapter.

As shown in Figure, the EDFs were forward pumped by 1480 nm laser diodes (LDs) via wavelength division multiplexing (WDM) coupler, with maximum output pump powers of 110 mW for single-pass amplifier and 170 mW for double-pass amplifier. An optical circulator 1 (OC1) was used to forward the input signal into the WDM and extract the twice amplified signal into the optical spectrum analyzer (OSA). In addition, the OC1 prevents the amplified signal and backward ASE from propagating into the input part. Another optical circulator 2 (OC2) was placed between the amplifiers to reflect back the amplified signal from Bi-EDFA via connecting port 3 with port 1 of the OC2, thus the transmitted signal via port 2 will be amplified again in the first stage amplifier. A tunable laser source (TLS) was used as an input to the amplifier and a programmable optical attenuator (POA) was used to obtain the power of the input signal.

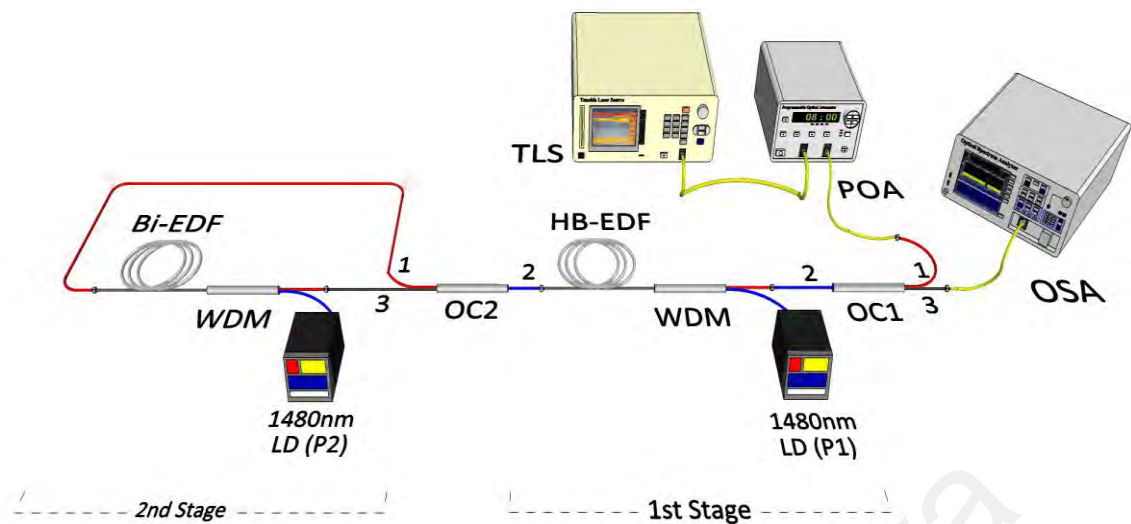
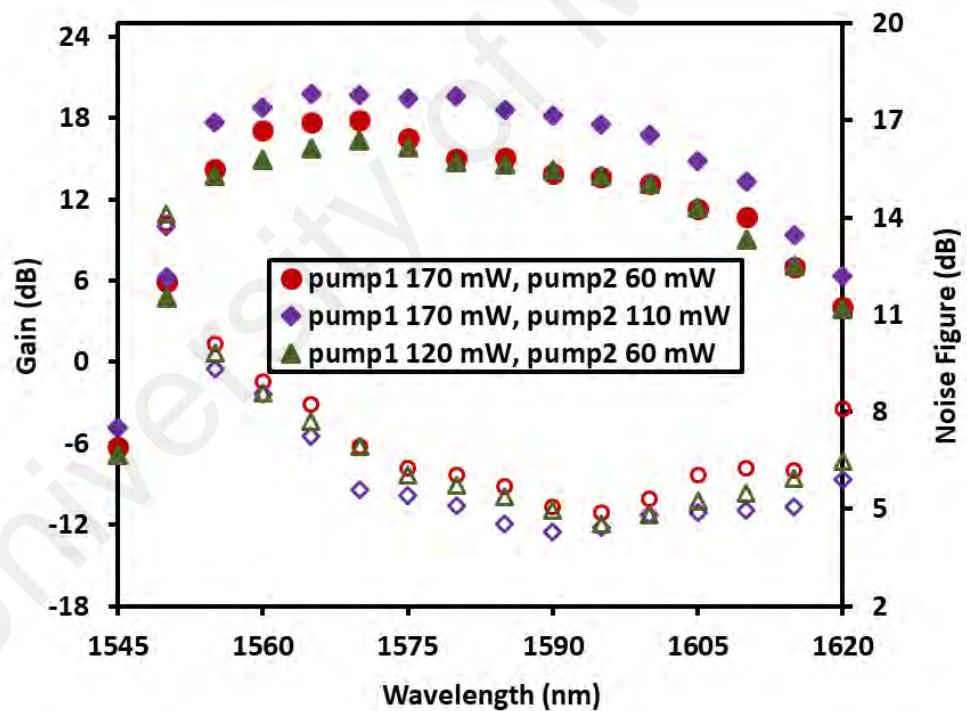


**Figure 5.6:** The proposed triple-pass hybrid EDFA.

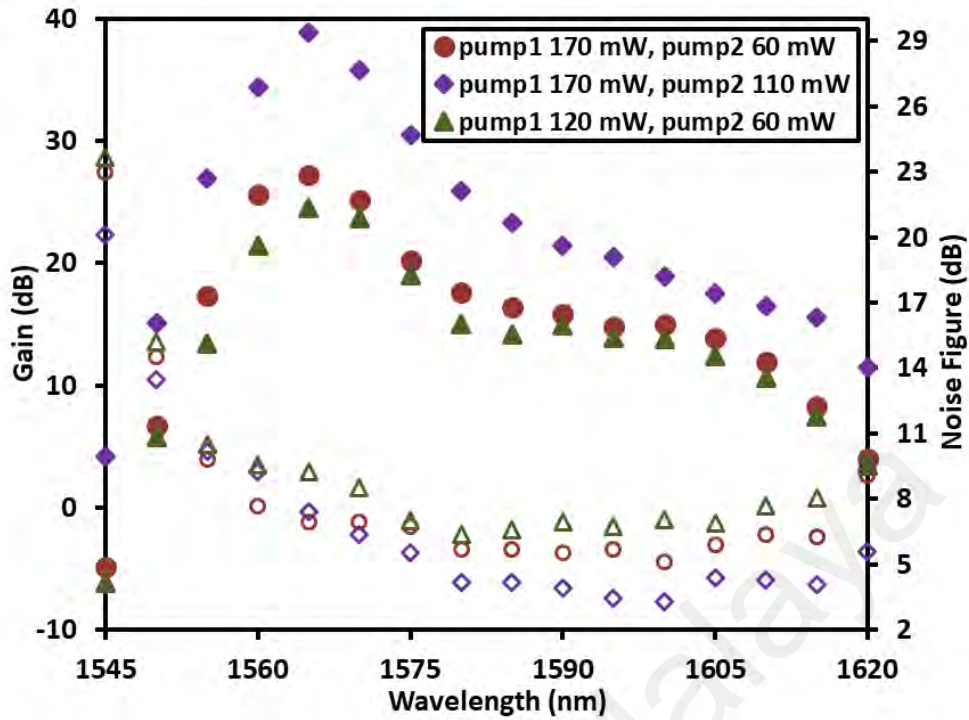
### 5.3.1 The effect of changing pump power

The pump power of both 1480 nm LDs in the proposed triple-pass amplifier were adjusted to obtain a higher and flatter gain spectrum. Figure 5.7 compares the gain and noise figure performance of the proposed amplifier at various combination of LD pump powers at two input signals power of -10 and -30 dBm. During this experiment, the length of Bi-EDF and HB-EDF were fixed at 49 cm and 150 cm, respectively. The pump power for HB-EDF (P1) was first fixed at 170 mW while the pump power for Bi-EDF (P2) was varied from 60 mW to 110 mW. As shown in Figure 5.7(a), the gain spectrum of the triple-pass amplifier rises by 21% with a lesser gain variation of 1.4 dB when the pump power of P2 increased to 110 mW at input signal power of -10 dBm. For instance, the gain improved from 14.9 to 19.6 dB at 1580 nm when the pump power increased from 60 mW to 110 mW. No significant changes on the gain spectrum were observed with the decrement of P1 power from 170 mW to 120 mW while the P2 power remained at 60 mW. On the other hand, the corresponding noise figure has reduced by 12% when the LD pump powers of P1 and P2 were fixed at 170 and 110 mW, respectively.

At input signal power of -30 dBm, the overall gain spectrum of the proposed amplifier was significantly enhanced by about 42% when the pump power of P2 was increased from 60 to 110 mW while P1 was fixed at 170 mW as shown in Figure 5.7(b). For instance, the gain was improved from 27.2 to 38.8 dB at input signal of 1565 nm when the pump power of P2 was increased from 60 mW to 110 mW. The corresponding noise figure was also reduced by about 12%, which is due to the higher gain with the higher P2 power. On the other hand, at a fixed P2 power of 60 mW, the overall gain spectrum was also slightly increased as the P1 power is increased from 120 to 170 mW. Therefore, the optimum pump powers for flat gain and wide-band operation are considered to be 170 mW for HB-EDF and 110 mW for Bi-EDF, respectively.



(a)



(b)

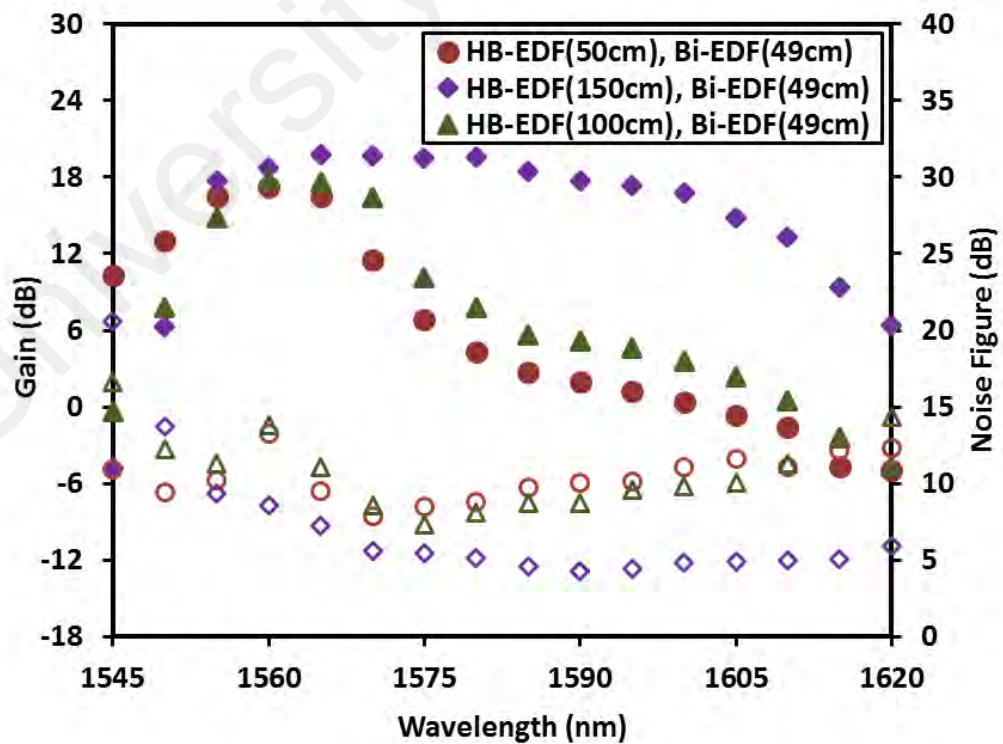
**Figure 5.7:** Gain and noise figure performance of the proposed triple-pass amplifier with different combinations of LD pump power at input signal power of (a) -10 dBm and (b) -30 dBm.

### 5.3.2 The effect of changing the HB-EDF length

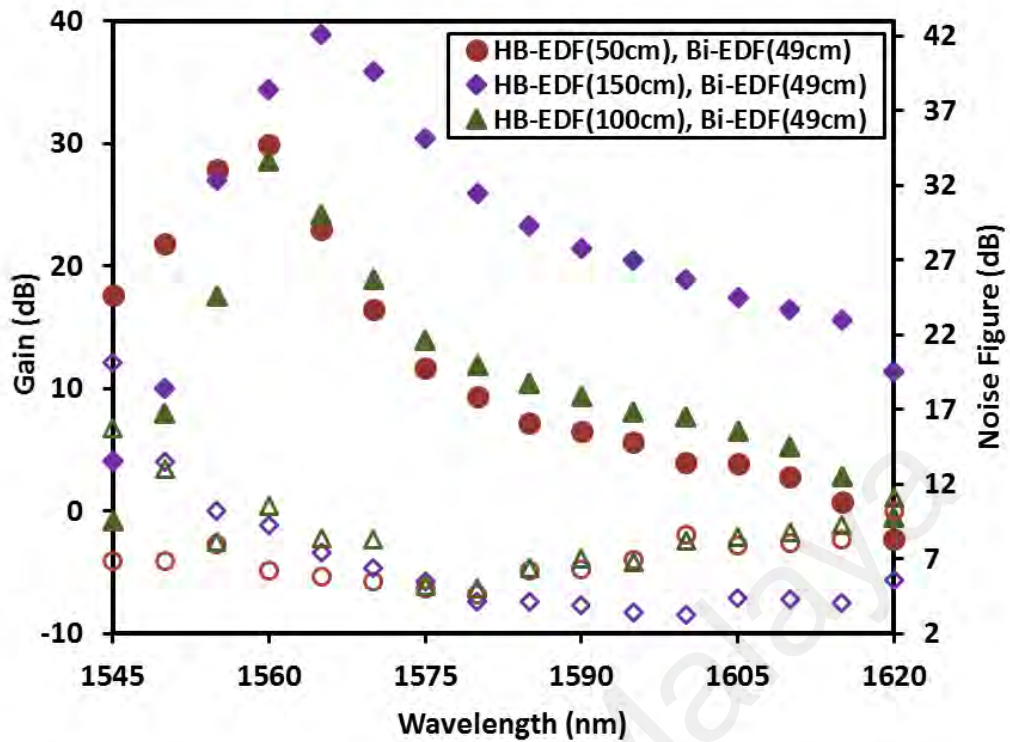
The effect of HB-EDF length (at the first stage) on the triple-pass amplifier performance is investigated in this subsection. Figure 5.8 shows the amplifier performance at various HB-EDF lengths when P1 and P2 are fixed at 170 and 110 mW, respectively. During this experiment, the length of Bi-EDF was fixed at 49 cm. It shows that the gain spectrum improves with the increase of HB-EDF length for both input signal powers. At the longest HB-EDF length of 150 cm and input signal power of -10 dBm, a flat gain of 18.5 dB was obtained with gain variation less than 2 dB across a wavelength region from 1555 nm to 1600 nm as illustrated in Figure 5.8(a). This is attributed to the enhancement of the population inversion of the erbium ions in the fiber, which increases with the EDF length. Furthermore, its corresponding noise figure was observed to be

lower at longer HB-EDF. Nevertheless, the EDF gain amplification was dominant in C-band region when the HB-EDF length reduced to 50 cm and 100 cm.

At lower input power of -30 dBm, the gain spectrum of the triple-pass amplifier was improved by about 14% within a wavelength span from 1555 to 1620 nm as the HB-EDF length was increased from 50 cm to 150 cm as depicted in Figure 5.8(b). For instance, the gain improved from 23 to 38.8 dB at 1565 nm when the HB-EDF length increases from 50 cm to 150 cm. This is owing to the increased in the number of erbium ions, which increases the population inversion and thus increase the attainable gain. However, the gain spectrum only rises by about 6% when the HB-EDF length was increased from 50 cm to 100 cm. The corresponding noise figure has also significantly reduced when the length of HB-EDF is increased from 50 to 150 cm for both input signal powers. The noise figure was maintained below 10 dB at the flat gain region when the input signal is fixed at -10 dBm.



(a)



(b)

**Figure 5.8:** The comparison of the gain and noise figure of the triple-pass EDFA at different lengths of HB-EDF at two input signal powers of (a) -10 dBm and (b) -30 dBm.

### 5.3.3 Amplification performance comparison

It is found in the previous section that the optimum length for HB-EDF and Bi-EDF are 150 cm and 49 cm, respectively for triple pass amplification. Figure 5.9 shows the amplified spontaneous emission (ASE) spectra for three different arrangements; single-pass Bi-EDF, double-pass HB-EDF and triple-pass amplifier (with the Bi-EDF and HB-EDF). The ASE for single-pass Bi-EDF and double-pass HB-EDF were measured separately in the single stage configuration. In the experiment, both fibers were forward pumped by 1480 nm with the maximum pump power of 170 mW. It is observed that the Bi-EDF provides emission in the conventional band range from 1530 nm to 1560 nm, while the emission of the double-pass HB-EDF is shifted to longer wavelength in the L-

band region. This indicates that the 1550 nm photons were absorbed by the Erbium ions to emit in longer wavelength with the use of longer EDF. It is also shown in the figure that the ASE of the combined fibers in the triple-pass arrangement covers a wider wavelength region from 1510 to 1615 nm.

The gain and noise figure spectra of both single-pass Bi-EDFA and double-pass HB-EDFA were measured separately and compared with the proposed triple-pass amplifier as shown in Figure 5.10. As clearly seen from the figure, the gain spectrum of the proposed amplifier was higher as compared with single-pass Bi-EDFA and double-pass HB-EDFA over C- and L-band wavelength span. This is owing to the combination of both stages of EDFAs which increased the effective EDF length of the amplifier and thus the gain. At input signal of -10 dBm, a high and flat gain of 18.5 dB was achieved with gain fluctuation of less than 1 dB within 45 nm wavelength span as illustrated in Figure 5.10(a). The corresponding noise figure of the proposed amplifier was varied from 1.8 to 6.3 dB within the flat gain region from 1555 to 1600 nm. The comparatively lower noise at L-band wavelength region owing to the higher gain characteristic and lower loss characteristic at the longer wavelength. On the other hand, the double-pass HB-EDFA has shown higher noise figure spectrum due to the increased of backward propagating ASE power at the input part of the amplifier, which reduces the population inversion and thus increases the noise figure.

At input signal power of -30 dBm, the triple-pass hybrid amplifier provides higher gain spectrum compared with those of single pass Bi-EDFA and double pass HB-EDFA across wide-band wavelength region. For instance, at 1565 nm region, the proposed amplifier achieves a maximum gain of 39 dB as shown in Figure 5.10(b). This is 2.9 dB and 24.4 dB higher than the gain of double pass HB-EDFA and single pass Bi-EDFA at the same wavelength, respectively. The gain improvement is due to the combination of both stages of EDFA which increases the effective EDF length of the amplifier and thus

the gain. The corresponding noise figure is less than 9.2 dB within the wavelength region from 1560 nm to 1620 nm.

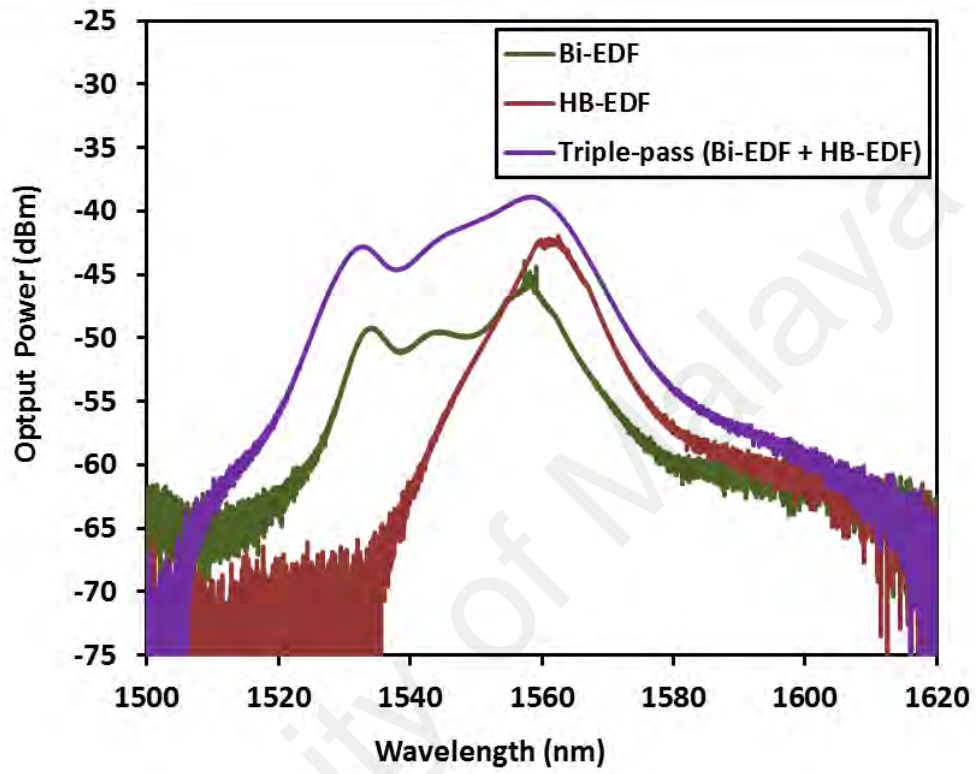
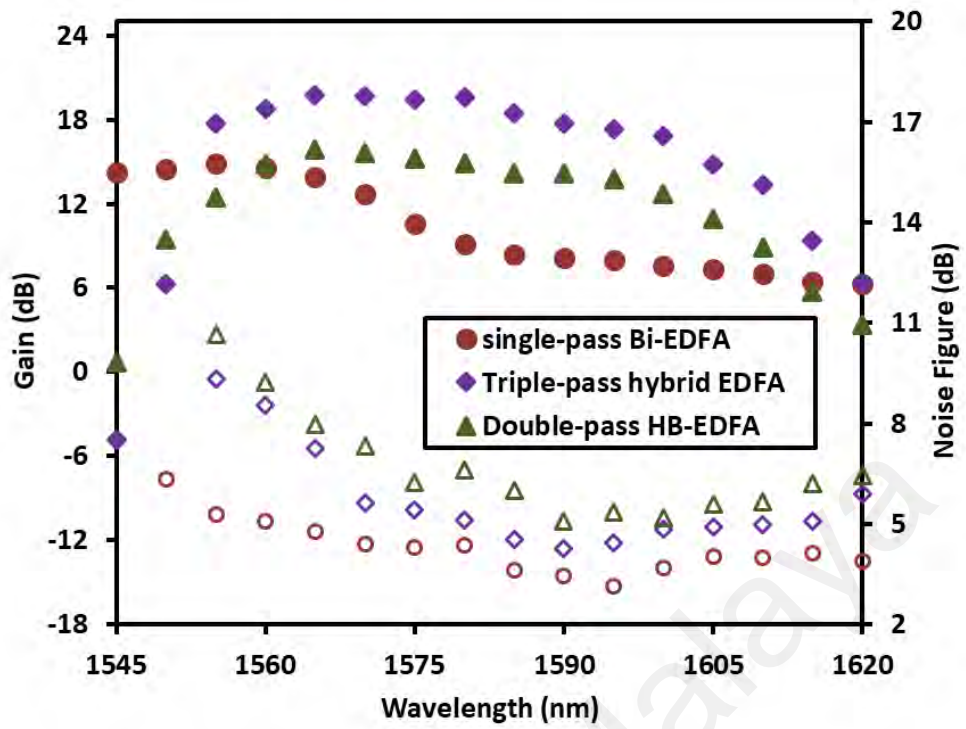
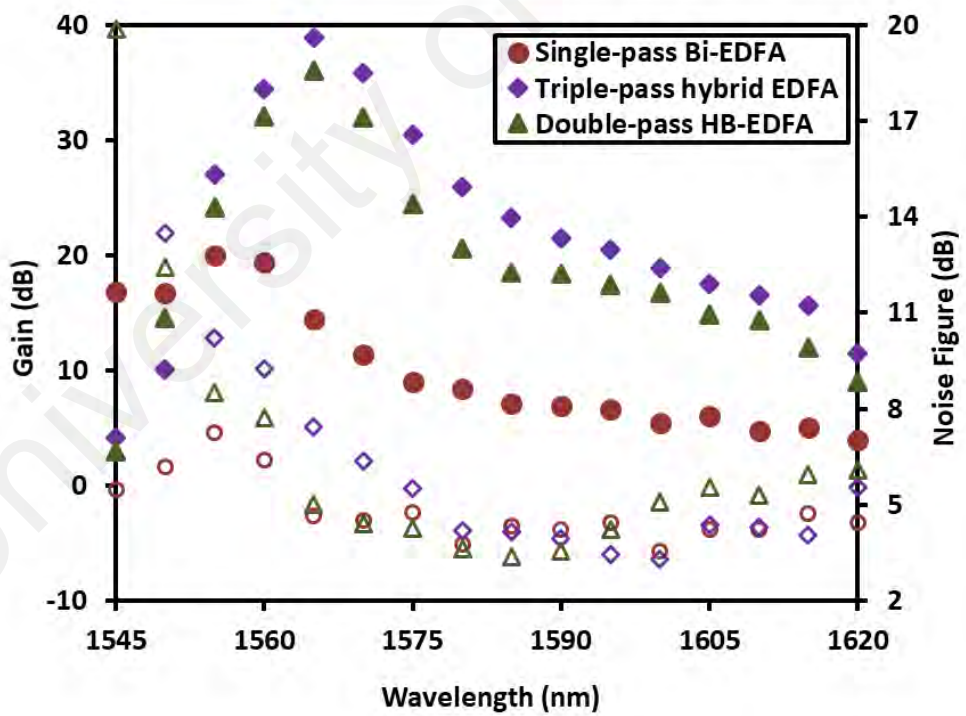


**Figure 5.9:** The ASE spectra from HB-EDF and Bi-EDF under pump power of 170 mW.



(a)



(b)

**Figure 5.10:** Comparison of the gain and noise figure performances of the proposed triple-pass amplifier with single-pass Bi-EDFA and double-pass HB-EDFA at input signal powers of (a) -10 dBm and (b) -30 dBm.

### 5.3.4 New pump power distribution scheme

The configuration in Figure 5.6 was improvised by integrating a 1480 nm optical coupler with split ratio 40/60 in the proposed triple-pass amplifier to distribute the pump power of a 1480 nm LD to the two stages of the amplifier as shown in Figure 5.11. 60% of the pumping power was channel to HB-EDF in the first stage while the residual fraction of the pump power was dispensed to Bi-EDF in the 2nd stage of the amplifier. This setup minimized the cost of the amplifier by reducing the use of 1480 nm LD in the configuration. The pump power of the 1480 nm LD in the figure was set at 280 mW which is comparable to the total power of the two LDs in Figure 5.6. The performance of both proposed triple-pass amplifiers will be compared and investigated.

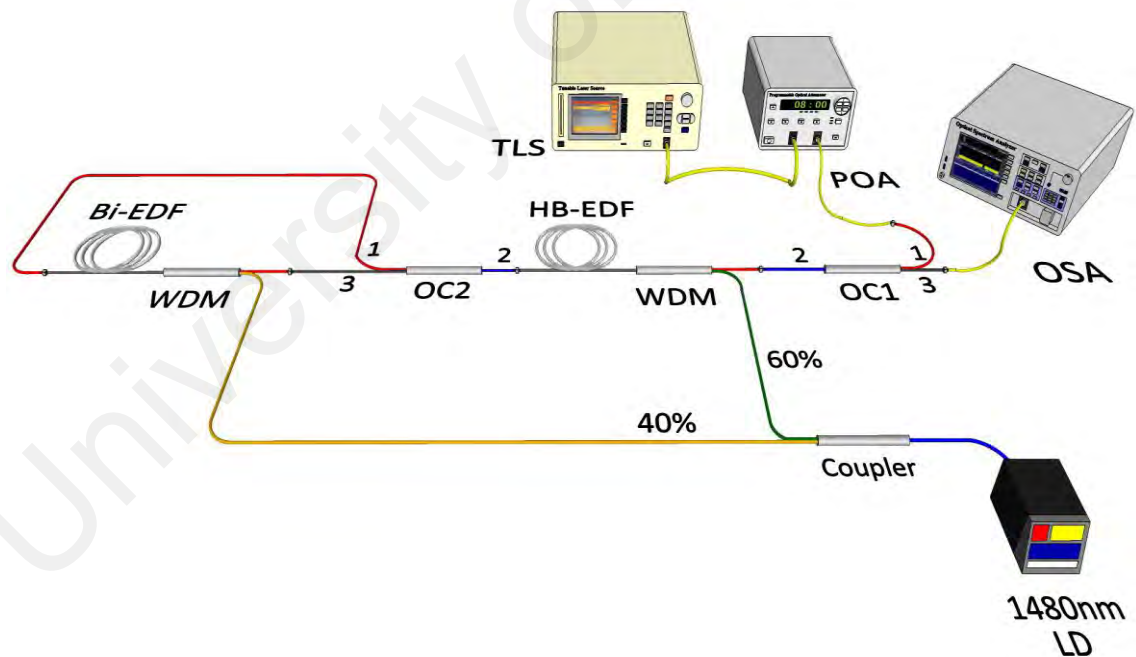


**Figure 5.11:** The enhanced triple-pass hybrid EDFA with distribution pumping scheme.

The experiment was repeated by incorporating a 40/60 optical coupler at the output of a 1480 nm LD pump. Figure 5.12 compares the gain and noise figure of both configurations at high input signal power of -10 dBm. As illustrated from the figure, the improvised configuration has a slight lower average gain of 17.2 dB within wavelength span from 1555 to 1600 nm. However, lower noise figure which below 8 dB within the flat gain region was observed in the improvised configuration. This improvised configuration with distributed pumping scheme is more compact and cost-effective while having a comparable performance with the conventional dual-pump amplifier of Figure 5.6.

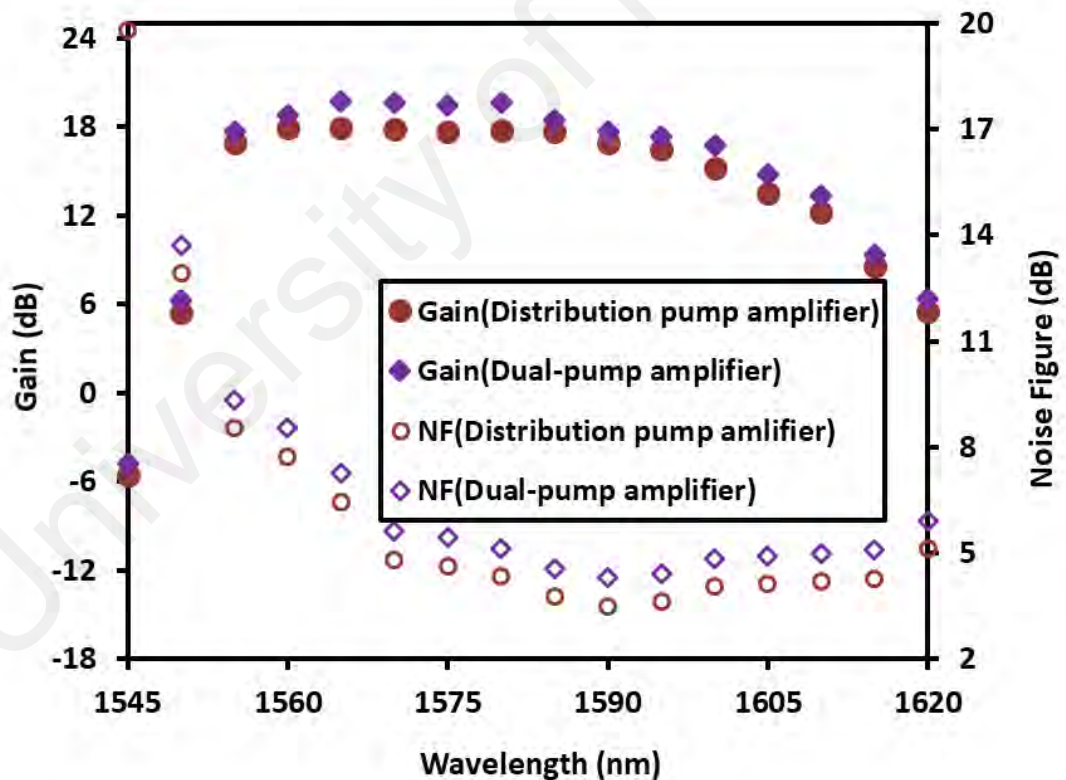


**Figure 5.12:** Gain and noise figure characteristics for two different configurations at high input signal power of -10 dBm.

## 5.4 Summary

A compact optical amplifier with a flat gain characteristic over wide-band wavelength span is successfully demonstrated using a hybrid active gain medium in serial configuration. At first, a dual-stage hybrid optical amplifier with total EDF length of only 3 meters was successfully achieved by using a combination of 1 m long of HB-EDF and 2 m long of Zr-EDF in partial double-pass configuration as the gain medium. In the experiment, the optimum power of 1480 nm and 980 nm laser diodes were obtained at 100 mW and 120 mW, respectively. At input signal of -10 dBm, a flat gain of 17.2 dB with a gain fluctuation of less than 2.3 dB was obtained within a wide-band wavelength region from 1540 to 1595 nm. The corresponding noise figure was kept below 10.6 dB within a flat gain wavelength region. The low cost and compactness of this hybrid amplifier has the potential to be used in the DWDM system.

A triple-pass hybrid EDF amplifier was also successfully demonstrated by incorporating two stages of EDFA using HB-EDF and Bi-EDF in first and second stage, respectively. For realizing flat gain and wide-band amplification, both EDFs are pumped by 1480 nm with the optimum pump power of 170 mW for HB-EDF in the first stage and 110 mW for Bi-EDF in the second stage. At high input power of -10 dBm, a flat gain of about 18.5 dB with gain variation less than 2 dB is observed across 45 nm bandwidth ranging from 1555 to 1600 nm. The corresponding noise figure varied from 4.8 to 9.3 dB within the flat gain region. The comparison performance between partial and triple-pass amplification are illustrated in Table 5.2.

**Table 5.2:** Performance summary of partial double-pass and triple-pass amplifiers.

<b>Merit</b>	<b>Partial double-pass Amplifier</b>	<b>Triple-pass Amplifier</b>
<b>Erbium concentration for EDFs</b>	Zr-EDF: 2800 ppm HB-EDF: 12500 ppm	Bi-EDF: 3250 ppm HB-EDF: 12500 ppm
<b>Total optimum Length</b>	3 m	1.99 m
<b>Laser diode</b>	1480 nm for 1 <sup>st</sup> stage 980 nm for 2 <sup>nd</sup> stage	1480 nm for both stages
<b>Optimum pump power</b>	120 mW for Zr-EDF 100 mW for HB-EDF	170 mW for HB-EDF 110 mW for Bi-EDF
<b>Flat gain and noise figure achievement</b>	Gain 17.2 dB Noise figure was kept below 10.6 dB within a flat gain wavelength region.	Gain 18.5 dB Noise figure varied from 4.8 to 9.3 dB within the flat gain region.
<b>Wide-band span</b>	1540-1595 nm	1555-1600 nm
<b>Gain fluctuation</b>	2.3 dB	1.8 dB

## CHAPTER 6: CONCLUSIONS AND FUTURE WORKS

### 6.1 Conclusions

This thesis successfully present a thorough study on demonstrating compact optical amplifiers with flat gain characteristic over wide-band wavelength span using a hybrid active gain medium. The optical amplifier was realized using short length of Erbium-doped fibers (EDFs) as the gain medium. Three types of EDFs with a significantly high Erbium ions concentration were employed in this study; Zirconia based EDF (Zr-EDF), Hafnium Bismuth based EDF (HB-EDF) and Bismuth based EDF (Bi-EDF). Both Zr-EDF and HB-EDF were fabricated by using modified chemical vapor deposition (MCVD) in conjunction with solution doping (SD) process. The Zr-EDF and HB-EDF have absorption losses of 80 dB/m and 100 dB/m, which can be translated to the erbium ion concentrations of 4000 ppm and 12500 ppm, respectively. On the other hand, The Bi-EDF was fabricated from a perform that was prepared by a melting method. The absorption loss of Bi-EDF is found to be 0.55 dB/m, which is equivalent to 3250 wt.ppm of Erbium ion concentration. By using these EDFs, an advanced EDFA was successfully developed with wide-band and flat gain spectrum characteristics, which are essential to increase the capacity of DWDM system.

At first, efficient L-band optical amplifiers were successfully achieved and demonstrated using two types of new EDFs; Zr-EDF and HB-EDF as a gain medium. Both fibers have significantly high Erbium dopants and thus suitable for L-band amplification application. It is found that the optimum length for L-band operation was 3 m and 1.5 m for the Zr-EDFA and HB-EDFA, respectively. The double-pass EDFA provides a higher and flatter gain spectrum compared to that of single-pass arrangement. The double-pass Zr-EDFA demonstrates a flat gain of 17.1 dB (3.8 dB higher than the single-pass one) with gain variation of less than 1 dB within more than 40 nm wavelength

region. The noise figure, on the other hand, varies from 6 to 10 dB within the flat gain region at input signal power of -10 dBm. It is observed that the double-pass amplifier provides a higher noise figure compared to the single-pass scheme due to the high amplified spontaneous emission generation at input part of the EDFA. It is also clearly seen that the gain of the amplifier that pumped at 1480 nm are higher as compared to that the one pumped at 980 nm.

For HB-EDF, an efficient flat gain of about 15 dB was achieved at gain variance of around 1 dB over wavelength area from 1560 to 1605 nm in double-pass configuration. At low input signal power of -30 dBm, the maximum gain of 36 dB was obtained at wavelength of 1565 nm for double-pass HB-EDFA. The noise figure was maintained below 9 dB within the L-band region. As compared to HB-EDFA, the Zr-EDFA has relatively higher gain especially at wavelength region from 1565 to 1610 nm. However, a shorter length of 1.5 m was used for the HB-EDF amplifier which is half of the Zr-EDF length due to high erbium ion concentration of the HB-EDF. As well, the new HB-EDFA provided wider bandwidth amplification started from 1545 nm. The corresponding noise figure of the proposed HB-EDFA was lower as compared to that of Zr-EDFA.

A compact wide-band EDFA with flat gain characteristic operating in both C and L-band regions was also successfully developed using very short length of the EDF sections. The efficient amplifier was designed based on a hybrid gain medium combining Bi-EDF and HB-EDF with total length of 1.99 m in double-pass parallel configuration. In the experiment, the 1480 nm pump powers were fixed at 90 and 170 mW for C- and L-band wavelength region, respectively. As compared to other hybrid amplifier, a combination of Bi-EDF and HB-EDF provided flat gain of 14 dB with gain fluctuation less than 1.5 dB over 75 nm wavelengths from 1535 to 1605 nm at high input power of -10 dBm. For input signal power of -30 dBm, a wide-band amplification from 1535 to 1590 nm was demonstrated with gain varies from 13 to 27 dB. On the other hand, the

corresponding noise figures were maintained below 12 dB over wide-band region for both input signal powers. A wide-band EDFA operating in both C- and L- band wavelength regions was also obtained using two pieces of Zr-EDFs as gain medium with total length of 3.5 m in double-pass parallel configuration. In the experiment, the pump powers were fixed at the optimum values of 170 and 280 mW for C- and L-band wavelength region, respectively. The proposed amplifier also provided a wide-band and high flat gain of 17.1 dB with gain fluctuation less than 1.5 dB within wavelength region from 1525 to 1600 nm at input signal power of -10 dBm.

A dual-stage amplifier was also successfully demonstrated based on partial double-pass configuration using hybrid active gain medium. The dual stage amplifier with total EDF length of only 3 meters was successfully achieved by using a combination of 1 m long of HB-EDF and 2 m long of Zr-EDF. At the optimum pumping power and input signal of -10 dBm, a flat gain of 17.2 dB with a gain fluctuation of less than 2.3 dB was obtained within a wide-band wavelength region from 1540 to 1595 nm. The corresponding noise figure was kept below 10.6 dB within a flat gain wavelength region.

A new amplifier scheme of triple-pass was also proposed and implemented with shorter length of hybrid gain medium in this study. This amplifier incorporated two stages of EDFA using HB-EDF and Bi-EDF in first and second stage, respectively. For realizing flat gain and wide-band amplification, HB-EDF and Bi-EDF was pumped by 1480 nm laser diode at the optimum pump power of 170 mW and 110 mW, respectively. At high input power of -10 dBm, a flat gain of about 18.5 dB was achieved with gain variation less than 2 dB across 45 nm bandwidth ranging from 1555 to 1600 nm. The corresponding noise figure varied from 4.8 to 9.3 dB within the flat gain region. Finally, a new pump distribution technique was also introduced to reduce the amplifier's cost and its compactness. The triple-pass amplifier was successfully improvised by splitting the 1480 nm pump in ratio 40/60 to distribute the pump power efficiently to the two stages of the

amplifier. The improvised amplifier achieved a flat gain of 17.2 dB with the corresponding noise figure below 8 dB to operate within 1555 to 1600 nm wavelength region. In summary, various configurations of advanced EDFA were studied to provide wide-band and flat gain amplification, which is essential to increase the capacity of DWDM system.

## 6.2 Future works

This thesis has focused on developing advanced EDFAs configured with hybrid gain medium using short length of EDFs with high erbium ion concentration in order to achieve wide-band and flat gain operation. The proposed amplifiers could be used in future dense wavelength division multiplexing (DWDM) communication system. Nevertheless, further improvements can be made to this research work. Brief suggestions for future research work are given as follows:

1. The short length of 1.5 m long HB-EDF provides an acceptable amplification performance at L-band region. However, the gain is slightly lower compared to Zr-EDF at the optimum length of 3 m. Future work should focus on improving the HB-EDF so that its amplification performance is comparable with the conventional fiber with lower concentration.
2. For triple-pass amplifier system, the pumping distribution technique demonstrates a cost reduction since only one laser diode was utilized to pump two stages. Nevertheless, further cost reduction could be achieved by replacing the optical circulators with a low-cost device such as fiber Bragg grating. Designing of one optical circulator for both stages having the ability to reflect any incoming signal, also seems attractive in future work.

3. Although there is advancement in optical fiber manufacturing technology, there is still a lack of theoretical work. Future work should focus on theoretical and simulation studies especially on designing new active fibers or new configurations.

University of Malaya

## REFERENCES

- Abass, A., Abdul-Razak, M. J., Mohammed, H. H., Kadhim, S. M., & Salih, M. A. J. D. J. O. E. S. (2019). Optical Fiber Amplifiers: Optimization and Performance Evaluation. *12*(1), 66-72.
- Abass, A. K., Abdul-Razak, M. J., Salih, M. A. J. E., & Journal, T. (2014). Gain characteristics for C-band erbium doped fiber amplifier utilizing single and double-pass configurations: A comparative study. *32*(9 Part (A) Engineering), 2165-2173.
- Ali, M. H., Abdullah, F., Jamaludin, M. Z., Al-Mansoori, M. H., Al-Mashhadani, T. F., & Abass, A. K. J. J. o. t. O. S. o. K. (2014). Simulation and experimental validation of gain-control parallel hybrid fiber amplifier. *18*(6), 657-662.
- Allah, B. A., Naji, A., Khan, S., ALKhateeb, W., Harun, S., & Ahmad, H. J. I. J. o. P. S. (2011). A novel wide-band dual function fiber amplifier. *6*(5), 1118-1126.
- Almukhtar, A. A., Al-Azzawi, A. A., Cheng, X., Paul, M., Ahmad, H., & Harun, S. (2019). *The effect of 980 nm and 1480 nm pumping on the performance of newly Hafnium Bismuth Erbium-doped fiber amplifier*. Paper presented at the Journal of Physics: Conference Series.
- Anthony, R., Lahiri, R., Biswas, S. J. O.-I. J. f. L., & Optics, E. (2014). Gain clamped L-band EDFA with forward-backward pumping scheme using fiber Bragg grating. *125*(11), 2463-2465.
- Bakar, A. A. A., Mahdi, M., Al-Mansoori, M., Shaari, S., & Zamzuri, A. J. A. o. (2009). Opto-optical gain-clamped L-band erbium-doped fiber amplifier with C-band control signal. *48*(12), 2340-2343.
- Bebawi, J., Kandas, I., El-Osairy, M., & Aly, M. J. A. S. (2018). A Comprehensive Study on EDFA Characteristics: Temperature Impact. *8*(9), 1640.
- Bebawi, J. A., Kandas, I., El-Osairy, M. A., & Aly, M. H. J. A. S. (2018). A comprehensive study on EDFA characteristics: temperature impact. *8*(9), 1640.
- Becker, P. M., Olsson, A. A., & Simpson, J. R. (1999). *Erbium-doped fiber amplifiers: fundamentals and technology*: Elsevier.
- Berkdemir, C., & Özsoy, S. J. O. C. (2005). An investigation on the temperature dependence of the relative population inversion and the gain in EDFAs by the modified rate equations. *254*(4-6), 248-255.
- Berkdemir, C., & Özsoy, S. J. O. E. (2005). The temperature dependent performance analysis of EDFAs pumped at 1480 nm: A more accurate propagation equation. *13*(13), 5179-5185.
- Bhadra, S., & Ghatak, A. (2016). *Guided Wave Optics and Photonic Devices*: CRC Press.

- Cheng, X. S., Hamida, B. A., Naji, A. W., Ahmad, H., & Harun, S. W. J. L. P. L. (2011). 67 cm long bismuth-based erbium doped fiber amplifier with wideband operation. *8*(11), 814-817.
- Cheng, X. S., Parvizi, R., Ahmad, H., & Harun, S. W. J. I. P. J. (2009). Wide-band bismuth-based erbium-doped fiber amplifier with a flat-gain characteristic. *1*(5), 259-264.
- Cokrak, A. C., Altuncu, A. J. I. U.-J. o. E., & Engineering, E. (2004). Gain and noise figure performance of erbium doped fiber amplifiers (EDFA). *4*(2), 1111-1122.
- Desurvire, E. J. i. P., & applications. (1992). Erbium-doped fiber amplifiers.
- Dong, J., Wei, Y., Wonfor, A., Penty, R., White, I., Lousteau, J., . . . Jha, A. J. I. P. T. L. (2011). Dual-Pumped Tellurite Fiber Amplifier and Tunable Laser Using Er<sup>3+</sup>/Ce<sup>3+</sup> Codoping Scheme. *23*(11), 736-738.
- Duarte, J., Paul, M. C., Das, S., Dhar, A., Leitão, J. P., Ferreira, M. F., & Rocha, A. M. J. O. M. E. (2019). Optical amplification performance of erbium doped zirconia-ytria-alumina-baria silica fiber. *9*(6), 2652-2661.
- Durak, F. E., & Altuncu, A. J. O. C. (2017). The effect of ASE reinjection configuration through FBGs on the gain and noise figure performance of L-Band EDFA. *386*, 31-36.
- Durak, F. E., & Altuncu, A. J. O. F. T. (2018). All-optical gain clamping and flattening in L-Band EDFAs using lasing-controlled structure with FBG. *45*, 217-222.
- Ellison, A., Dickinson, J., Goforth, D., Harris, D., Kohli, J., Minelly, J., . . . Yadlowsky, M. (1999). *Hybrid erbium silicate conventional-band fiber amplifier with ultra-low gain ripple*. Paper presented at the Optical Amplifiers and Their Applications.
- Emami, S. D., Hajireza, P., Abd-Rahman, F., Abdul-Rashid, H. A., Ahmad, H., & Harun, S. W. J. P. I. E. R. (2010). Wide-band hybrid amplifier operating in S-band region. *102*, 301-313.
- Emmanuel, D., & Zervas, M. (1994). Erbium-doped fiber amplifiers: principles and applications. In: New York: Wiley Interscience.
- Firstov, S., Firstova, E., Alyshev, S., Khopin, V., Riumkin, K., Melkumov, M., . . . Dianov, E. J. L. P. (2016). Recovery of IR luminescence in photobleached bismuth-doped fibers by thermal annealing. *26*(8), 084007.
- Firstov, S., Riumkin, K., Khagai, A., Alyshev, S., Melkumov, M., Khopin, V., . . . Dianov, E. J. L. P. L. (2017). Wideband bismuth-and erbium-codoped optical fiber amplifier for C+L+U-telecommunication band. *14*(11), 110001.
- Gangwar, R., Singh, S., Singh, N. J. O.-I. J. f. L., & Optics, E. (2010). Gain optimization of an erbium-doped fiber amplifier and two-stage gain-flattened EDFA with 45 nm flat bandwidth in the L-band. *121*(1), 77-79.

- Geguo, D., & Guofu, C. J. S. i. C. S. A. M. (1999). Gain performances of 980 nm-pumped erbium-doped fiber amplifiers. *42*(3), 286-292.
- Ghosh, B., Pal, R. R., Mukhopadhyay, S. J. O.-I. J. f. L., & Optics, E. (2011). A new approach to all-optical half-adder by utilizing semiconductor optical amplifier based MZI wavelength converter. *122*(20), 1804-1807.
- Giles, C. R., & Desurvire, E. J. J. o. l. t. (1991). Modeling erbium-doped fiber amplifiers. *9*(2), 271-283.
- Goel, N. K., Pickrell, G., & Stolen, R. J. O. F. T. (2014). An optical amplifier having 5 cm long silica-clad erbium doped phosphate glass fiber fabricated by “core-suction” technique. *20*(4), 325-327.
- Hamida, B., Azooz, S., Jasim, A., Eltaif, T., Khan, S., Ahmad, H., & Harun, S. W. J. O. (2016). Flat-gain wide-band erbium doped fiber amplifier with hybrid gain medium. *127*(5), 2481-2484.
- Hamida, B. A., Cheng, X. S., Naji, A. W., Ahmad, H., Al-Khateeb, W., Khan, S., . . . Materials. (2012). Optical amplifier with flat-gain and wideband operation utilizing highly concentrated erbium-doped fibers. *21*(01), 1250005.
- Hamzah, A., Azrin, N., Saris, N. J. J. o. T., Electronic, & Engineering, C. (2018). Flat-gain and Wideband EDFA by using Dual Stage Amplifier Technique. *10*(2-6), 25-29.
- Hamzah, A., Paul, M. C., Harun, S. W., Huri, N., Lokman, A., Pal, M., . . . Yoo, S. J. L. P. (2011). Compact fiber laser at L-band region using Erbium-doped Zirconia fiber. *21*(1), 176-179.
- Harun, S. W., Parvizi, R., Cheng, X., Parvizi, A., Emami, S., Arof, H., . . . Technology, L. (2010). Experimental and theoretical studies on a double-pass C-band bismuth-based erbium-doped fiber amplifier. *42*(5), 790-793.
- Harun, S. W., Paul, M. C., Huri, N., Hamzah, A., Das, S., Pal, M., . . . Technology, L. (2011). Double-pass erbium-doped zirconia fiber amplifier for wide-band and flat-gain operations. *43*(7), 1279-1281.
- Harun, S. W., Tamchek, N., Poopalan, P., & Ahmad, H. J. I. P. T. L. (2003). Double-pass L-band EDFA with enhanced noise figure characteristics. *15*(8), 1055-1057.
- Hayashi, H., Sugimoto, N., & Tanabe, S. J. O. F. T. (2006). High-performance and wideband amplifier using bismuth-oxide-based EDF with cascade configurations. *12*(3), 282-287.
- Htein, L., Fan, W., Watekar, P. R., & Han, W.-T. (2012). Amplification by white light-emitting diode pumping of large-core Er-doped fiber with 12 dB gain. *Optics letters*, *37*(23), 4853-4855.
- Huri, N., Hamzah, A., Arof, H., Ahmad, H., & Harun, S. W. J. L. P. (2011). Hybrid flat gain C-band optical amplifier with Zr-based erbium-doped fiber and semiconductor optical amplifier. *21*(1), 202-204.

- Idachaba, F., Ike, D. U., & Orovwode, H. (2014). Future trends in fiber optics communication.
- Jauregui, C., Otto, H.-J., Breilkopf, S., Limpert, J., & Tünnermann, A. J. O. e. (2016). Optimizing high-power Yb-doped fiber amplifier systems in the presence of transverse mode instabilities. *24*(8), 7879-7892.
- Jayarajan, P., Kuppusamy, P., Sundararajan, T., Thiyagupriyadharsan, M., AhamedYasar, Z., Maheswar, R., & Amiri, I. S. J. R. i. P. (2018). Analysis of temperature based power spectrum in EDFA and YDFA with different pump power for THz applications. *10*, 160-163.
- Jia, Y., Wei, E., Wang, X., Zhang, X., Morrison, J. C., Parikh, M., . . . Edmunds, B. J. O. (2014). Optical coherence tomography angiography of optic disc perfusion in glaucoma. *121*(7), 1322-1332.
- Jianga, S., Hwang, B.-C., Luo, T., Seneschal, K., Smektala, F., Honkanen, S., . . . Peyghambarian, N. (2000). *Net gain of 15.5 dB from a 5.1 cm long Er/sup 3+/-doped phosphate glass fiber*. Paper presented at the Optical Fiber Communication Conference. Technical Digest Postconference Edition. Trends in Optics and Photonics Vol. 37 (IEEE Cat. No. 00CH37079).
- Jung, M., Chang, Y. M., & Lee, J. H. (2012). *Performance Comparison between 980 and 1480 nm Pumping for Er3+/-doped Bismuth Fiber Amplifiers*. Paper presented at the National Fiber Optic Engineers Conference.
- Kaler, R., Kaler, R. J. O.-I. J. f. L., & Optics, E. (2011). Gain and Noise figure performance of erbium doped fiber amplifiers (EDFAs) and Compact EDFAs. *122*(5), 440-443.
- Kir'yanov, A., Siddiki, S., Barmenkov, Y., Das, S., Dutta, D., Dhar, A., . . . Didenko, S. J. O. M. E. (2017). Hafnia-yttria-alumina-silica based optical fibers with diminished mid-IR (> 2  $\mu$ m) loss. *7*(7), 2511-2518.
- Kumar, G., Kumar, S. J. O., & Electronics, Q. (2019). Flat gain C+ L band using optical amplifiers for 200 $\times$  14 Gbps DWDM system. *51*(1), 34.
- Ladaci, A., Girard, S., Mescia, L., Robin, T., Cadier, B., Laurent, A., . . . Ouerdane, Y. J. I. J. o. Q. E. (2018). Validity of the McCumber Theory at High Temperatures in Erbium and Ytterbium-Doped Aluminosilicate Fibers. *54*(4), 1-7.
- Latiff, A., Zakaria, Z., Jaafar, A., Rafis, H., Gannapathy, V. J. I. J. o. R. i. E., & Tech. (2013). Comparative Study on Single-And Double-Pass Configurations for Serial Dual-Stage High Concentration EDFA. *2*(12), 139-143.
- Li, X., Liu, X., Gong, Y., Sun, H., Wang, L., & Lu, K. J. L. P. L. (2009). A novel erbium/ytterbium co-doped distributed feedback fiber laser with single-polarization and unidirectional output. *7*(1), 55.
- Liaw, S.-K., & Huang, Y.-S. J. E. I. (2008). C+ L-band hybrid amplifier using FBGs for dispersion compensation and power equalisation. *44*(14), 844-845.

- Liaw, S., Huang, C., & Hsiao, Y. J. L. P. L. (2008). Parallel-type C+ L band hybrid amplifier pumped by 1480 nm laser diodes. *5*(7), 543.
- Lin, M.-C., & Chi, S. J. I. p. t. l. (1992). The gain and optimal length in the erbium-doped fiber amplifiers with 1480 nm pumping. *4*(4), 354-356.
- Liu, H., Naumov, I. I., Geballe, Z. M., Somayazulu, M., John, S. T., & Hemley, R. J. J. P. R. B. (2018). Dynamics and superconductivity in compressed lanthanum superhydride. *98*(10), 100102.
- Long, H., Li, X., & Liu, H. J. L. P. (2011). Over 300 nm tunable broadband one-crystal noncollinear optical parametric amplification. *21*(1), 86-89.
- Lopez-Amo, M., Blair, L. T., & Urquhart, P. J. O. I. (1993). Wavelength-division-multiplexed distributed optical fiber amplifier bus network for data and sensors. *18*(14), 1159-1161.
- Mahran, O., & Aly, M. H. J. A. o. (2016). Performance characteristics of dual-pumped hybrid EDFA/Raman optical amplifier. *55*(1), 22-26.
- Mariyam, P. D., Aji, A. P., Chisnariandini, N., & Apriono, C. (2018). *Design of land optical fiber backbone communication network in North Sumatera*. Paper presented at the 2018 International Conference on Information and Communications Technology (ICOIACT).
- Markom, A., Paul, M. C., Dhar, A., Das, S., Pal, M., Bhadra, S. K., . . . Harun, S. J. O. (2017). Performance comparison of enhanced Erbium–Zirconia–Yttria–Aluminum co-doped conventional erbium-doped fiber amplifiers. *132*, 75-79.
- Martin, R., & Quimby, R. J. J. B. (2006). Experimental evidence of the validity of the McCumber theory relating emission and absorption for rare-earth glasses. *23*(9), 1770-1775.
- Mochida, Y., Yamaguchi, N., & Ishikawa, G. J. J. o. l. t. (2002). Technology-oriented review and vision of 40-Gb/s-based optical transport networks. *20*(12), 2272-2281.
- Mori, A. J. J. o. t. C. S. o. J. (2008). Tellurite-based fibers and their applications to optical communication networks. *116*(1358), 1040-1051.
- Mynbaev, D. K. J. I. J. o. H. S. E., & Systems. (2016). Fundamental and Technological Limitations of Optical Communications. *25*(01n02), 1640010.
- Naji, A., Hamida, B. A., Cheng, X., Mahdi, M. A., Harun, S., Khan, S., . . . Ahmad, H. J. I. J. o. P. S. (2011). Review of Erbium-doped fiber amplifier. *6*(20), 4674-4689.
- Naji, A. W., Ibrahim, H. F., Ahmed, B., Harun, S. W., & Mahdi, M. A. (2010). *Theoretical analysis of triple-pass erbium-doped fiber amplifier*. Paper presented at the International Conference on Computer and Communication Engineering (ICCCE'10).

- Nilsson, J., Yun, S., Hwang, S., Kim, J., & Kim, S. J. I. P. T. L. (1998). Long-wavelength erbium-doped fiber amplifier gain enhanced by ASE end-reflectors. *10*(11), 1551-1553.
- Norouzi, M., Badeka, P., Chahande, P., & Briley, B. (2013). *A survey on rare earth doped optical fiber amplifiers*. Paper presented at the IEEE International Conference on Electro-Information Technology, EIT 2013.
- Novak, S., & Moesle, A. J. J. o. L. T. (2002). Analytic model for gain modulation in EDFAs. *20*(6), 975.
- Ohara, S., & Sugimoto, N. J. O. I. (2008). Bi<sub>2</sub>O<sub>3</sub>-based erbium-doped fiber laser with a tunable range over 130 nm. *33*(11), 1201-1203.
- Ohishi, Y., Mori, A., Yamada, M., Ono, H., Nishida, Y., & Oikawa, K. J. O. I. (1998). Gain characteristics of tellurite-based erbium-doped fiber amplifiers for 1.5- $\mu$ m broadband amplification. *23*(4), 274-276.
- Pal, A., Dhar, A., Das, S., Chen, S. Y., Sun, T., Sen, R., & Grattan, K. T. J. O. e. (2010). Ytterbium-sensitized Thulium-doped fiber laser in the near-IR with 980 nm pumping. *18*(5), 5068-5074.
- Paul, M. C., Dhar, A., Das, S., Pal, M., Bhadra, S. K., Markom, A., . . . Harun, S. J. I. P. J. (2015). Enhanced Erbium-Zirconia-Yttria-Aluminum Co-Doped Fiber Amplifier. *7*(5), 1-7.
- Paul, M. C., Harun, S. W., Huri, N., Hamzah, A., Das, S., Pal, M., . . . Kalita, M. J. J. o. L. T. (2010a). Wideband EDFA based on erbium doped crystalline zirconia yttria alumino silicate fiber. *28*(20), 2919-2924.
- Paul, M. C., Harun, S. W., Huri, N., Hamzah, A., Das, S., Pal, M., . . . Kalita, M. J. O. I. (2010b). Performance comparison of Zr-based and Bi-based erbium-doped fiber amplifiers. *35*(17), 2882-2884.
- Pedersen, B., Thompson, B., Zemon, S., Miniscalco, W., & Wei, T. J. I. p. t. l. (1992). Power requirements for erbium-doped fiber amplifiers pumped in the 800, 980, and 1480 nm bands. *4*(1), 46-49.
- Pradhan, D., & Mishra, V. J. I. J. C. S. N. (2015). Analysis and Review of EDFA. *6*(4).
- Qiao, L. (2019). Optical amplifier. In: Google Patents.
- Qiu, Y., Dong, X., & Zhao, C. J. L. P. (2010). Spectral characteristics of the erbium-bismuth co-doped silica fibers and its application in single frequency fiber laser. *20*(6), 1418-1424.
- Qureshi, K. K. (2014). Multi-wavelength laser. In: Google Patents.
- Qureshi, K. K., Tam, H. J. O., & Technology, L. (2012). Multiwavelength fiber ring laser using a gain clamped semiconductor optical amplifier. *44*(6), 1646-1648.

- Saris, N. N. H., Hamzah, A., Ambran, S. J. J. o. A. R. i. A. S., & Technology, E. (2017). Investigation on Gain Improvement of Erbium Doped Fiber Amplifier (EDFA) By Using Dual Pumped Double Pass Scheme. 7(1).
- Sergeyev, S., Vanin, E., & Jacobsen, G. (2002). *Gain-clamped dynamics in EDFA with combined electronic feed-forward–optical feedback control*. Paper presented at the Optical Fiber Communication Conference.
- Shen, J.-L., Lee, Y.-C., & Huang, C.-C. J. A. o. (2009). L-band automatic-gain-controlled erbium-doped fiber amplifier utilizing C-band backward-amplified spontaneous emission and electrical feedback monitor. 48(5), 842-846.
- Singh, M. J. J. o. O. C. (2018). A review on hybrid optical amplifiers. 39(3), 267-272.
- Singh, S., & Kaler, R. J. I. P. T. L. (2012). Flat-gain L-band Raman-EDFA hybrid optical amplifier for dense wavelength division multiplexed system. 25(3), 250-252.
- Singh, S., & Kaler, R. J. I. P. T. L. (2013). Novel optical flat-gain hybrid amplifier for dense wavelength division multiplexed system. 26(2), 173-176.
- Singh, S., & Kaler, R. S. J. O. E. (2015). Review on recent developments in hybrid optical amplifier for dense wavelength division multiplexed system. 54(10), 100901.
- Suzuki, N., Miura, H., & Uto, K. (2016). *Demonstration of 100 Gb/s/λ-based Coherent PON System Using New Automatic Gain Controlled EDFA with ASE Compensation Function for Upstream*. Paper presented at the ECOC 2016; 42nd European Conference on Optical Communication.
- SW, H., HA, A.-R., SZ, M.-Y., MR, T., & Ahmad, H. J. I. E. E. (2006). Dual-stage Er/Yb doped fiber amplifier for gain and noise figure enhancements. 3(23), 517-521.
- Urquhart, P. J. I. P. J. (1988). Review of rare earth doped fibre lasers and amplifiers. 135(6), 385-407.
- Vienne, G. G., Caplen, J. E., Dong, L., Minelly, J. D., Nilsson, J., & Payne, D. N. J. J. o. l. t. (1998). Fabrication and characterization of Yb<sup>3+</sup>: Er<sup>3+</sup> phosphosilicate fibers for lasers. 16(11), 1990.
- Volet, N., Spott, A., Stanton, E. J., Davenport, M. L., Chang, L., Peters, J. D., . . . Reviews, P. (2017). Semiconductor optical amplifiers at 2.0-μm wavelength on silicon. 11(2), 1600165.
- Wang, P., Yang, J., & Zhang, X. J. O. E. (2018). Stability improvement in a gain-clamped L-band erbium-doped fiber amplifier through hybrid gain control. 57(5), 056105.
- Wood, D. L., Nassau, K., Kometani, T., & Nash, D. J. A. o. (1990). Optical properties of cubic hafnia stabilized with yttria. 29(4), 604-607.
- Wysocki, P. F., Park, N., & DiGiovanni, D. J. O. I. (1996). Dual-stage erbium-doped, erbium/ytterbium-codoped fiber amplifier with up to+ 26-dBm output power and a 17-nm flat spectrum. 21(21), 1744-1746.

- Xia, B., Pudo, D., & Chen, L. R. J. I. P. T. L. (2003). Comparison of the static and dynamic properties of single- and double-pass partially gain-clamped two-stage L-band EDFAs. *15*(4), 519-521.
- Xunsi, W., Qihua, N., Tiefeng, X., Xiang, S., Shixun, D., & Na, G. J. J. o. R. E. (2008). Tm<sup>3+</sup>-doped tellurite glass with Yb<sup>3+</sup> energy sensitized for broadband amplifier at 1400–1700 nm bands. *26*(6), 907-911.
- Yang, D., Pun, E. Y. B., Wang, N., & Lin, H. J. J. B. (2010). Radiation and gain behaviors in Tm<sup>3+</sup>-doped aluminum germanate substrate glasses and thermal ion-exchanged waveguide. *27*(5), 990-996.
- Yang, J., Ma, Y., OuYang, Y., Liu, C., & Zhang, J. (2014). *A comprehensive study on gain stabilization of Er-doped fiber amplifier in C-band with uniform fiber Bragg grating-pair*. Paper presented at the International Symposium on Photonics and Optoelectronics 2014.
- Yang, J., Meng, X., Liu, C. J. O., & Technology, L. (2016). Accurately control and flatten gain spectrum of L-band erbium doped fiber amplifier based on suitable gain-clamping. *78*, 74-78.
- Yeniay, A., & Gao, R. (2001). *L-band EDFA gain and gain flatness enhancement via co-propagating C-band seed technique*. Paper presented at the Proceedings 27th European Conference on Optical Communication (Cat. No. 01TH8551).
- Yi, L., Zhan, L., Taung, C., Luo, S., Hu, W., Su, Y., . . . Leng, L. J. O. e. (2005). Low noise figure all-optical gain-clamped parallel C+ L band Erbium-doped fiber amplifier using an interleaver. *13*(12), 4519-4524.
- Yücel, M., Göktaş, H. H., & Akkaya, G. (2012). *Optimization of the three stages L band EDFA*. Paper presented at the 2012 20th Signal Processing and Communications Applications Conference (SIU).
- Yusoff, N. M., Abas, A., Hitam, S., & Mahdi, M. J. O. C. (2012). Dual-stage L-band erbium-doped fiber amplifier with distributed pumping from single pump laser. *285*(6), 1383-1386.

## LIST OF PUBLICATIONS AND PAPERS PRESENTED

**Almukhtar, A. A.,** Al-Azzawi, A. A., Reddy, P. H., Das, S., Dhar, A., Paul, M. C., ... & Harun, S. W. (2019). Wideband optical fiber amplifier with short length of enhanced erbium–zirconia–yttria–aluminum co-doped fiber. *Optik*, 182, 194-200.

**Almukhtar, A. A.,** Al-Azzawi, A. A., Ahmad, B. A., Cheng, X. S., Reddy, P. H., Dhar, A., ... & Harun, S. W. (2019). Flat-gain and wide-band partial double-pass erbium co-doped fiber amplifier with hybrid gain medium. *Optical Fiber Technology*, 52, 101952.

**Almukhtar, A. A.,** Al-Azzawi, A. A., DASb, S., Dhar, A., Paul, M. C., Jusoh, Z., ... & Yasin, M. (2018). An efficient L-band Erbium-doped fiber amplifier with Zirconia-Yttria-Aluminum co-doped silica fiber. *Journal of Non-Oxide Glasses Vol*, 10(3), 65-70.

**Almukhtar, A. A.,** Al-Azzawi, A. A., Reddy, P. H., Das, S., Dhar, A., Paul, M. C., ... & Harun, S. W. (2019). An efficient L-band Zirconia Yttria Aluminum Erbium co-doped fiber amplifier with 1480 nm pumping. *Journal of Nonlinear Optical Physics & Materials*, 1950018.

**Almukhtar, A. A.,** Al-Azzawi, A. A., Jusoh, Z., Razak, N. F., Reddy, P. H., ... & Harun, S. W. (2019). Flat-gain optical amplification within 70 nm wavelength band using 199 cm long hybrid erbium fibers. *Optoelectronics and Advanced Materials–Rapid Communications*, 13(7-8), 391-395.

**Almukhtar, A. A.,** Al-Azzawi, A. A., Cheng, X. S., Reddy, P. H., Dhar, A., Paul, M. C., & Harun, S. W. The Enhanced Triple-pass Hybrid Erbium Doped Fiber Amplifier using Distribution Pumping Scheme in a Dual-stage Configuration. *Optik* (under Review).

## LIST OF CONFERENCE PAPER

**Almukhtar, A. A.,** Al-Azzawi, A. A., Cheng, X. S., Paul, M. C., Ahmad, H., & Harun, S. W. (2019, January). The effect of 980 nm and 1480 nm pumping on the performance of newly Hafnium Bismuth Erbium-doped fiber amplifier. In *Journal of Physics: Conference Series* (Vol. 1151, No. 1, p. 012013). IOP Publishing.

University of Malaya